A NITROGEN-RESPONSIVE SMALL PEPTIDE SIGNALING MECHANISM MODULATES PLANT ROOT SYSTEM ARCHITECTURE

By

Katerina Sibala Lay-Pruitt

A DISSERTATION

Submitted to
Michigan State University
in partial fulfillment of the requirements
for the degree of

Genetics and Genome Sciences—Doctor of Philosophy

2021

ABSTRACT

A NITROGEN-RESPONSIVE SMALL PEPTIDE SIGNALING MECHANISM MODULATES PLANT ROOT SYSTEM ARCHITECTURE

By

Katerina Sibala Lay-Pruitt

The plant root system changes dynamically in response to environmental cues. Plants utilize their root system for uptake of essential mineral nutrients that are heterogeneously distributed in the soil environment. Nutrient-dependent modulation of root system architecture (RSA) traits such as primary root growth, lateral root emergence, and the angles at which these roots grow allows for optimization of nutrient acquisition. Among signaling pathways by which plants may sense the availability of nutrients from the environment, small signaling peptide (SSP) pathways play important roles in optimizing root functions. These SSP pathways may further regulate molecular processes underlying RSA, such as the biosynthesis and transport of the major plant growth hormone, auxin. Characterization of these nutrient-responsive SSP pathways is thus of great importance and critical for understanding plant development in nutrient-poor environments. For my dissertation, I have identified and characterized a nitrogen (N)-responsive SSP pathway modulating root gravitropic response and lateral root development. Co-regulation of these RSA components by this module is proposed to prevent root outgrowth into N-poor regions and drive deeper root growth towards mobile nitrate (NO_3^-) resources stratified deeper in the soil profile. **First**, I show that a signaling pathway involving the CLAVATA3/EMBRYO SURROUNDING REGION-RELATED (CLE) family of peptides and the CLAVATA1 (CLV1) receptor kinase, which is involved in N-dependent repression of lateral root emergence, also enhances root gravitropic

response under N-limited conditions. Transcriptomic profiling of a *clv1* mutant and *CLE3* overexpressing lines identified *Arabidopsis thaliana* CENTRORADIALIS (ATC), a mobile protein previously characterized for its role in flowering regulation, as a downstream target of CLE-CLV1 signaling. Loss of *ATC* function significantly weakens root gravitropic response and has a moderate impact on lateral root emergence under low NO_3^- availability. *ATC* promoter activity and protein localization are also detected throughout the phloem and in the root columella cells, which are major centers for gravity sensing. **Second**, I demonstrate the relevance of ATC function on the molecular processes underlying root gravitropic response. While mutation in *ATC* does not impact gravity sensing via amyloplast sedimentation, it does inhibit the asymmetric transport of auxin needed for gravitropic bending. I determine that this occurs via the significant reduction of the PIN3 auxin efflux transporter in the vasculature and root tip of *atc* mutant lines. **Lastly**, I examine how the known roles of ATC in floral development could be implicated in root developmental processes. ATC binds to phosphatidic acid and phosphatidylserine, which is contrary to the binding capacity of its homolog FLOWERING LOCUS T (FT) to phosphatidylcholine and may contribute to its activity in N-limited environments. I also investigate the interaction of ATC and the transcription factor FD in the transcriptional regulation of *PIN3*. Although FD appears to have an impact on root gravitropic response, FD inhibits the expression of *PIN3,* suggesting potentially complex control of this gene via floral regulatory components. Taken together, the results presented in this dissertation contribute greatly to our understanding of how plant root architecture alters in response to N. These results can be further utilized in plant engineering strategies to regulate root growth in nutrient-limited soils.

ACKNOWLEDGEMENTS

First and foremost, I would like to thank my research advisor, Dr. Hideki Takahashi, for all the support, revisions, and professional advice he has given me throughout my graduate studies. I would like to acknowledge the members of the Takahashi lab who have helped me tremendously along the way, particularly Dr. Anne-Sophie Bohrer and Dr. Wei Dong. I would also like to thank Dr. Ricardo Giehl and Dr. Nicolaus von Wirén at IPK Gatersleben as well as Dr. Eva Benková and her lab at the Institute of Science and Technology Austria. Technical support from members of the Hoffmann-Benning, Hamberger, and Farré labs at MSU was also greatly appreciated. I would like to thank the Genetics and Genome Sciences Program, Dr. Cathy Ernst, and Alaina Burghardt for all their administrative help as well as my committee members: Dr. Susanne Hoffmann-Benning, Dr. Gregg Howe, and Dr. Beronda Montgomery. Lastly, I would like to thank my friends and family, especially Dylan Pruitt, for all their support throughout this process.

This research was funded by National Science Foundation grant no. 1444549 and by the USDA NIFA National Needs Training grant no. 2015-38420-23697.

TABLE OF CONTENTS

LIST OF TABLES vii

LIST OF FIGURES viii

KEY TO ABBREVIATIONS x

CHAPTER 1. Nutrient-responsive small signaling peptides and their influence on the root system architecture 1
- Abstract 2
- Introduction 3
- Nitrogen-responsive SSPs 5
- Phosphorus-responsive SSPs 8
- SSP-dependent changes on RSA have an impact on nutrient homeostasis 10
- Transcriptomic studies reveal potential SSP candidates for functional characterization 12
- Gene expression reveals potential for nutrient-dependent crosstalk involving SSP pathways 13
- Conclusions 14
- Project goals and significance 18

CHAPTER 2. Nitrogen-responsive CLE-CLV1 signaling promotes root gravitropic response through the activity of *Arabidopsis thaliana* CENTRORADIALIS 21
- Abstract 22
- Introduction 23
- Methods 25
  - Plant growth and culture 25
  - Root phenotyping 26
  - Microarray analysis 26
  - Quantitative real-time polymerase chain reaction 27
  - Generation of transgenic plant lines 28
  - Microscopy 29
- Results 30
  - CLV1 signaling is involved in maintenance of root gravitropism 30
  - ATC controls root gravitropic response under low NO_3^- availability 34
  - ATC has a moderate impact on lateral root phenotypes 36
  - Localization of *ATC* promoter activity and protein expression 38
  - ATC exhibits nuclear localization in the primary root 43
- Discussion 45

CHAPTER 3. *Arabidopsis thaliana* CENTRORADIALIS alters auxin transport mechanisms via PIN3 auxin efflux transporter activity 48
- Abstract 49

Introduction 49
Methods 52
Plant growth and culture 52
Root phenotyping 52
Quantitative real-time polymerase chain reaction 52
Microscopy 52
Results 54
Mutation in *ATC* disrupts auxin transport in the root tip 54
ATC regulates expression of PIN3 to maintain root gravitropism 57
ATC does not affect PIN3 relocalization but may stabilize expression at the columella during gravistimulation 59
N-dependent ATC signaling mediates *PIN3* expression and root gravitropism 61
Discussion 63

CHAPTER 4. Characterization of the flowering repressor protein *Arabidopsis thaliana* CENTRORADIALIS as a novel regulator of root growth 65
Abstract 66
Introduction 66
Methods 70
Plant growth and culture 70
Root phenotyping 70
Agroinfiltration of *N. benthamiana* leaves 70
Luciferase transactivation assay 72
Protein expression and lipid binding assay 72
Results 73
ATC binds to phosphatidic acid and phosphatidylserine 73
FD function influences root gravitropic response 75
ATC and FD independently influence *PIN3* expression 76
Discussion 78

CHAPTER 5. Conclusions and future directions 80
Summary 81
Future work 84
Lateral root development 84
ATC-mediated regulation of PIN3 85
Expanding the CLE-CLV1-ATC signaling model 87
Conclusion 88

APPENDICES 89
Appendix A. Supplemental Data for Chapter 2 90
Appendix B. Supplemental Data for Chapter 3 97
Appendix C. Supplemental Data for Chapter 4 101

REFERENCES 106

LIST OF TABLES

Appendix Table A.1. List of primers used in Chapter 2 91

Appendix Table A.2. Differentially expressed genes in *CLE3* overexpressing lines and *clv1-15*..... 92

Appendix Table B.1. List of primers used in Chapter 3 98

Appendix Table C.1. List of primers used in Chapter 4 102

LIST OF FIGURES

Figure 1.1. Small signaling peptide (SSP) signaling modules influencing root system architecture (RSA) and nutrient response, uptake, and homeostasis 5

Figure 1.2. CLE-CLV1 signaling module represses lateral root primordia development. 19

Figure 2.1. CLV1 signaling is involved in the maintenance of root gravitropism..... 32

Figure 2.2 ATC is a downstream target of CLE3-CLV1 signaling..... 33

Figure 2.3. ATC regulates root gravitropism under low NO_3^- availability 35

Figure 2.4. Lateral root phenotypes of *ATC* mutants and overexpressing lines 37

Figure 2.5. *ATC::GFP* localization in the root 39

Figure 2.6. *ATC* promoter activity is localized to the phloem companion cells and columella cells..... 40

Figure 2.7. ATC protein is localized to the phloem companion cells and surrounding tissues below the elongation zone 41

Figure 2.8. *ATC* promoter activity and protein localization in the columella cells 42

Figure 2.9. Nuclear localization of GFP-ATC in the primary root..... 44

Figure 2.10. Potential nuclear localization of GFP-ATC in the columella cells of gravistimulated roots 45

Figure 3.1. Lugol's staining of *atc* mutant root tips 54

Figure 3.2. Distribution of *DR5::GFP* in the root tip during gravistimulation 55

Figure 3.3. Distribution of DII-VENUS in the root tip during gravistimulation..... 56

Figure 3.4. Reduction of PIN3-GFP expression in *atc-2* mutant lines 58

Figure 3.5. Relocalization of PIN3 in the columella is unaffected by *ATC* mutation 60

Figure 3.6. PIN3 expression is reduced in *atc-2* during gravistimulation..... 61

Figure 3.7. *PIN3* expression in *atc* mutant lines and its influence on root gravitropic response 62

Figure 4.1 Lipid binding profiling of His-ATC..... 74

Figure 4.2 Overlay of His-ATC on a dilution series of PS, PA, and PC 75

Figure 4.3. Root gravitropic response in *fd* mutants 76

Figure 4.4. *PIN3::Fluc* transactivation assay 77

Figure 5.1. Proposed model of N-responsive CLE-CLV1-ATC signaling to regulate root architecture 82

Figure 5.2. Localization of CLV1 and ATC modulating PIN3-mediated auxin transport during gravitropic response 83

Appendix Figure A.1. Root phenotyping of *clv1* mutants 93

Appendix Figure A.2. Root phenotyping of *CLE3* overexpressing lines 94

Appendix Figure A.3. Root phenotyping of *atc* mutants 95

Appendix Figure A.4. Plasmid maps of ATC reporter constructs 96

Appendix Figure B.1. Effect of *ATC* mutation on PIN2 and PIN7 expression 99

Appendix Figure B.2. Root phenotyping of *pin3* mutant lines 100

Appendix Figure C.1. Validation of His-ATC through SDS-PAGE and Western Blot .. 103

Appendix Figure C.2. Plasmid maps of pEAQ vectors 104

Appendix Figure C.3. Plasmid maps of dual luciferase vectors 105

KEY TO ABBREVIATIONS

RSA	Root system architecture
SSP	Small signaling peptide
LRR-RK	Leucine-rich repeat receptor kinase
sORF	Small open reading frames
NRT	Nitrate transporter
CLE	Clavata3/embryo surrounding region related
AON	Autoregulation of nodulation
CLV	CLAVATA
CEP	C-terminally encoded peptide
RGF/GLV/CLEL	Root growth factor/Golven/CLE-like
LPR	Low phosphate root
PDR	Phosphate deficiency response
PLT	PLETHORA
IDA	Inflorescence deficient in abscission
PSY	Plant peptide containing sulfated tyrosine
PIP	PAMP-induced secreted peptide
CIF	Casparian strip integrity factor
GSO	GASSHO1/SCHENGEN3
RALF	Rapid alkalinization factor
FER	FERONIA
HAE	HAESA

PSK	PHYTOSULFOKINE
CAPE	Cysteine-rich secretory proteins, antigen 5, and pathogenesis-related 1 protein
NMR	Nuclear magnetic resonance
LC-MS/MS	Liquid chromatography with tandem mass spectrometry
BAM	Barely any meristem
CRN	CORYNE
RPK	Receptor-like protein kinase
SERK	Somatic embryogenesis receptor-like kinases
ATC	Arabidopsis thaliana CENTRORADIALIS
IAA	Indole-3-acetic acid
GFP	Green fluorescent protein
NLS	Nuclear localization signal
PIN	PIN-FORMED
N	Nitrogen
S	Sulfur
P	Phosphorous
SE	Sieve elements
CC	Companion cells
QC	Quiescent center
SCN	stem cell niche
FT	FLOWERING LOCUS T
FD	FLOWERING LOCUS D

TFL1	TERMINAL FLOWERING 1
LRC	Lateral root cap
Col-0	Columbia 0
L*er*	Landsberg *erecta*
PI	Propidium Iodide
DAPI	4,6’-diamidino-2-phenylindole
PC	Phosphatidylcholine
PA	Phosphatidic acid
PS	Phosphatidylserine
PG	Phosphatidylglycerol
PE	Phosphatidylethanolamine
PI	Phosphatidylinositol
BSA	Bovine serum albumin
FLuc	Firefly luciferase
RLuc	*Renilla* luciferase

CHAPTER 1

Nutrient-responsive small signaling peptides and their influence on the root system architecture

This chapter has been adapted from the following review article published in the open access journal, *International Journal of Molecular Sciences*:

Lay, K. S. & Takahashi, H. Nutrient-responsive small signaling peptides and their influence on the root system architecture. *Int. J. Mol. Sci.* **19,** 3927 (2018). https://doi.org/10.3390/ijms19123927

Abstract

The root system architecture (RSA) of plants is highly dependent on the surrounding nutrient environment. The uptake of essential nutrients triggers various signaling cascades and fluctuations in plant hormones to elicit physical changes in RSA. These pathways may involve signaling components known as small signaling peptides (SSPs), which have been implicated in a variety of plant developmental processes. This chapter reviews known nutrient-responsive SSPs with a focus on several subclasses that have been shown to play roles in root development. Most functionally well-characterized cases of SSP-mediated changes in RSA are found in responses to nitrogen (N) and phosphorus (P) availability, but other nutrients have also been known to affect the expression of SSP-encoding genes. These nutrient-responsive SSPs may interact downstream with leucine-rich repeat receptor kinases (LRR-RKs) to modulate hormone signaling and cellular processes impacting plant root development. SSPs responsive to multiple nutrient cues potentially act as mediators of crosstalk between the signaling pathways. Phenotypes associated with SSP pathways are complicated because of functional redundancy within peptide and receptor families and due to their functionality partly requiring post-translational modifications. As genomic research and techniques progress, novel SSP-encoding genes have been identified in many plant species. Understanding and characterizing the roles of SSPs influencing the root phenotypes will help elucidate the processes that plants use to optimize nutrient acquisition in the environment.

Introduction

Plants require macronutrients and micronutrients from the soil to grow and develop. Due to various geological processes and soil chemistry, these nutrients are heterogeneously distributed in patches and gradients[1]. Thus, plants, as sessile organisms, must use their root systems to navigate the soil profile to maximize nutrient acquisition and maintain nutrient homeostasis. The collective physical characteristics of root growth are known as the root system architecture (RSA); this term encompasses such spatial parameters as primary root length, lateral root length and density, and proliferation of root hairs[2]. RSA of most plant species is highly plastic depending on the nutrient environment[3]. Nutrients are taken up by the plant root system, triggering signaling cascades that alter gene expression and hormone levels, which affect cell growth and differentiation of the root meristems[4]. However, there are many steps in these pathways that remain to be characterized.

One way in which plants sense changes in nutrient availability in the environment and convey the information to downstream physiological processes is through the expression of nutrient-responsive small signaling peptides (SSPs). SSPs are a class of proteins ranging from 5–75 amino acids in length. Many SSPs are derived from nonfunctional precursor proteins to be cleaved and post-translationally-modified to mature forms which then carry out their function as short- or long-distance mobile signals. However, other SSP families may be derived from functional precursors, the 5’ region of mRNA, primary transcripts of miRNA, or small open reading frames (sORFs)[5]. These SSP signaling pathways typically involve the secretion of peptide and perception by leucine-rich repeat receptor kinases (LRR-RKs), although some SSPs have been

hypothesized to act in a receptor-independent manner, such as antimicrobial peptides[6,7]. These LRR-RKs are composed of a family of transmembrane proteins containing an extracellular LRR domain; perception of the SSP ligand occurs through binding with this domain to generate further downstream signals that may regulate physiological and developmental processes. While LRR-RKs are numerous in Arabidopsis (>200 predicted members), most that are known to interact with SSPs are members of the Type XI clade[8,9]. Yet, there is a high numerical disparity between the thousands of putative SSP-encoding genes and the hundreds of LRR-RKs, and many of these pairings remain to be identified or characterized in relationship to plant development.

Regardless of the current lack of receptor identification, SSPs have been implicated in a broad range of downstream processes throughout the plant, such as meristem maintenance, cell proliferation and expansion, reproduction, and response to pathogens[6,10–13]. In the root specifically, SSPs have roles in lateral root development, nodulation, and root hair growth[14–17]. These processes may be linked to the physiological responses of plants to the soil nutrient environment as SSP-encoding gene expression is modulated in roots by changes in the nutrient availability.

This review examines how nutrient signals are interpreted by SSP pathways to alter root morphology for the improvement of nutrient uptake. Most current evidence suggests that a few SSP families play important roles in regulating macronutrient-responsive changes in RSA, particularly in regard to N- or P-availability or maintaining nutrient uptake and homeostasis (Figure 1.1) However, transcriptomic experiments have identified multiple SSP families that are responsive to nutrient cues. Additionally, certain SSPs are found to be responsive to more than one type of nutrient, suggesting they may

represent signals allowing potential crosstalk between the pathways. Lastly, current challenges and novel approaches in the field of SSP research will be addressed.

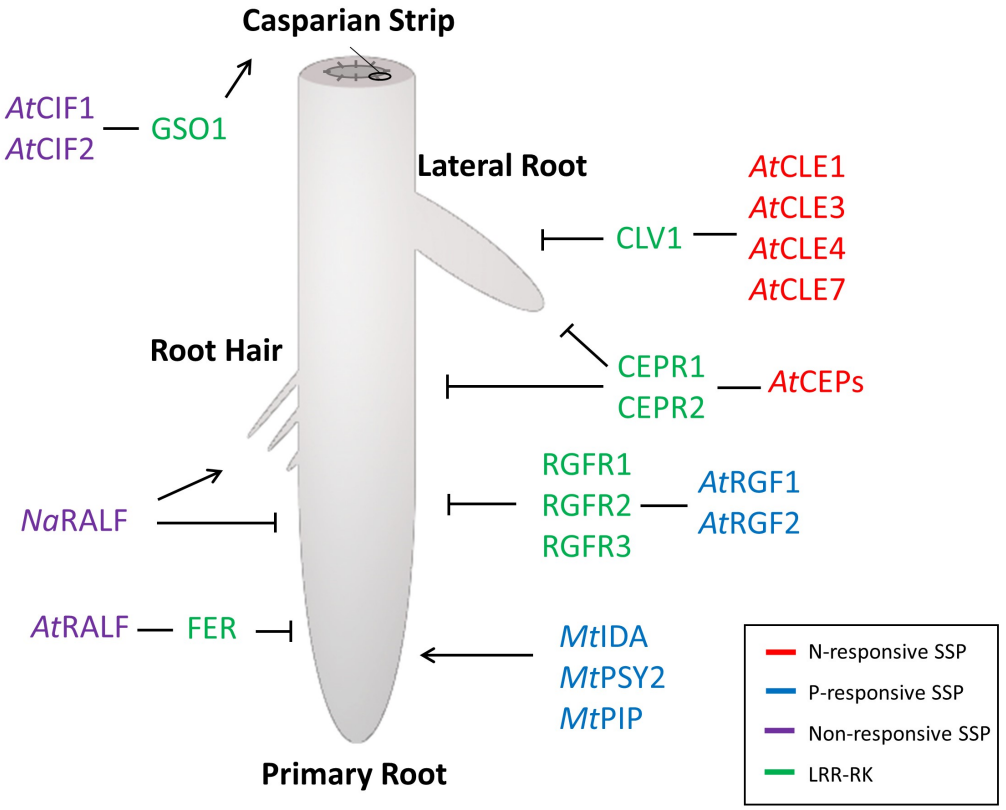

Figure 1.1 Small signaling peptide (SSP) signaling modules influencing root system architecture (RSA) and nutrient response, uptake, and homeostasis. Arrows and bars indicate promotion or repression of growth, respectively. Red: SSPs that are responsive to N-availability at the transcriptional level. Blue: SSPs responsive to P, at the transcriptional level. Purple: SSPs non-responsive to N or P but influencing the nutrient uptake or homeostasis. Green: LRR-RKs.

Nitrogen-responsive SSPs

Variation in availability of the essential macronutrient nitrogen (N) is known to elicit significant changes in plant RSA. Within the soil profile, nitrate (NO_3^-) is highly mobile and easily leaches due to the flow of water; in certain plant species, this may encourage

the root system that is “steep, cheap, and deep” to acquire NO_3^- that has stratified in deeper soil levels[18]. Moderate reduction in N availability leads to an increase in lateral root length as plants forage for available N resources, while severe N-starvation inhibits the growth of primary and lateral roots in favor of survival strategies[3]. Additionally, alternate N sources, such as ammonium (NH_4^+) can elicit different changes in RSA. When N-depleted plants grow into a NO_3^--rich patch, lateral root elongation is stimulated in order to acquire more N, but in NH_4^+-rich patches, more lateral roots are initiated and existing roots become more branched[19,20]. Under homogeneously excess NO_3^- conditions, the RSA profile exhibits long primary roots with short lateral roots, while excess NH_4^+ inhibits primary root growth[1]. NO_3^- supply after a period of N-starvation also induces root hair development[21]. Molecular characterization of how NO_3^- modulates RSA has been studied in depth and involves complex interactions between the NITRATE TRANSPORTER 1.1 (NRT1.1) and auxin signaling pathways[4,22,23]. The N-responsive SSP pathways, described below, may interact with or be part of these pre-existing processes, but direct evidence for their mechanistic interactions has not yet been determined.

N availability alters the expression of various SSPs linked to these observed changes in RSA. One peptide family in which select members have exhibited N-responsiveness is the CLAVATA3/ EMBRYO SURROUNDING REGION-RELATED (CLE) family. CLEs are 12–13 amino acid peptides that control plant development at various stages. While there are thirty-two CLE family members in Arabidopsis, more have been identified in leguminous species where CLE peptides are known to be involved in the autoregulation of nodulation (AON) in addition to RSA response[24,25]. The CLE family has been extensively characterized in relation to its involvement in the regulation of shoot

and root apical meristem differentiation through CLAVATA3 (CLV3)-CLAVATA1 (CLV1)- and CLE40-ARABIDOPSIS CRINKLY 4 (ACR4)-mediated signaling, respectively[26,27]. Other members, however, have been shown to influence the root architecture in an N-dependent manner. Under severe N-starvation, *CLE3* (in addition to *CLE1*, *CLE4*, and *CLE7*) gene expression is induced, and mature CLE3 peptides are produced and secreted from the root pericycle, which bind to the CLV1 LRR-RLK expressed in the phloem companion cells. This interaction signals to yet uncharacterized downstream components to repress the lateral root development. This model was suggested from an experiment validating the ligand-receptor relationship in transgenic Arabidopsis lines that overexpress *CLE3*, in which a correlation between a decrease in lateral root density and an increase in *CLE3* transcript accumulation was observed when *CLV1* was present[14]. Additionally, while the *CLE3* peptide-encoding gene is induced by NO_3^- starvation, it is induced by NH_4^+ supply after N starvation[28], indicating these peptides may fine tune the response in the RSA to the type of N source available.

Another SSP family with members exhibiting responsiveness to N is the C-TERMINALLY ENCODED PEPTIDE (CEP) family. The fifteen members of this family of Arabidopsis are processed to mature 15-amino-acid peptides hydroxylated at the proline residues[29]. Overexpression of multiple *CEP* genes leads to the repression of primary root growth and lateral root initiation, while the knockout lines of *CEP3* generate larger root systems with a higher lateral root density under N-limited conditions[30]. The *CEP* gene expression increases in roots undergoing local N-starvation, and mature CEP peptides translocate to the shoot as long-distance signals to interact with the CEPR1 and CEPR2 LRR-RKs, thereby inducing a shoot-derived signal mediated by the CEP

DOWNSTREAM1 (CEPD1) and CEPD2 polypeptides[31]. This signaling cascade results in the upregulation of nitrate transporters (NRT2.1) in roots locally exposed to relatively N-sufficient or N-rich environments to compensate for N starvation at the distant part of the root system[32]. Despite potential functional redundancy, individual CEP peptides may still be involved in the more specified processes governing RSA. CEP5, which putatively binds to CEPR1 to repress root growth, is negatively regulated by auxin, during lateral root initiation[33]. In *Medicago truncatula*, low N upregulates *MtCEP1*, which interacts with the CEPR1 homolog COMPACT ROOT ARCHITECTURE 2 (MtCRA2) to inhibit the lateral root growth[34,35]. Additionally, like members of the CLE family, CEP peptide families play important roles in other aspects of N-dependent root morphology in leguminous plant species, specifically in the regulation of root nodulation[36].

Phosphorus-responsive SSPs

Phosphorus (P) is another essential macronutrient known to impact RSA. P is relatively immobile in the soil and is typically localized in higher concentrations in the topsoil layer[37]. P deficiency, in fact, causes shorter primary roots and denser lateral roots and root hairs in Arabidopsis, likely to promote a more advantageous RSA profile for enhanced P-uptake[38]. Several additional molecular studies indicate that RSA modulation is linked to changes in P-availability. One major pathway involves the interaction between the LOW PHOSPHATE ROOT1 (LPR1) ferroxidase and the PHOSPHATE DEFICIENCY RESPONSE 2 (PDR2) ATPase—two proteins expressed in the root apical meristem that regulate the primary root growth inhibition due to P-starvation[39]. The S-DOMAIN RECEPTOR KINASE 1-6 (SDK6) and AtPUB9 proteins are also involved in P-responsive

lateral root development, while ETHYLENE INSENSITIVE 3 (EIN3) directly binds to ROOT HAIR DEFECTIVE 6-like 4 (RSL4), to regulate P-responsive root hair development[40,41]. While much is known about the genetic control of these pathways in response to P-availability, it is not yet known how P-responsive SSP signaling is directly related to these studied pathways.

One of the best characterized SSP families responsive to P-availability is the ROOT GROWTH FACTOR/GOLVEN/CLE-LIKE (RGF/GLV/CLEL) family. *RGF1*, *RGF2*, and *RGF3* are induced in the meristematic cortex and epidermis of the root tip under inorganic phosphate (Pi) deprivation[42]. These three peptides were previously established to act redundantly to control root longitudinal growth[43]. A more recent study shows RGF2 and RGF1 independently alter different aspects of the primary root growth. Mutation of *RGF2* causes primary root growth inhibition and a hypersensitivity to low P environments, while RGF1 was shown to control circumferential root growth through the repression of radial cellular divisions in response to Pi deficiency. These changes are proposed to occur through the RGF-mediated signaling pathways, acting on manipulating gradients of PLETHORA (PLT) transcription factors throughout the root meristem[43]. Through an extensive search for peptide receptors by photoaffinity labeling experiments, three LRR-RKs (RGFR1, RGFR2, and RGFR3) have been shown to interact with the RGF peptides to maintain the root meristem[44]. RGF-peptide signaling may directly modulate RSA in response to P-availability, but these pathways have not yet been linked to previously established P-responsive signaling pathways, such as the LPR1-PDR2-mediated pathway that inhibits primary root growth under P-deficiency[4,39].

While the RGF/GLV/CLEL family regulates RSA in response to P-availability in Arabidopsis, other families of SSPs have been suggested to play a role in the response based on experiments in *M. truncatula*. Members of the INFLORESCENCE DEFICIENT IN ABSCISSION (*Mt*IDA), PLANT PEPTIDE CONTAINING SULFATED TYROSINE (*Mt*PSY), and PAMP-INDUCED SECRETED PEPTIDE (*Mt*PIP) families are upregulated upon P-deficiency, but exogenous application of synthetic *Mt*IDA18, *Mt*PSY2, and 9 *Mt*PIP peptides enhances the total root length, especially of the primary root[45]. It is, therefore, possible that SSP signaling pathways responding to P-stress may elicit contrary effects on RSA in different plant species. Direct receptors for these peptides have not yet been characterized in *M. truncatula*.

SSP-dependent changes on RSA have an impact on nutrient homeostasis

SSP pathways governing root developmental processes may still influence the ability of plants to acquire various nutrients, even if the expression of the SSP-encoding gene is not responsive itself to nutrient availability. The function of the CASPARIAN STRIP INTEGRITY FACTOR (CIF) sulfated peptides represents an example of such constitutive actions of SSPs[46,47]. CIF1 and CIF2, which are expressed in the root stele, interact with the endodermis-localized GASSHO1 (GSO1)/SCHENGEN3 LRR-RK to maintain the formation of the Casparian strip, a structure composed of suberin in the root endodermis that prevents water and nutrients from freely entering the vasculature. Interactions between these peptides and the receptor were identified using photoaffinity labeling to probe binding with members of the Type XI LRR-RK clade. Loss of CIF-GSO1 signaling impacts the homeostasis of potassium (K), as well as the micronutrients zinc

and magnesium, and can also increase shoot sensitivity to an iron-excess, as the loss of the Casparian strip integrity may lead to ion leakage between the xylem and the soil[48]. Alternatively, SSP signaling can promote RSA changes that improve nutrient uptake. Expression of the RAPID ALKALINIZATION FACTOR (RALF) peptides in the root is linked to a shorter primary root growth and increased cytoplasmic calcium levels. In Arabidopsis, these RALF peptides interact with the FERONIA (FER) LRR-RK to repress cell elongation in the root; however, in *Nicotiana attenuata*, NaRALF1 additionally promotes root hair formation, which is proposed to improve P-uptake[49,50]. These examples indicate that SSP signaling modules involved in RSA modulation potentially affect the ability of plants to take up essential nutrients, even if the SSP-encoding gene does not exhibit responsiveness to that specific nutrient cue.

Other non-nutrient responsive SSP pathways are known to impact and modulate RSA, which may indirectly affect nutrient uptake. Many of these established pathways have been shown to have downstream effects on cell structure and maintenance. Among the members of the CLE family, CLE40-ACR signaling is integral for the maintenance of the root apical meristem[27]. IDA peptides in Arabidopsis signal to the HAESA (HAE) and HAESA-LIKE2 LRR-RKs to promote lateral root emergence through an enhanced cell separation[15]. PHYTOSULFOKINE (PSK) also interacts with its receptor PSKR to enhance root growth through cell elongation[51]. While these developmental modules have not yet been studied in relation to nutrient cues, modulation of these RSA phenotypes may aid in the uptake of certain nutrients from the heterogeneous soil environment.

Transcriptomic studies reveal potential SSP candidates for functional characterization

Only a small percentage of SSPs have been functionally characterized for their involvement in nutrient response and RSA. Potential candidates for further research are largely identified after their nutrient responsiveness exhibited at the transcriptional level. Relevance of SSPs to regulatory pathways responding to nutrient availability and their potential influence on root development can be mined from the transcriptome datasets examining the effect of nutrient supply on gene expression or RSA. Microarray data of Arabidopsis grown on split-root media, with half of the root system exposed to N-replete environments and the other half in N-deficient conditions, shows a differential expression of thirty-one SSPs (including various CLEs and CEPs) from multiple SSP families[52,53]. These differentially expressed SSPs are proposed to be responsive to long-distance N-signals or be active as mobile signals for communication between root segments. These pathways could contribute to the downstream changes in RSA observed between split root conditions, namely, the compensatory root growth observed in nitrate-rich environments when distal root segments experience N-limitation[53]. Additionally, nitrate supplementation after N-starvation has been shown to induce root hair formation in a process mediated by TGA1 and TGA4 transcription factors[21]. Among potential TGA1/TGA4 downstream targets are CAP (Cysteine-rich secretory proteins, Antigen 5, and Pathogenesis-related 1 protein) (CAPE) peptides, which belong to an SSP family initially investigated for its role in pathogen response and salt tolerance[54,55]. These CAPEs are differentially expressed after NO_3^- supply, but this response is ablated in

the *tga1/tga4* double knockout; however, the direct effect of CAPE expression on root hair phenotype, once again, remains to be observed or functionally characterized.

N and P are indeed the well-characterized macronutrients affecting the SSP-mediated changes in RSA, likely because they induce the most dramatic visible changes in root morphology. However, other macronutrients, such as sulfur (S) and K, as well as various micronutrients may also act through SSP pathways to influence growth and metabolism in the root. Analysis of *M. truncatula* transcriptome after S- and K-deprivation showed that seventy-two SSP-encoding genes were differentially regulated by S, and one (*Mt*Legin13) was downregulated by a K-deficiency[45]. Additional research must be conducted on these SSPs to identify the downstream processes and potential effects on the RSA.

Gene expression reveals potential for nutrient-dependent crosstalk involving SSP pathways

One further challenge to interpret the impact of nutrients on the RSA is that most of the experiments reported in the literature only examine the effect of a single nutrient. Plants growing in soil, however, experience combinatorial nutrient cues that could independently cause contradictory changes in RSA. The moderate effects of certain nutrients, such as S and K, on RSA may also be magnified when combined with fluctuations in other nutrient availabilities[56]. Crosstalk mechanisms between the molecular pathways likely exist to fine-tune RSA in response to these complex environments. These mechanisms may involve SSPs, as certain SSP-encoding genes have been shown to respond to multiple nutrient deficiencies.

These cues may be derived from different functional forms of the same nutrient. For example, *CLE3* expression is repressed by NO_3^-, the more desirable source of N used by the plant, but highly induced by NH_4^+[28,57]. This can potentially be used as a sensing mechanism for an N-context in the surrounding environment and lead to less lateral roots emerging in the NH_4^+-rich areas and a higher proliferation in the comparatively NO_3^--rich patches to maximize the N-uptake efficiency. Other SSPs may still act as integrators for diverse nutrient cues. CLE2, which is also implicated in the lateral root development through interactions with CLV1, is responsive to not only NO_3^- but also to sulfate and phosphate, while other CLE family members exhibit responsiveness to glucose and iron availabilities[58]. These trends are not specific to Arabidopsis and have recently been examined in a large-scale study exposing *M. truncatula* to N, P, K, and S starvation and resupply. Two hundred forty nutrient-responsive SSPs were purportedly involved in the receptor-mediated signaling; while 61% of these genes were responsive to a single macronutrient deprivation in the roots, the remainder, including the *Mt*CLE family members *Mt*CLE05 and *Mt*CLE34, were responsive to two or three conditions[45]. Research remains limited on the effect of multiple nutrient cues acting through individual SSP pathways.

Conclusions

The field of SSP research is greatly expanding. In Arabidopsis, over a thousand peptide encoding genes have been identified[59]. Likewise, in the *M. truncatula*, recent genome re-annotations have identified 1970 homologs of known SSP gene families and 2455 potentially novel SSP-encoding genes[45]. Increasing study of SSPs has led to the

development of the PlantSSP database (http://bioinformatics.psb.ugent.be/webtools/PlantSSP/), which predicts close to 40,000 SSPs and over 4000 SSP families based on the annotations of 32 plant species, many of which have agricultural relevance[60]. Despite such an expansion of information through in silico re-annotations, knowledge of how these nutrient-responsive SSPs influence RSA remains limited, particularly in these crop species, due to the lack of phenotype correlation and identification of receptors or downstream signaling targets, among other challenges. Still, many strategies have been employed to expand the SSP signaling research and establish connections between the nutrient environment and root physiology.

Many experiments performed to study SSPs have relied on forward and reverse genetics using transgenic overexpression lines of peptide-encoding genes or knockout mutant lines. One study has also suggested the use of antagonistic peptides to artificially generate a dominant-negative effect to examine the loss of peptide activity[61]. However, these tools are complicated by a functional redundancy within the peptide families[14,43]. Some peptides, such as CLE1, CLE3, and CLE4 of Arabidopsis, may even have identical mature peptide sequences and overlap in tissue localization[62]. Single mutant studies may not be efficient enough to fully characterize the roles of redundant SSP families; loss of function mutants created using T-DNA insertions are difficult to generate due to the small size of SSP-encoding genes, and alternative strategies, such as generating antagonistic peptides, may still not result in detectable RSA phenotypes. Emergent technologies, such as gene editing, may aid in studying these complex pathways. CRISPR/Cas9 has been used to generate individual knockouts in CLE-peptide encoding genes[63]. The high specificity of this gene editing system was shown to be effective for generating mutants

in this family, which has been difficult in the past due to the small gene size of the CLE family members. While many of the mutants generated using this approach still did not have detectable developmental phenotypes because of the redundancy of peptide sequences, CRISPR/Cas9 has also been shown to be effective in generating higher order mutants within peptide families. This method has been used to generate multiplex knockout lines of the 6 RGF/GLV/CLEL family members; while the stable mutant has not yet been characterized phenotypically, the method was shown to be highly specific with no off-target effects[64].

Another specific consideration is that many experiments rely on the use of exogenously applied synthetic peptides. While these may indeed phenocopy the transgenic overexpression lines and provide a relatively quicker means of analysis, many synthetically-generated peptides lack post-translational modifications that are necessary for proper biological functioning of the SSPs[9]. Conserved post-translational modifications within many Arabidopsis SSP families have been identified using the structural analysis methods, such as nuclear magnetic resonance (NMR) and LC–MS/MS[65,66]. Additionally, the concentration at which they are applied to the medium greatly exceeds the physiological levels, which are estimated to be in the nanomolar range[61].

Lastly, challenges are present not only in studying SSPs themselves, but also in determining associated LRR-RKs. Many studies on the downstream developmental effects of SSP pathways rely on using the mutant lines of proposed receptors. However, SSPs may bind to multiple receptors and individual receptors may also interact with multiple SSPs[44,46,47]. Furthermore, receptors may be functionally redundant, which can complicate the understanding of how the SSP pathways impact plant development. For

example, the CLV3 peptide can be perceived by both CLV1 and the BARELY ANY MERISTEM (BAM) kinase to regulate stem-cell specification; the *clv1 bam* double mutant results in a much more severe phenotype than the single mutants in *clv1* or *bam*[67]. This redundancy in the receptor kinase function is also observed with the CLV2-CORYNE (CRN) complex and the RECEPTOR-LIKE PROTEIN KINASE 2 (RPK2)[68–71], and in the root apical meristem, where CLE40 can bind to both CLV1 and ACR4[72]. Aside from issues of redundancy, LRR-RKs may form hetero- and homo-dimeric protein complexes with leucine-rich repeat (LRR) proteins, associated with additional kinases[68–73], or with coreceptors, such as somatic embryogenesis receptor-like kinases (SERKs), further complicating the identification and study of peptide-receptor pairings[74,75].

While there remain significant technical challenges, SSP signaling modules identified recently have shown a great promise as regulators of root development, controlled in response to nutrient environmental cues. SSP signaling and biology can be applied to various agricultural practices. Improving the basic understanding of these pathways and how they mediate nutrient-responsive changes in the RSA in model organisms such as Arabidopsis and *M. truncatula* may be further translated in crops or other leguminous species. More directly, application of validated synthetic peptides to seeds or plants growing in nutrient-limited environments is proposed as a non-transgenic means to improve plant growth and yield. Current research in the field has identified the key roles of SSPs in N- and P-responsive root development, as well as other SSPs either responsive to other nutrients or influential in nutrient uptake and homeostasis. Large-scale genomic datasets have also introduced a better understanding of the number and variation in the putative SSP families, which could potentially impact the RSA or be

involved in the crosstalk of various nutrient cues. Further research advancement in this area to elucidate the roles of potentially hundreds of nutrient-responsive SSPs is imperative to fully understand the integration of nutrient cues in RSA phenotypes.

Project goals and significance

Despite the importance of understanding how SSP pathways integrate nutrient signals in the modulation of root architecture, there remains a lack of functional characterization of the downstream effects of many of these pathways. Likewise, the roles of these pathways in the regulation of certain complex root architectural traits, such as root gravitropic response, are understudied. In this dissertation, I have characterized a N-responsive SSP pathway involved in the regulation of primary root gravitropic response and, to a lesser extent, lateral root emergence.

Previously, the Takahashi lab has shown that low N induces the expression of members of the CLE family of SSPs, which interact with the CLV1 LRR-RK to inhibit the development of the lateral root primordia during N starvation[14,76] (Figure 1.2). The specific targets of this signaling module, however, remained uncharacterized in this initial study. Furthermore, CLV1 may have additional involvement in the regulation of other root developmental phenotypes due to its localization in the initials of the columella, epidermis, and lateral root cap within the root apical meristem, as observed by other groups[72]. Through transcriptomic analysis of microarray data collected from root tissues of *clv1* mutants and CLE3 overexpressing lines, a putative downstream target of this pathway, *Arabidopsis thaliana* CENTRORADIALIS (ATC) was determined. ATC is a mobile antiflorigen protein known to interact with the bZIP transcription factor FD to alter the

expression of floral development genes[77]. Despite the established role of ATC in flowering, its characteristics as a mobile signaling protein and involvement in transcriptional regulation prompted further study of yet unknown functions of this antiflorigen in roots downstream of the CLE-CLV1 signaling pathway.

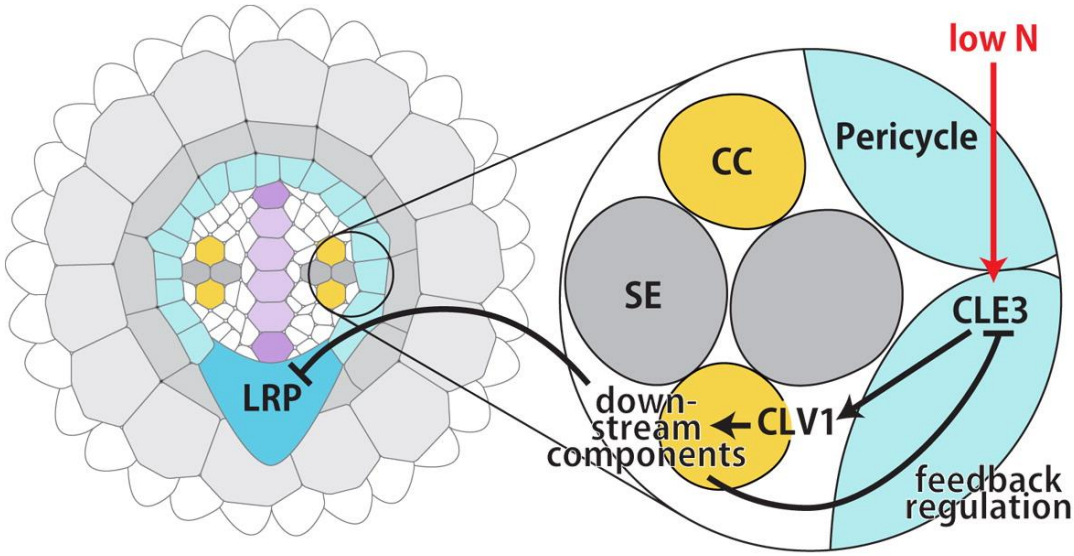

Figure 1.2. CLE-CLV1 signaling module represses lateral root primordia development. CC: Columella cells, SE: sieve elements, LRP: lateral root primordia. From Araya *et al.* (2014) (Ref. 80).

In this dissertation, I present three major findings that are relevant to the N-responsive SSP pathway involving the function of the CLE-CLV1 signaling module and its downstream target ATC in modulating RSA development: (i) the CLE-CLV1-ATC pathway is primarily required for the maintenance of root gravitropic response and has a moderate effect on lateral root emergence under low N availability (Chapter 2); (ii) this signaling module regulates auxin growth hormone transport mechanisms integral for gravitropic root bending (Chapter 3); the unique feature of phospholipid binding capacity of ATC and its interaction with the bZIP transcription factor FD are implicated in the N-

dependent adaptation mechanisms of root growth (Chapter 4). I hypothesize the CLE-CLV1-ATC signaling module functions to regulate root growth based on the way that N is stratified in the soil environment through the promotion of deeper root growth towards N resources and prevention of lateral root outgrowth into N-poor environments in higher soil strata. The research described in this dissertation contributes further to our understanding of how nutrient-responsive SSP pathways can modulate RSA through the regulation of hormone transport and integration of systemic signaling components to efficiently respond to the environment.

CHAPTER 2

Nitrogen-responsive CLE-CLV1 signaling promotes root gravitropic response through the activity of *Arabidopsis thaliana* CENTRORADIALIS

Results from this chapter have been submitted for publication as part of the following manuscript:

Lay-Pruitt, K. S., Araya, T., Abualia, R., Giehl, R. F. H., Benková, E., von Wirén, N. & Takahashi, H. Nitrogen-responsive small peptide signaling modulates root gravitropism.

Abstract

Nitrogen (N) availability significantly impacts the development of plant root system architecture (RSA) as plants must balance foraging and survival strategies. A signaling pathway involving the CLE family of small signaling peptides and the CLV1 leucine-rich repeat receptor kinase has been shown to repress lateral root development when plants are undergoing N starvation. However, CLV1 is not only expressed in the root vasculature but also in the columella initial cells of the primary root tip, suggesting a role for this receptor in the regulation of other root phenotypes in response to N availability. This chapter describes the role of the CLE-CLV1 signaling pathway in root gravitropic response modulated in a N-dependent manner. Analysis of downstream targets of CLE3-CLV1 signaling has revealed *Arabidopsis thaliana* CENTRORADIALIS (ATC), a mobile protein previously characterized as a flowering repressor, as a putative regulator of root growth. Mutation or overexpression of *ATC* results in only moderate changes in lateral root density; however, *ATC* expression has a strong effect on the maintenance of root gravitropic response under minimal nitrate (NO_3^-) treatments. *ATC* promoter activity is present in the phloem companion cells and columella cells. The translational fusion of GFP and ATC protein is also present in the phloem and exhibits nuclear localization in the elongation and transition zones of the root. Upon gravistimulation, GFP-ATC protein further accumulates in the columella cells, suggesting a function of ATC in gravity sensing or auxin hormone transport mechanisms in this region. Together, these results demonstrate a dual role of the CLE-CLV1-ATC signaling pathway in the coupling of lateral root inhibition and enhancement of root gravitropic response to potentially promote root growth towards deeper, N-rich environments within the soil profile.

Introduction

The macronutrient nitrogen (N) is essential for plant growth and survival. N is typically taken up by the plant root system in the inorganic forms of nitrate (NO_3^-) or ammonium (NH_4^+), converted to glutamine, and assimilated into amino acids[78]. Due to their respective charges, these inorganic N forms are distributed throughout the soil heterogeneously. Positively charged NH_4^+ is typically retained in the topsoil since it is unable to migrate through negatively charged soil particles; on the other hand, negatively charged NO_3^-, which is the preferential N source for many plant species, readily moves through the soil profile and expected to be more highly concentrated in deeper soils. Thus, the plant root system must adapt to this differential localization of N sources and develop mechanisms of efficient acquisition by altering growth strategies.

Plant root system architecture (RSA) describes the spatiotemporal arrangement of roots and encompasses such traits as primary root length, lateral root length and density, and the angles at which these roots grow[2]. Proliferation of roots into nutrient-rich areas and repression of root growth into less ideal environments is a critical resource management strategy for plants, and plant response to N serves as a well-characterized example of this phenomenon[3,20,79]. In *Arabidopsis thaliana*, moderate N limitation leads to an increased rate of lateral and primary root elongation, which is proposed to act as a "foraging" mechanism for roots to seek out more N sources[3]. When N resources are severely limited, root growth is significantly restricted as plants prioritize survival[1].

One example of this survival strategy is the strong repression of lateral root emergence under low N availability[3,14]. A molecular mechanism underlying this response has been shown to involve the activity of a N-responsive small signaling peptide (SSP)

pathway. In this signaling module, low N induces the transcription of genes encoding the CLAVATA3/EMBRYO-SURROUNDING REGION (CLE) family of peptides in the root pericycle cells. The mature forms of these peptides diffuse from the pericycle and interact with the CLV1 leucine-rich repeat receptor kinase in the phloem companion cells where it transmits signals to prevent the emergence of late-stage lateral root primordia[14]. While targets of this CLE-CLV1 signaling interaction are also proposed to feedback regulate CLE peptide encoding gene expression, the exact downstream components of this pathway have remained uncharacterized[14,80].

In addition to this role in the regulation of lateral root development, the CLV1 receptor is also involved in plant developmental processes in the shoot and root apical meristems. In the shoot apical meristem, CLV1 interacts with the CLV3 peptide (another member of the CLE peptide family) to repress the expression of the WUSCHEL (WUS) transcription factor to regulate stem cell fate[81]. In a study by Stahl *et al*. (2013), CLV1 was also shown to be expressed in the first tier of columella cells in the root tip, where it coordinately acts with the CLE40-ACR4 peptide-receptor kinase interaction to similarly regulate stem cell fate in the root apical meristem[72]. However, the function of CLV1 or the CLE-CLV1 signaling module in this region has not been fully studied in relation to N-responsive RSA development.

This chapter expands on the role of CLE-CLV1 signaling in the regulation of N-responsive root architecture. In addition to the repression of lateral root development, the CLE-CLV1 interaction maintains root gravitropic response under low NO_3^- availability through promoting the expression of a mobile antiflorigen protein[77], *Arabidopsis thaliana* CENTRORADIALIS (ATC). While *ATC* knockout mutation and overexpression has

moderate effect on lateral root density, it significantly impacts root gravitropic response under low N availability. *ATC* promoter activity is also localized to both the phloem and the columella cells of the root tip region. GFP-ATC translational fusion protein is present in the phloem and exhibits nuclear localization in surrounding pericycle and endodermal cells in the transition and elongation zones. While GFP-ATC is not present in the columella cells of vertically growing seedlings, it accumulates in this region when plants experience a gravity stimulus. The results presented in this chapter characterize ATC as a novel regulator of N-responsive root developmental processes downstream of the CLE-CLV1 signaling pathway.

Methods

Plant growth and culture

Arabidopsis thaliana seeds were surface sterilized with a solution of 5% sodium hypochlorite and 1% Tween 20 for 15 minutes and rinsed 5 times with sterile water. Seeds were sown on 120x120 mm square petri plates containing MGRL media[82] for which the amount of NO_3^- as the sole N source was adjusted to the indicated concentrations. These plates were then stratified in the dark for two days at 4°C. Seedlings were germinated and grown in Percival growth chambers for 5 or 10 days under a 16-hour day/8-hour night light cycle with a daytime light intensity of 45 µmol of photons $s^{-1}m^{-2}$. The growth chambers were set to a temperature of 22 ° C. The mutant lines used in study are *clv1-1*[83], *clv1-15*[14] (ET13689)[84], *atc-2* (isolated from SALK_021699C)[85], and *atc-4* (isolated from CS926917)[85]. *CLV1::CLV1-GFP* and *CLE3*-overexpressing lines *CLE3ox-12* and *CLE3ox-17* are described previously[14].

Root phenotyping

Root images were taken using an Epson Perfection V700 Photo Scanner. For primary root gravitropism assays and root growth rate measurements, five-day-old seedlings were turned 90 degrees for two hours and were scanned at 30-minute intervals. Root tip reorientation was defined as a difference between root angle at the zero time point and the angle after two hours of gravistimulation. Root length rates were calculated by tracing the primary root at the zero time point compared to the primary root length at the two hour time point and calculating the rate of growth per minute for each genotype and condition combination. For lateral root density measurements, seedlings were grown for 10 days on MGRL media supplemented with the indicated concentration of NO_3^-. Lateral root density was defined as the number of lateral roots per length of primary root in millimeters. Root angles, lengths, and lateral root densities were measured using ImageJ (Fiji)[86] and graphed as raincloud plots using *raincloudplots* R package[87].

Microarray analysis

Seedlings were grown for 10 days on MGRL media supplemented with 0.1 mM NO_3^-. RNA was isolated from whole root tissues in triplicate for L*er*, Col-0, and *clv1-15* lines and in duplicate for *CLE3ox-12* and *CLE3ox-17*. Hybridization of the ATH-1 array (Affymetrix) was performed according to the manufacturer's protocol. Expression values were normalized by Microarray Suite version 5.0 (MAS 5.0) and Present/Marginal/Absent calls were determined using the *affy* R package[46]. Significance testing was conducted using the *limma* R package[47], which performed a moderated *t*-test for each probe per contrast (*clv1-15* vs. L*er*, *CLE3ox-17* vs. Col-0, and *CLE3ox-12* vs. Col-0). The resulting

p-values were adjusted for multiple tests using the Benjamini-Hochberg method[48]. Differentially expressed genes (DEGs) in the *clv1-15* vs. L*er* and the *CLE3ox-17* vs. Col-0 contrasts were determined by using both an adjusted *p*-value cutoff of 0.05 and a fold change cutoff of 2. For the *CLE3ox* lines, these cutoff thresholds for differential expression were only applied to the *CLE3ox-17* vs. Col-0 contrast to take into account the greater levels of *CLE3* expression in *CLE3ox-17* compared to *CLE3ox-12*[17]. DEGs were further filtered by their directionality of expression prior to hierarchical clustering: either induced in *clv1-15* and repressed in *CLE3ox* lines, or vice versa, to reflect expression patterns predicted for downstream targets of CLE-CLV1 signaling. Multiple Experiment Viewer (MeV) 4.9.0 was used to generate a heat map for visualization of expression patterns. Filtered DEGs were clustered using the hierarchical clustering function in MeV with the Pearson correlation distance metric and average linkage clustering method. The Gene Expression Omnibus (GEO) accession number for this microarray dataset is GSE169744.

Quantitative real-time polymerase chain reaction

Total RNA was isolated from flash-frozen whole root tissue using the E.Z.N.A. Plant RNA extraction kit (Omega Bio-tek) according to manufacturer's protocols. Samples were standardized to 500 ng of total RNA and treated with DNase using the Turbo DNA-free Kit (Invitrogen). First strand cDNA was synthesized with oligo-dT primers and Superscript III Reverse Transcriptase (Invitrogen). Quantitative real-time PCR was performed with SYBR Green Master Mix (Life Technologies) and run on the QuantStudio5

platform (Applied Biosystems). *ACTIN 2* (AT3G18780) and *EF-1α* (AT1G18070) were used as housekeeping genes. Primer sequences are listed in Appendix Table A.1.

Generation of transgenic plant lines

The *ATC* overexpressing construct (*ATCox*) was generated by cloning the coding sequence of *ATC* amplified from genomic DNA of *A. thaliana* Col-0 accession downstream of the CaMV 35S constitutive promoter in the pH35GS binary vector[88].

The transgenic reporter lines were made by using the binary vector pBI101-Hm[89], which has a replacement of the kanamycin resistance gene in pBI101 (Clontech) with the hygromycin resistance gene for plant selection. The ATC promoter-GFP (*ATC::GFP*) fusion was made as follows. The 2047-bp 5'-flanking region of *ATC* was amplified by PCR using primers NheI-ATC-F-2047-2 and NcoI-ATC-R-2. The coding sequence of GFP[90] was amplified by PCR using primers NcoI-GFP-F-3 and SacI-GFP-R-3. These PCR-amplified DNA fragments were cloned into pCR-Blunt vector (Invitrogen) and fully sequenced. After this subcloning step, the plasmids were digested using restriction enzymes to obtain the *ATC* promoter region as the NheI- and NcoI-ended fragment, and the GFP coding sequence as the NcoI- and SacI-ended fragment, respectively. These two fragments were cloned into the pBI101-Hm vector by replacing the GUS coding sequence between the XbaI and SacI sites to obtain the *ATC::GFP* fusion construct.

The *ATC::GFP-NLS* and *ATC::GFP-ATC* translational fusion constructs were made by InFusion cloning (Clontech). Primers for the InFusion cloning were designed to remove the stop codon of GFP and to direct homologous recombination to create the GFP-NLS and GFP-ATC in-frame translational fusions. For the *ATC::GFP-NLS* construct,

the NLS region was PCR amplified from pBGYN[88] using SacI-NLS-F and SacI-NLS-R primers. For the *ATC::GFP-ATC* construct, the *ATC* coding sequence was PCR amplified using SacI-ATC-F and SacI-ATC-R. These PCR-amplified fragments were used for the InFusion cloning into the SacI-digested *ATC::GFP*. The resultant binary plasmids were sequenced to confirm the successful removal of a stop codon and the recombination event, and introduced into *Agrobacterium tumefaciens* GV3101 (pMP90)[91] by freeze-thaw transformation[92]. *Arabidopsis thaliana* Col-0 accession was transformed with *ATC::GFP* and *ATC::GFP-NLS*, while *atc-2* plants were transformed with *ATC::GFP-ATC* by following a standard floral-dip method[93]. Hygromycin-resistant transformants were selected and propagated to obtain T3 homozygous transgenic segregants. Primer sequences are listed in Appendix Table A.1.

Microscopy

Olympus FV10i and Zeiss LSM 780 confocal laser-scanning microscopes were used for imaging of *CLV1::CLV1-GFP*, *ATC::GFP*, *ATC::GFP-NLS*, and *ATC::GFP-ATC*. GFP was visualized using a 473-nm (FV10i) or a 488-nm (LSM780) laser for excitation and capturing emission at a wavelength range of 490-540 nm (FV10i) or 490-560 nm (LSM780), respectively. Counterstaining of the cell walls within the root was performed by dipping roots in 1 µg/ml propidium iodide (PI) for 5 minutes. PI staining was visualized using a 559-nm (FV10i) or 561-nm (LSM780) laser for excitation and capturing emission at 570-670 nm (FV10i) or 580-700 nm (LSM780), respectively. Tile scans and Z-stacks were obtained using the ZEN Black (Zen 2.3 SP1 FP1) while orthogonal views of Z-stacks were prepared with ZEN 2.6 (blue edition) software. Nuclear staining was performed by

fixing roots in 4% formaldehyde in phosphate buffered saline (PBS) for 3 minutes, washing with PBS, and incubating in 1 ug/ml 4',6-diamidino-2-phenylindole (DAPI) for 5 minutes. DAPI-stained nuclei were visualized a 405-nm laser and capturing emission at 420-460 nm on the Olympus FV10i confocal laser-scanning microscope.

Results

CLV1 signaling is involved in maintenance of root gravitropism

The CLV1 receptor kinase has been independently reported to be present in multiple cell types of the primary root tissues at distant locations[14,72]. I examined the expression of *CLV1::CLV1-GFP* translational fusion expressed in the *clv1-4* mutant line[14] to validate the dual localization of the CLV1 receptor in these locations within the same experimental root system. Consistent with previous observations, CLV1-GFP localization was found in the phloem companion cells (Figure 2.1a) where it binds CLE peptides secreted from the surrounding pericycle cells in the vasculature to inhibit the development of lateral root primordia under severely limited N supply[14]. In the root tip, CLV1-GFP was expressed in the first tier of columella cells (columella initials) below the quiescent center as well as in epidermis initials and lateral root cap initials (Figure 2.1b) where it maintains the activity of the root meristem[72]. These distinct patterns of CLV1 localization suggest a systematic coordination of CLE peptide hormone signaling for lateral root development and processes governing stem cell maintenance at the root tip.

The second and third tiers of columella cells act as the major gravity-sensing centers within the root tip[94]. To determine whether CLV1 expressed in the columella initials influences root gravitropism, the angles of root tip reorientation were analyzed in

clv1 mutant seedlings over a two-hour time course (Appendix Figure A.1a). The *clv1-15* mutant[14], which carries a *Ds* transposon insertion in the coding region of the kinase domain of *CLV1* (Figure 2.1c), clearly showed defects in gravitropic responses upon two hours of gravistimulation compared to the Landsberg *erecta* (L*er*) wild-type under low NO_3^- conditions (Figure 2.1d). Root gravitropic response of the *clv1-1* mutant line, which contains a point mutation in the kinase domain, was also weaker under lower NO_3^- availability, although these effects were not statistically significant (Appendix Figure A.1b). Conversely, the *CLE3* overexpressing lines (*CLE3ox*) in the Columbia-0 (Col-0) background[14] showed stronger root gravitropism than the wild-type with increasing NO_3^- supplementation (Figure 2.1e, Appendix Figure A.2a). The root growth rates over the two-hour interval of gravistimulation were not significantly different among genotypes and conditions tested (Appendix Figure A1.c, Appendix Figure A.2b). These results provided evidence that the loss of CLV1-dependent signaling in *clv1-15* substantially reduces the ability of roots to respond to a gravistimulus under NO_3^--limited conditions, whereas the constitutive overexpression of *CLE3* in the *CLE3ox* lines contributes to maintaining the root gravitropic response even under NO_3^--replete conditions. Together, these data show CLE3-CLV1 signaling modulates root gravitropism in response to NO_3^- availability.

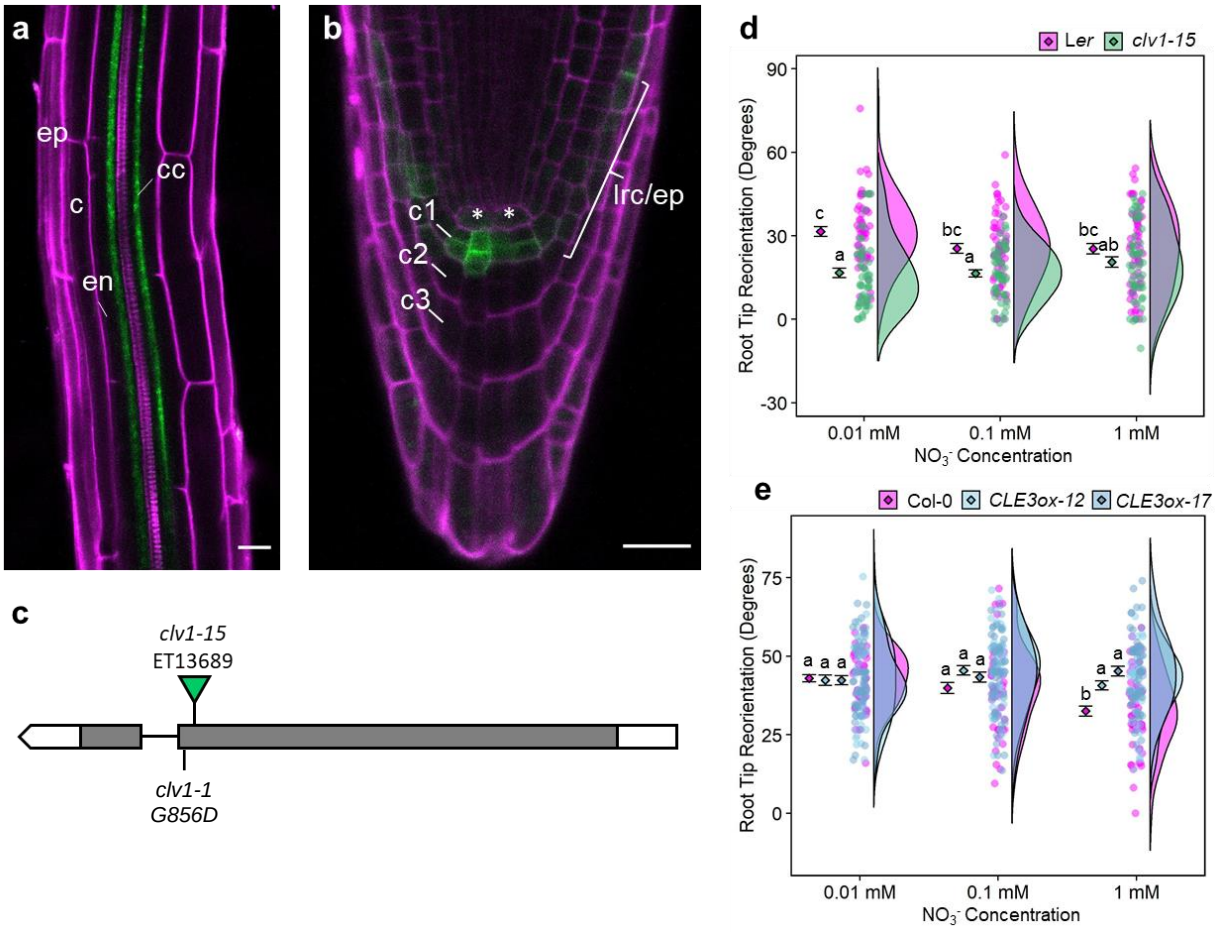

Figure 2.1. CLV1 signaling is involved in the maintenance of root gravitropism. a-b) *CLV1::CLV1-GFP* localization in the primary root. CLV-GFP signal is present in the phloem (a) as well as the first tier of columella cells and epidermal and lateral root cap initials in the root tip (b). The PI counter staining is shown in magenta. Root tissue layers are labeled as ep: epidermis, c: cortex, en: endodermis, cc: companion cells, lrc/ep: lateral root cap and epidermal initials. Columella tiers are numbered and the quiescent center is indicated with asterisks. Scale bar = 20 µm. c) Gene model of *CLV1* (AT1G75820) with location of the *clv1-1* (Gly 856 to Asp) and *clv1-15* (ET13689) mutations. Green triangle indicates *Ds* insertion. d-e) Root gravitropism of 5-day-old *clv1-15* mutants compared to L*er* (n=53-59) (d) and *CLE3* overexpressing lines compared to Col-0 (n=54-59) (e) on media supplemented with increasing NO_3^- concentrations. Mean-and-error plots are shown alongside raincloud plots indicating individual data points and distributions by genotype. Significant differences between genotype and condition combinations were determined using Tukey's test (p<0.05) following a two-way ANOVA and are indicated by lowercase letters.

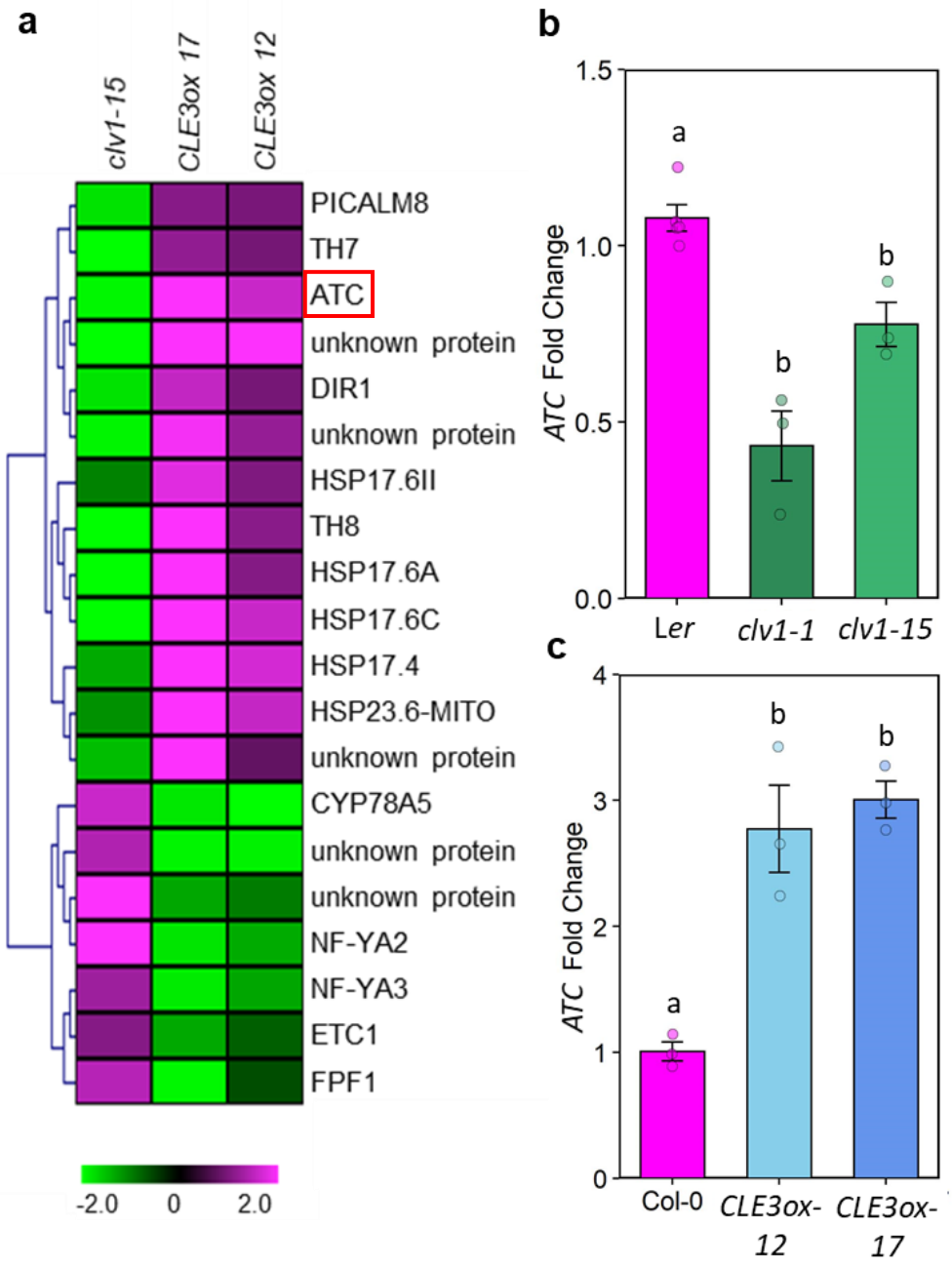

Figure 2.2 ATC is a downstream target of CLE3-CLV1 signaling. a) Heat map of differentially expressed genes (adj. *p*-value<0.05) in *clv1-15* compared to L*er* and *CLE3* overexpressing lines compared to Col-0. Colors represent $\log_2$ fold changes in expression compared to the wild-type. Red box indicates AT2G27550 (ATC). b-c) *ATC* transcript expression in *clv1* mutants (b) and *CLE3ox* lines (c). For each condition, n=3 biological replicates. Significant differences between genotype and condition combinations were determined using Tukey's test (p<0.05) following a one-way ANOVA and are indicated by lowercase letters.

ATC controls root gravitropic response under low NO_3^- availability

To identify targets of CLE3-CLV1-dependent signaling in root gravitropism, whole root transcriptome profiles of *clv1-15* mutants and *CLE3*ox lines were analyzed. Differentially expressed genes in these lines compared to their respective wild-type accessions were further selected if their expression patterns were consistent with downstream targets of CLE-CLV1 signaling: either induced in *clv1-15* and repressed in *CLE3ox* or the inverse pattern. Twenty candidate genes were obtained after this filtering procedure (Figure 2.2a, Appendix Table A.2). Within the subset of genes repressed in the *clv1-15* mutant and induced in the *CLE3ox* lines, *Arabidopsis thaliana CENTRORADIALIS* (ATC, AT2G27550) was among the most differentially expressed (Fig. 2.2a, Appendix Table A.2). ATC is a homolog of the major florigen FLOWERING LOCUS T (FT)[95], but has been shown to suppress flowering under short-day conditions[77].

To investigate the role of ATC in root gravitropism, *atc-2* and *atc-4* mutants, which contain T-DNA insertions in the gene body of *ATC*, were obtained (Figure 2.3a). Both *atc* knockout mutant alleles had substantially weaker gravity responses than Col-0 at 0.01 mM NO_3^- without significant differences in their root growth rates (Figure 2.3b, Appendix Figure A.3). Additionally, there was an increase in *ATC* expression in Col-0 roots as NO_3^- concentration in the growth media decreased (Figure 2.3c), supporting the observed weakening of the gravitropic response in the *atc* mutants (Figure 2.3b, Appendix Figure A3). Transformation of the *atc-2* mutant line with a translational fusion construct *ATC::GFP-ATC* (Appendix Figure A.4c) restored the weakened gravitropic response phenotype under the 0.01 mM NO_3^- treatment (Figure 2.3d). These observations provided

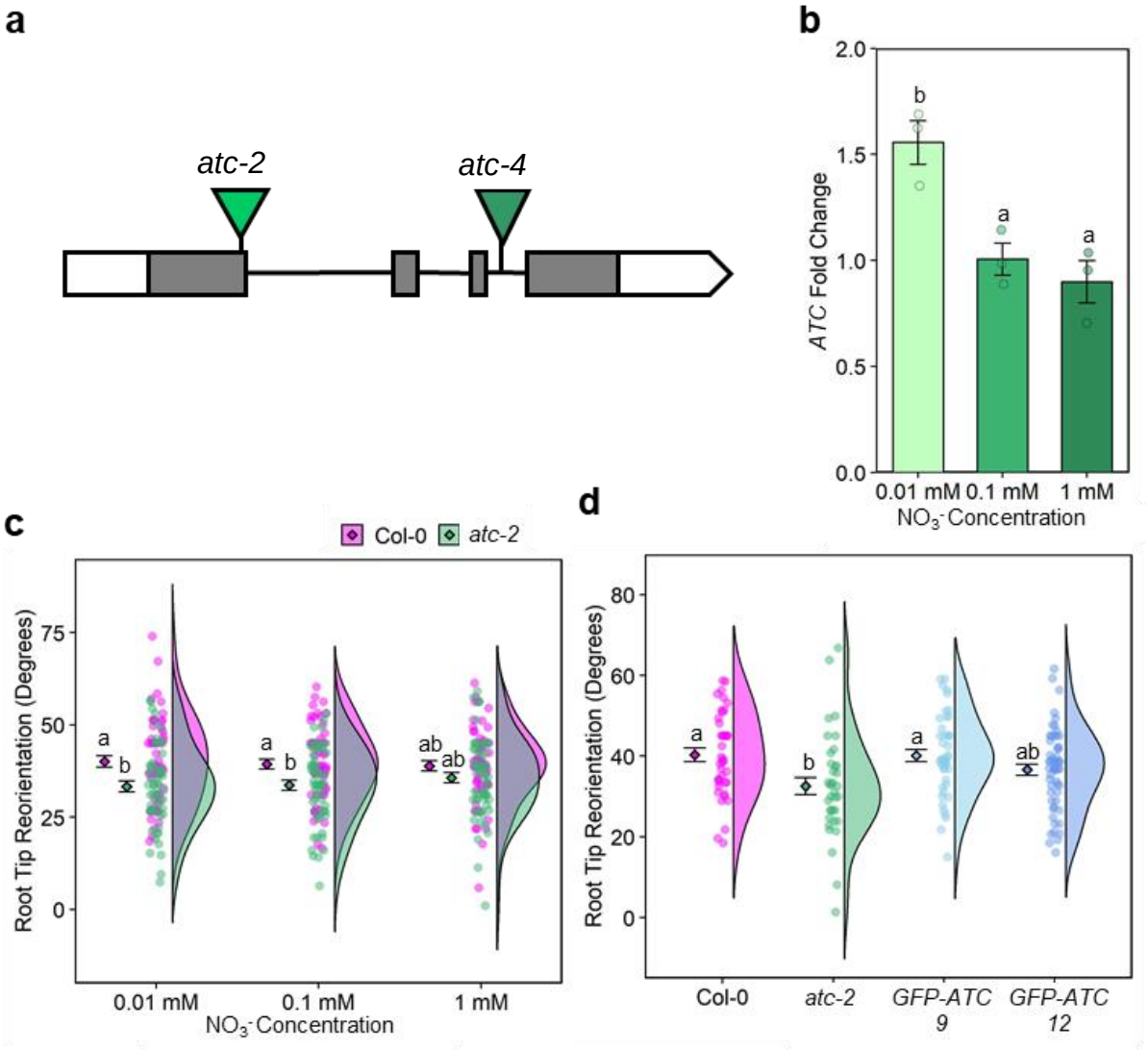

Figure 2.3. ATC regulates root gravitropism under low NO_3^- availability a) Gene model of *ATC* (AT2G27550) with the location of *atc-2* (SALK_021699C) and *atc-4* (CS926917). Green triangles denote T-DNA insertions. b) Transcript expression of *ATC* under increasing NO_3^- supplementation. For each condition, n=3 biological replicates. c) Root gravitropism of *atc* mutants under increasing NO_3^- concentrations (n=56-59). Mean-and-error plots are shown alongside raincloud plots indicating individual data points and distributions by genotype. d) Restoration of gravitropic response in *atc-2* mutants expressing *ATC::GFP-ATC*. Mean-and-error plots are shown alongside raincloud plots indicating individual data points with distributions by genotype. Significant differences between genotype and condition combinations were determined using Tukey's test (p<0.05) following a two-way (Fig 2.3c) or one-way (Fig 2.3a, d) ANOVA and are indicated by lowercase letters.

evidence that ATC positively regulates primary root gravitropism under N-limited conditions.

ATC has a moderate impact on lateral root phenotypes

As the CLE-CLV1 signaling pathway has been previously characterized as a regulator of N-responsive lateral root development, the effect of ATC expression on lateral root density was examined on a spectrum of NO_3^- concentrations. The *atc-2* mutant had significantly higher lateral root density under the 0.01 mM NO_3^- condition, but not at higher concentrations (Figure 2.4a, c). Conversely, the *ATC* overexpression line (*ATCox*) showed a phenotype of reduced lateral root density at 1 mM NO_3^- (Figure 2.4b-c), indicating that ATC does influence lateral root emergence in an N-dependent manner. However, mutants in *clv1* and *CLE3* overexpressing lines do show much stronger lateral root emergence phenotypes consistent across NO_3^- availabilities[14], suggesting that other potential downstream components (Figure 2.2a, Appendix Table A.2) may have a stronger or additive effect on this phenotype compared to ATC. Still, these findings provide evidence for the coordination of two RSA phenotypes in response to N-availability that could drive root growth to N resources and prevent root outgrowth into less advantageous environments.

I also performed a qualitative assessment of lateral root gravitropic set point angle (GSA) between wild-type and *ATC* knockout mutant and *ATCox* lines (Figure 2.4d). Despite an effect on primary root gravitropic response, mutation in *ATC* did not seem to affect the GSA of lateral roots when compared to the wild-type. However, the lateral root GSA of the *ATCox* line was significantly reduced compared to Col-0 (Figure 2.4d),

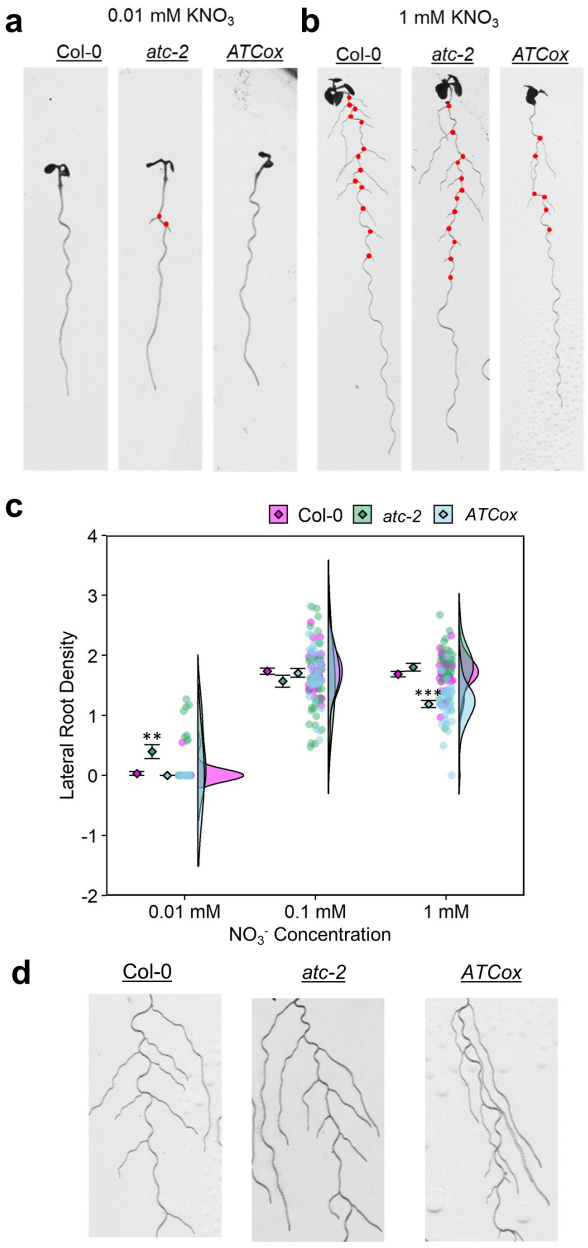

Figure 2.4. Lateral root phenotypes of *ATC* mutants and overexpressing lines. a-b) Representative images of 10-day-old seedlings grown on 0.01 mM NO_3^- media (a) and 1 mM NO_3^- media (c). Red dots indicate locations of lateral roots along the primary root. c) Lateral root density measurements across NO_3^- concentrations. Mean-and-error plots are displayed alongside individual data points and distributions for each genotype. Asterisks indicate significant results from Student's *t*-test performed between mutant and overexpressing lines compared to Col-0 within each NO_3^- condition (**p<0.01, ***p<0.001). d) Representative images of lateral root gravitropic set point angle in wild-type, *atc-2,* and *ATCox* lines.

indicating a stronger response to gravity. Strengthening of GSA has been shown to drive deeper root growth in soil[96], which could enable plants to acquire nitrate resources more deeply stratified in the soil profile.

Localization of *ATC* promoter activity and protein expression

Previous findings for the function of ATC show that this protein acts in a non-cell autonomous manner to regulate flowering time[77]. In these studies, *ATC::GUS* activity was detected in the phloem of petioles, hypocotyls, and roots[77]; transcriptomic analysis of publicly available datasets on the Arabidopsis eFP browser also show strongest expression of ATC in the vasculature of root tissues, despite its role in floral initiation in the shoot[97,98]. Thus, a series of ATC reporter lines (Appendix Figure A.4) were generated to determine *ATC* promoter activity and protein localization in the root in order to understand how these patterns of expression could contribute to processes regulating root development.

To determine the tissue localization of *ATC* gene expression, I generated transgenic lines expressing GFP driven by the *ATC* promoter (*ATC::GFP*) (Appendix Figure A.4a). *ATC* promoter activity was found in the root phloem tissues (Figure 2.5a-b) similar to the localization domain of CLV1 (Figure 2.1a; ref. 72). However, due to its small size, GFP expressed in the phloem was diffused throughout the root tip, which was uninformative for understanding how the expression of ATC could contribute to root gravitropic response (Figure 2.5a, c).

I then generated lines expressing the translational fusion of GFP and a nuclear localization signal under control of the *ATC* promoter (*ATC::GFP-NLS*) (Appendix Figure

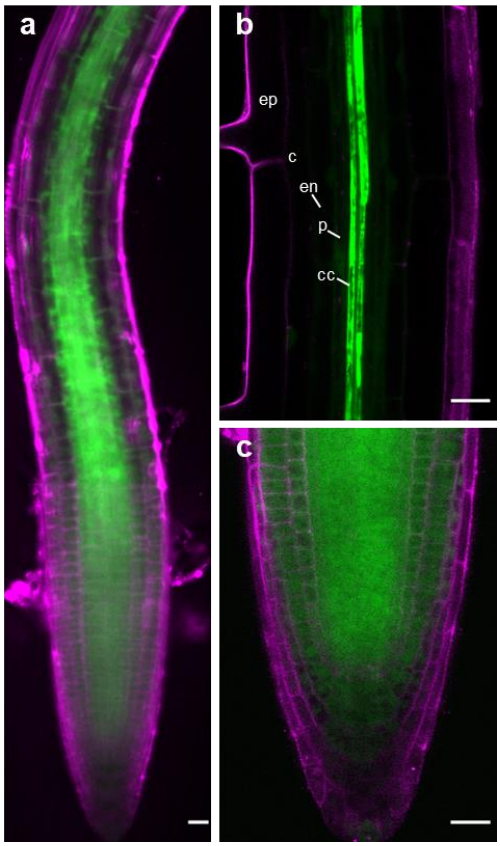

Figure 2.5. *ATC::GFP* localization in the root. a-c) Localization of *ATC::GFP* in the primary root from root tip to elongation zone (a), root hair zone (b) and root tip (c). Root tissue layers are labeled as ep: epidermis, c: cortex, en: endodermis, p: pericycle, cc: companion cells, and x: xylem. Scale bars = 20 μm

A.4b) to restrict expression of GFP in cell types where the *ATC* promoter is active. In these transgenic lines, the nuclear-localized GFP (GFP-NLS) was expressed in the vasculature and the root tip (Figure 2.6a). GFP-NLS was also predominantly expressed in the phloem companion cells above the meristematic zone and further up in the root hair zone (Figure 2.6b, c, e, f), while weaker fluorescence was detected in pericycle cells of the transition zone (Figure 2d, g). These patterns of expression indicate a potential role of ATC in the phloem and root tip coordinating root gravitropism in addition to its canonical role in flowering regulation[77].

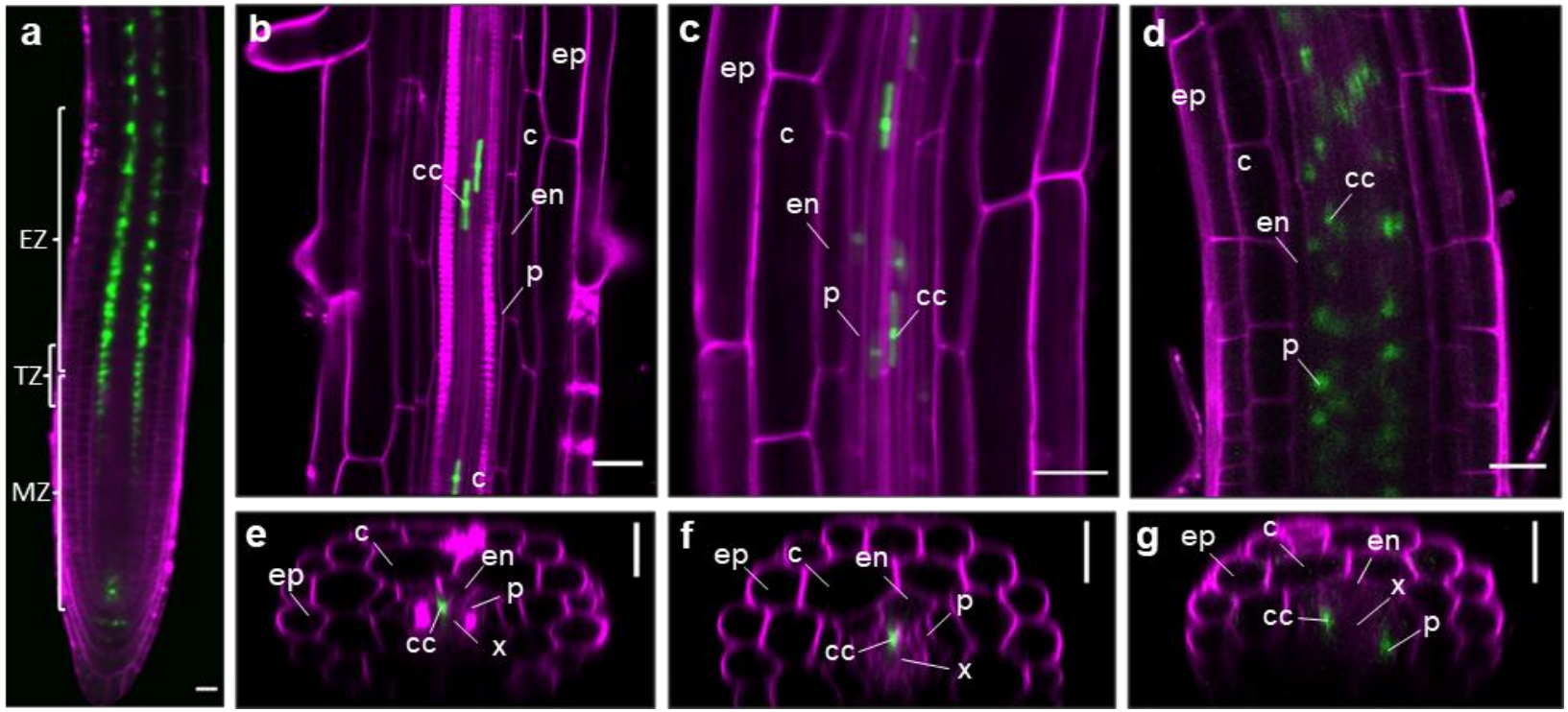

Figure 2.6. *ATC* promoter activity is localized to the phloem companion cells and columella cells. a-d) Localization of *ATC::GFP-NLS* in the root tip to elongation zone (a), root hair zone (b), elongation zone (c), and transition zone (d). e-g) Localization of *ATC::GFP-NLS* in root cross section slices of the root hair zone (e), elongation zone (f), and transition zone (g). The PI counter staining is shown in magenta. Root growth zones are labeled as EZ: elongation zone, TZ: transition zone, and MZ: meristematic zone. Root tissue layers are labeled as ep: epidermis, c: cortex, en: endodermis, p: pericycle, cc: companion cells, and x: xylem. Scale bar = 20 μm

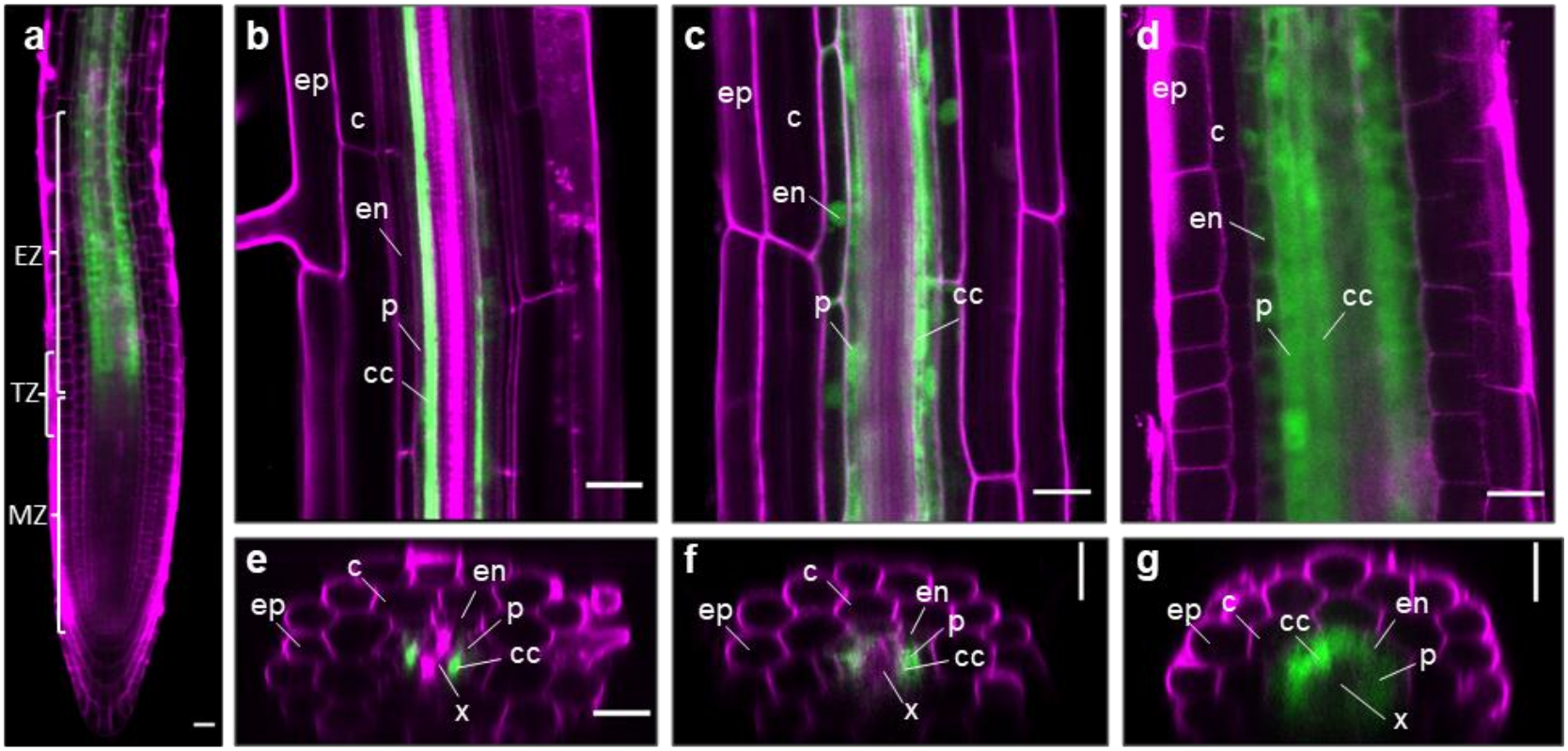

Figure 2.7. ATC protein is localized to the phloem companion cells and surrounding tissues below the elongation zone. a-d) Localization of *ATC::GFP-ATC* in the root tip to elongation zone (a), root hair zone (b), elongation zone (c), and transition zone (d). e-g) Localization of *ATC::GFP-NLS* in root cross section slices of the root hair zone (e), elongation zone (f), and transition zone (g). The PI counter staining is shown in magenta. Root growth zones are labeled as EZ: elongation zone, TZ: transition zone, and MZ: meristematic zone. Root tissue layers are labeled as ep: epidermis, c: cortex, en: endodermis, p: pericycle, cc: companion cells, and x: xylem. Scale bar = 20 μm

To further investigate the protein function of ATC in root gravitropism, I next expressed a translational fusion of GFP and ATC under control of the *ATC* promoter (*ATC::GFP-ATC*) (Appendix Figure A.4c) in the *atc-2* mutant background. Restored root gravitropism of these transgenic lines indicated that expression of GFP-ATC fusion protein complemented the loss of ATC function in *atc-2* (Figure 2.3d). Like GFP-NLS, GFP-ATC localized to the phloem companion cells in regions of the primary root above the meristematic zone and in the root hair zone (Figure 2.7). GFP-ATC also exhibited cytosolic localization and punctate patterns consistent with nuclear localization in the pericycle and endodermal cells of the transition zone above the primary root meristem (Figure 2.7c, d).

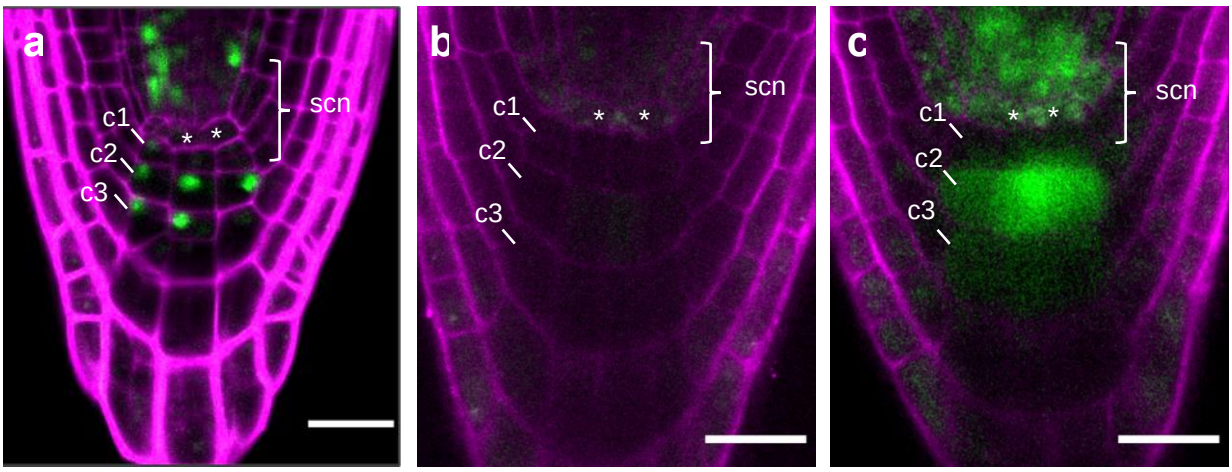

Figure 2.8. *ATC* promoter activity and protein localization in the columella cells. a) Localization of ATC::GFP-NLS in the columella cells and stem cell niche (SCN) of vertically growing seedlings. B) SCN and columella cell region in root tips of vertically growing seedlings expressing *ATC::GFP-ATC*. C) Localization of *ATC::GFP-ATC* in the columella cells and SCN after 90-degree gravistimulation for 30 minutes. PI counter staining is shown in magenta. Columella tiers are numbered and the quiescent center is indicated with asterisks. Seedlings used for imaging were grown 5 days on MGRL media supplemented with 0.01 mM NO_3^-. Scale bar = 20 μm

The expression of these GFP translational fusions was also detected in the columella cells of the root tip. GFP-NLS was expressed in the three tiers of columella cell files below the quiescent center, consistent with the location of gravity sensing in the root tip (Figure 2.8a). The expression of GFP-ATC protein was not immediately apparent in the primary root tip of vertically growing seedlings (Figure 2.8b). However, GFP-ATC accumulated in the stem cell niche and the second and third tier of columella cells after gravistimulation, which imply its action in maintaining root gravitropism (Fig. 2.8c).

ATC exhibits nuclear localization in the primary root

Huang *et al.* (2012) showed preliminary evidence of ATC protein localization in the nucleus. In this study, the interaction of FD and ATC in the nucleus was first demonstrated through bimolecular fluorescence complementation in *Nicotiana benthamiana* leaf cells. They also showed transient expression of a translational fusion of RFP and ATC (RFP-ATC) localized to the cytoplasm and nucleus in *N. benthamiana* leaves; however, upon co-infiltration with the translational fusion of GFP and FD (GFP-FD), RFP-ATC expression was restricted to the nucleus and co-localized with GFP-FD. Thus, it was hypothesized that the ATC-FD interaction stabilizes ATC localization to the nucleus where this complex regulates transcription of floral development genes[77].

Nuclear localization of ATC protein in the root could also implicate this protein or the ATC-FD protein complex in the transcriptional regulation of genes to maintain gravitropic response in these regions. In the transition and elongation zones of *ATC::GFP-ATC* roots, GFP-ATC appears to exhibit nuclear localization in the cell layers surrounding the phloem (Figure 2.7 c, d). This nuclear localization was confirmed by DAPI

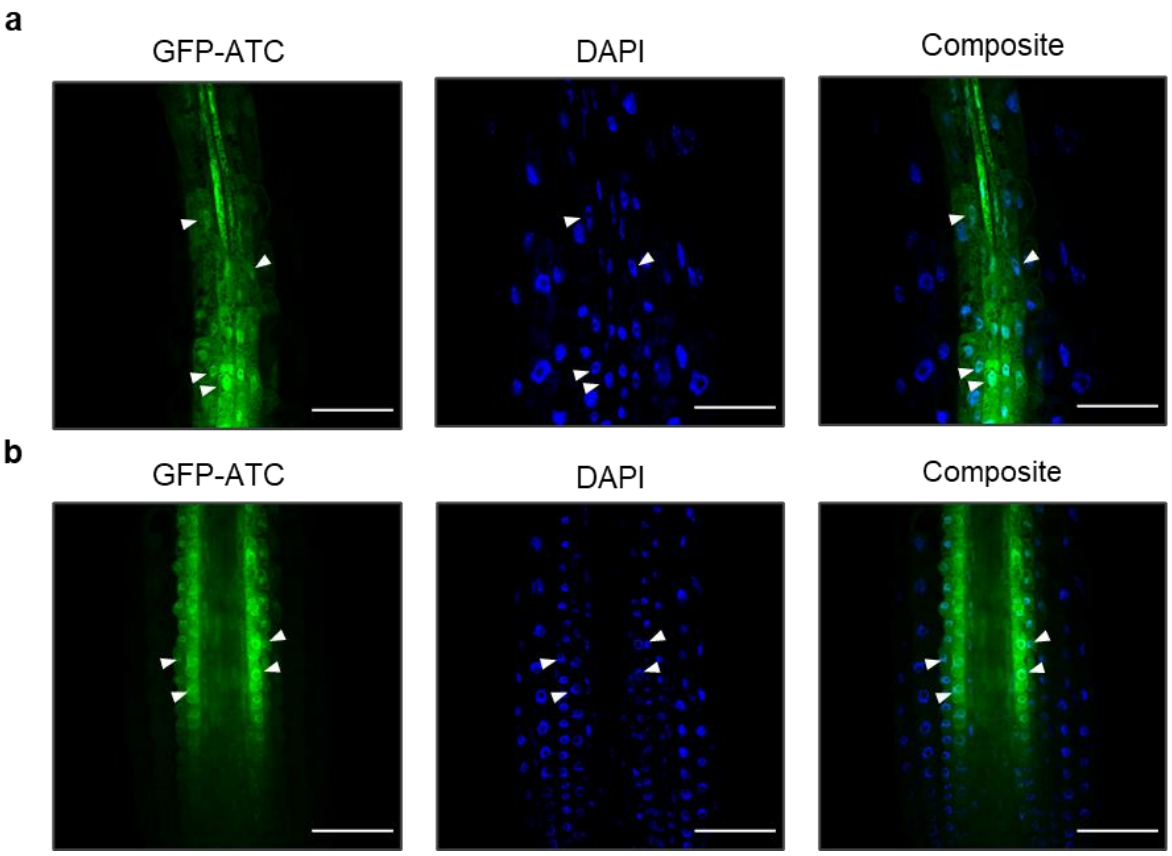

Figure 2.9. Nuclear localization of GFP-ATC in the primary root. a-b) Localization of *ATC::GFP-ATC* expression in the transition zone (a) and meristematic zone (b) in 5-day-old seedlings grown on 0.01 mM NO_3^- media. Panels from left to right indicate GFP-ATC expression, DAPI-stained nuclei, and co-localization of GFP-ATC and DAPI signals. White arrows indicate examples of co-localized nuclear signals. Scale bar = 50 μm

staining of *ATC::GFP-ATC* lines (Figure 2.9); GFP-ATC in these regions exhibits both cytosolic and nuclear localization in the pericycle and endodermal cells of these regions. Furthermore, weak GFP-ATC signals in the columella cells of gravistimulated seedlings were observed to exhibit punctate patterns which may possibly indicate nuclear localization within this region (Figure 2.10). Nuclear signals in these regions, however,

could not be confirmed via DAPI staining due to the stringency of the fixation process on the root tip and the transient nature of GFP-ATC expression in gravistimulated seedlings.

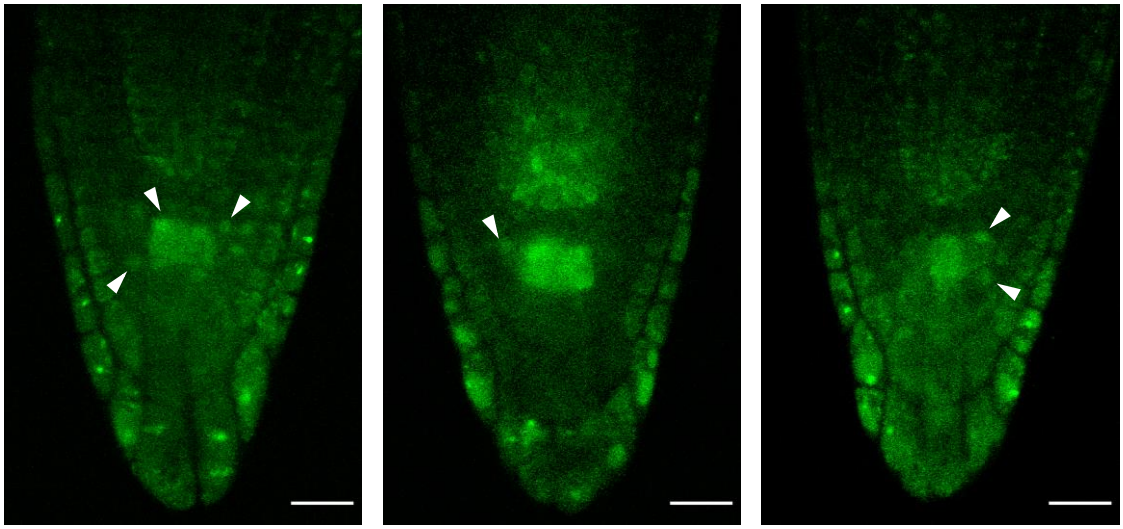

Figure 2.10. Potential nuclear localization of GFP-ATC in the columella cells of gravistimulated roots. White arrows highlight punctate signals of GFP-ATC. Scale bars: 20 μm.

Discussion

The results shown in this chapter provide evidence that the CLE-CLV1-ATC pathway serves as an integral regulator of N-responsive RSA. This signaling module acts to maintain root gravitropic response under low NO_3^- availability (Figure 2.3c, Appendix Figure A.1a-b) while moderately repressing lateral root development (Figure 2.4c). These alterations to root growth strategies specifically under limited N availability may be related to the way in which NO_3^- resources are available in the environment. In order to obtain NO_3^- in deeper soil layers, root gravitropism may become stronger when the plant experiences N starvation, coupled with repression of lateral root growth into N-poor regions in the upper soil layers. The results of experiments presented here also focus on

the effect of NO_3^- as the main nitrogen resource. Additional transcriptomic evidence has shown that CLE3 is not only induced by N-starvation, but also even further induced by NH_4^+ re-supplementation after starvation[28]. This could have further relevance for the environmental context of the proposed model as NH_4^+ is positively charged and retained in higher soils. While *Arabidopsis* can utilize NH_4^+ as a N resource, it does not do so preferentially because accumulation of NH_4^+ is toxic[99]. Further promotion of CLE-CLV1-ATC signaling by NH_4^+ derived signals could suppress lateral root elongation in NH_4^+-rich layers while promoting gravitropic response towards deeper NO_3^--enriched soils via the activity of ATC. While the phenotypes governed by the CLE-CLV1-ATC pathway lend support to this hypothesis, further experiments examining root systems in soil environments are necessary as stronger root gravitropic response has been shown to have contrary effects on the steepness of root architecture[96,100].

The localization of ATC expression in the columella cells and its protein accumulation in response to gravity stimulus (Figure 2.8) strongly suggests a role of this signaling protein in the regulation of root gravitropic response. However, the connection between ATC expression in mature regions of the root and the observed repression of lateral root emergence is less clear. Lateral roots first develop from the pericycle cells of the primary root; these initial cells undergo a series of anticlinal and periclinal cell divisions to create the lateral root primordia, which eventually emerges after the disruption of the overlaying cortical and epidermal cell layers[101]. Due to the age and nutritional status of the plants examined in this study, very few if any lateral root primordia were present and thus a connection between ATC expression and the development of the lateral root was not observed as clearly as the gravitropic root bending. ATC expressed in the phloem

companion cells of the root hair zone may once again act upstream of regulators that may have a more significant effect on this phenotype. Likewise, other targets of CLE-CLV1 signaling identified through microarray analysis (Figure 2.2a, Appendix Table A.2) could additionally or independently elicit a more significant impact on lateral root repression than ATC.

While the CLE-CLV1-ATC pathway is involved in the regulation of root gravitropic response, direct mechanisms of control needed to be explored further. Although ATC exhibited expression in the root phloem, studies to date focus on the function of this protein in flowering regulation due to its homology to the FT florigen[77,95]. The known interaction of ATC with the FD transcription factor could impact the transcription of genes involved in root development, which is partially supported by the potential nuclear localization observed for the ATC protein in the cells in the transition zone of the primary root. Given the localization of ATC expression in the root tip columella cells, one may hypothesize the role of ATC in the regulation of auxin transport processes underlying root gravitropism. Localization of ATC within these cell types mirrors the localization of key transporters of the growth hormone auxin, which has been implicated in a variety of N-responsive root architectural changes[22,23,79,102]. In the next chapter, I describe the connection between ATC and auxin transport mechanisms involved in auxin distribution in the root tip and regulation of root gravitropism.

CHAPTER 3

Arabidopsis thaliana CENTRORADIALIS alters auxin transport mechanisms via PIN3 auxin efflux transporter activity

Results from this chapter have been submitted for publication as part of the following manuscript:

Lay-Pruitt, K. S., Araya, T., Abualia, R., Giehl, R. F. H., Benková, E., von Wirén, N. & Takahashi, H. Nitrogen-responsive small peptide signaling modulates root gravitropism.

Abstract

The plant root system changes growth strategies depending on available nutrient resources in the surrounding environment. One potential way that plants may acquire nutrients and water from the environment is through the strengthening of root gravitropism, which enables stronger anchoring and deeper growth within the soil. Root gravitropic response involves changes in auxin flow within root tissues coordinated in part by the PIN family of auxin efflux transporters. This chapter describes how the N-responsive CLE-CLV1-ATC pathway is involved in the modulation of root gravitropic response by altering these patterns of auxin distribution in the root tip. Mutation in *ATC* does not appear to impact gravity sensing mechanisms such as level of starch statoliths or auxin concentration in the primary root tip; however, asymmetric auxin transport during gravistimulation is inhibited in the *atc-2* mutant. This restriction occurs through altered levels of the PIN3 auxin efflux transporter expression, significantly diminished in the *atc-2* mutant. Although trans-cytotic membrane relocalization of PIN3 is not affected by loss of ATC function, PIN3 further degrades in *atc-2* at a faster rate than in the wild-type in response to gravistimulation. It is suggested that the modulation of PIN3 expression occurs at the transcriptional levels specifically under low nitrate (NO_3^-) availability. This regulation of PIN3 by ATC may act as a mechanism to promote root gravitropic response to acquire (NO_3^-) resources stratified in deeper soil layers.

Introduction

The spatiotemporal arrangement of resources in the soil is proposed to elicit complex changes in RSA[1,3]. One possible plant root growth strategy of a “steep, deep,

and cheap" root system has been proposed as a mechanism for plants to quickly seek out N and water located in deeper soil levels[18]. This steepening of root architecture results from a strengthening of growth angle in alignment with the gravity vector, or root gravitropic response. Root gravitropic response is an important adaptation developed in land plants to improve anchoring of the root system and acquisition of water and nutrients located deeper in the soil profile[103].

Plant root gravitropic response is highly complex and involves communication within gravity sensing tissues at physical, molecular, and hormonal levels[104]. First, sensing of changes in the gravity vector occurs through actin filament-mediated sedimentation of starch-filled plastids called amyloplasts located in the columella cells of the root cap[105]. Physical collision of these amyloplasts with the endoplasmic reticulum on the bottom side of the columella cells is proposed to trigger Ca^{2+} signaling cascades[106]. Following these gravity sensing mechanisms, changes occur in the transport of the major plant growth hormone auxin at the root tip region. In a vertically growing root, auxin flows acropetally through the vasculature towards the root tip and is then transported away from the root tip basipetally[107]. This canonical flow of auxin is coordinated in part by a series of auxin influx transporters, such as AUX1[108], and efflux transporters, primarily members of the PIN transporter family[109]. Upon experiencing a gravity stimulus, PIN3 and PIN7 relocalize to the side of the columella cells in alignment with the gravity vector, shifting the flow of auxin preferentially to the lower side of the root[110,111]. In the root (contrary to its effect in cells in the shoot), auxin restricts cell elongation; as growth of cells on the lower side of the root is inhibited, coupled with enhanced cell elongation of the auxin-deprived cells on the upper side of the root, a bend in root growth results[112]. Modulation

of auxin transport pathways underlying root gravitropic responses has also recently been shown to influence how deeply RSA can be structured when plants are grown soil environment[96,100].

Auxin-responsive growth processes underlying RSA have been shown to be regulated by the availability of N. For example, the transceptor NRT1.1 acts as a dual nitrate (NO_3^-) and auxin transporter depending on the relative availability of NO_3^-[22,23]. Recently, other studies have shown that NO_3^- as well as ammonium (NH_4^+) impact auxin transport and biosynthesis mechanisms involved in the development of RSA[23,79,102]. However, the effect of how N impacts root gravitropic response, which could contribute to the steepening of the root system to acquire more N in deeper soils, remains understudied at the molecular level, despite potential relevance in the acquisition of N in crop species[113].

In this chapter, ATC, a downstream target of N-responsive signaling pathway involving CLE-CLV1 interaction, is demonstrated to regulate auxin transport mechanisms. While ATC function does not appear to impact processes involved in gravity sensing through starch-statolith sedimentation, loss of ATC function does impair auxin transport to the lower side of the root during turning. This dysregulation of auxin transport is proposed to occur due to the substantial loss of PIN3 auxin efflux transporter expression in the *atc* mutant.

Methods

Plant growth and culture

Plant growth and culture conditions were as described in Chapter 2 Methods. The mutant lines used in study are *atc-2* (isolated from SALK_021699C)[85], *pin3-4* (CS9363)[114], and *pin3-5* (CS9364)[114]. *PIN2::PIN2-GFP*[115], *PIN7::PIN7-GFP*[116], *PIN3::PIN3-GFP*[117], *DR5::GFP*[114], and DII-VENUS[118] lines were cross-fertilized with *atc-2* for microscopy.

Root phenotyping

Phenotyping of root gravitropism and root growth rates were as described in Chapter 2 methods.

Quantitative real-time polymerase chain reaction

Quantitative real-time polymerase conditions were as described in Chapter 2 Methods. Primer sequences are listed in Appendix Table B.1.

Microscopy

To visualize amyloplast localization in the root tip, roots were dipped in Lugol's solution (Sigma) for 5 minutes and then cleared by mounting onto a glass slide with two drops of Visikol for Plant Biology (Visikol). Light microscope images were taken using an Olympus CX31 light microscope with an Infinity 1 camera.

Olympus FV10i confocal laser-scanning microscopes were used for imaging of *DR5::GFP*, DII-VENUS and *PIN3::PIN3-GFP* lines. GFP was visualized using a 473-nm

(FV10i) or a 488-nm (LSM780) laser for excitation and capturing emission at a wavelength range of 490-540 nm (FV10i) or 505-560 nm (LSM780), respectively. VENUS was visualized using FV10i with the same setting. Counterstaining of the cell walls within the root was performed by dipping roots in 1 ug/ml propidium iodide (PI) for 5 minutes. PI staining was visualized using a 559-nm (FV10i) or 561-nm (LSM780) laser for excitation and capturing emission at 570-670 nm (FV10i) or 550-650 nm (LSM780), respectively. For *DR5::GFP* lines, seedlings were gravistimulated at 135 degrees for 16 hours. The mean GFP fluorescence for each root was quantified from maximum intensity projections of 12 Z-stack slices. Redistribution of *DR5::GFP* signals was determined as a ratio of mean fluorescent signal measured in the lower half of the root to the signal in the upper half of the root in the maximum projection images. For DII-VENUS lines, seedlings were gravistimulated at 90 degrees for 1 hour. Redistribution of DII-VENUS signals was determined as a ratio of mean VENUS fluorescent signal in the upper half of the root to the signal in the lower half of the root in single slice images.

PIN2-GFP and PIN7-GFP expression in roots and polar localization of PIN3-GFP at the plasma membrane of the columella cells were analyzed using a Zeiss LSM 800 vertical stage microscope with a 488-nm laser for excitation of GFP and an emission range of 505-550 nm. PIN3-GFP ratios were calculated by measuring the fluorescent signal on the bottom outer membrane of the columella cells and comparing it to the fluorescence of the upper outer membrane[119] after 60 minutes of 90-degree gravistimulation.

Fluorescence quantification was performed using ImageJ (Fiji)[86].

Results

Mutation in *ATC* disrupts auxin transport in the root tip

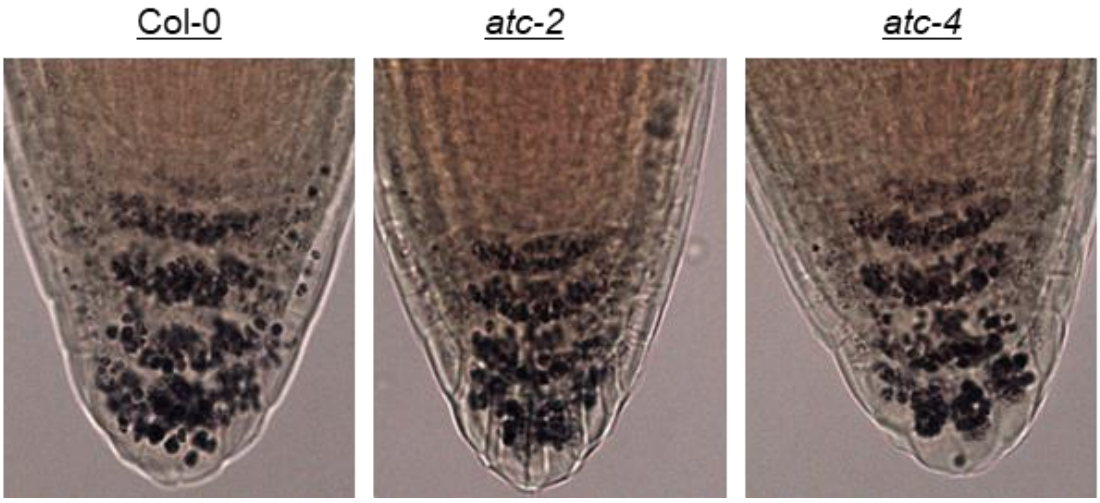

Figure 3.1. Lugol's staining of *atc* mutant root tips.

Gravitropic bending of the root relies first on the sensing of changes in the gravity vector through amyloplast sedimentation in root columella cells and the subsequent response in auxin transport mechanisms to direct auxin flow toward the lower side of the root[19]. Lugol's staining was performed on vertically growing seedlings under limited NO_3^- conditions in order to visualize amyloplasts within the columella cells. There was no difference in the levels of amyloplasts between Col-0 and *atc-2* or *atc-4* (Figure 3.1). These results suggest that ATC is not directly involved in mechanisms underlying gravity sensing.

Next the effect of ATC on changes in auxin distribution root gravitropic response was examined. When plant roots experience a gravity stimulus, auxin moves to the lateral root cap and epidermal cells toward the lower side of the root in the direction of gravity. This change in auxin distribution was first measured using the auxin-responsive reporter

DR5::GFP expressed in Col-0 and *atc-2* (Figure 3.2). Auxin levels as measured by this reporter were not different between these two genotypes (Figure 3.2b); however after 16 hours of gravistimulation at 135 degrees, the *DR5::GFP* signal ratio between the lower and upper side of the root was significantly lower in *atc-2*, which indicated a reduction in asymmetric auxin transport in this genotype (Figure 3.2a, c).

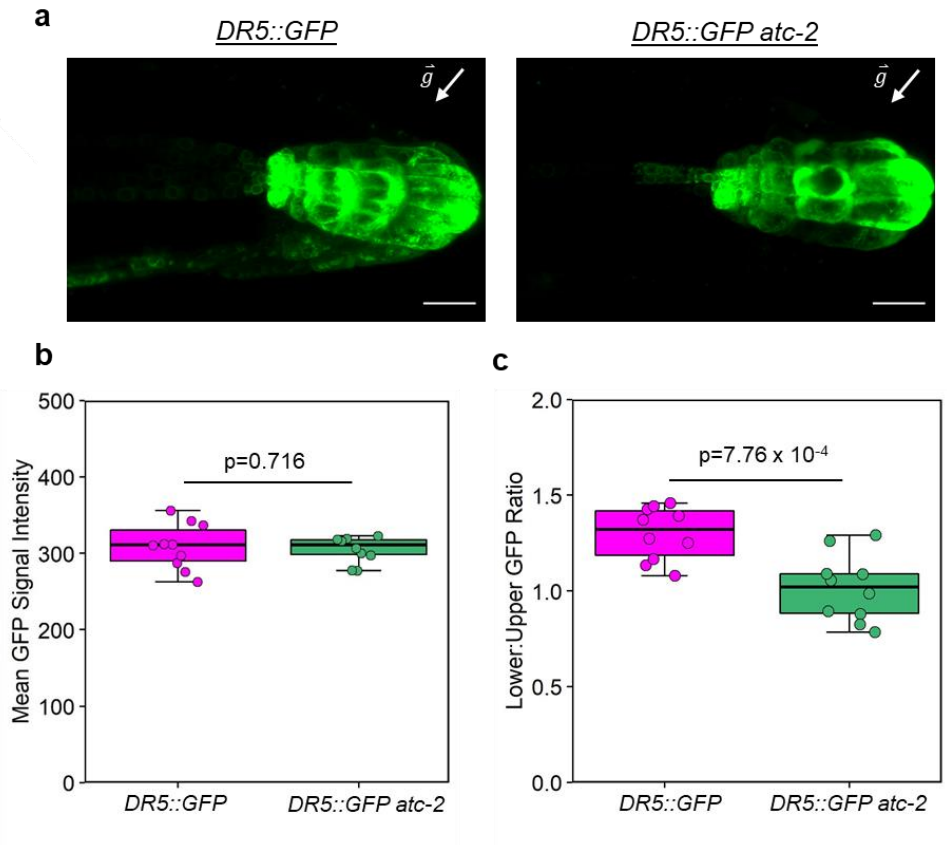

Figure 3.2. Distribution of *DR5::GFP* in the root tip during gravistimulation. a) Maximum intensity projections of *DR5::GFP* expression in the primary root of wild-type and *atc-2* after 16 hours of 135-degree gravistimulation on 0.01 mM NO_3^-. b) Mean GFP signal intensity of *DR5::GFP* expression below the quiescent center of wild-type (n=10) and *atc-2* mutant (n=10) plants. c) Quantification of GFP signal ratio of the lower to upper side of the primary root tip representing auxin distribution to the lower side of the root in *DR5::GFP* (n=10) and *DR5::GFP atc-2* (n=10). Results of a Student's *t*-test between wild-type and *atc-2* comparisons are indicated on each figure. $p<0.05$ indicates significant differences. Boxplots range from first to third quartile with median values indicated by the thick line and whiskers range from lowest to highest values. Scale bars = 20 μm. White arrows indicate direction of the gravity vector.

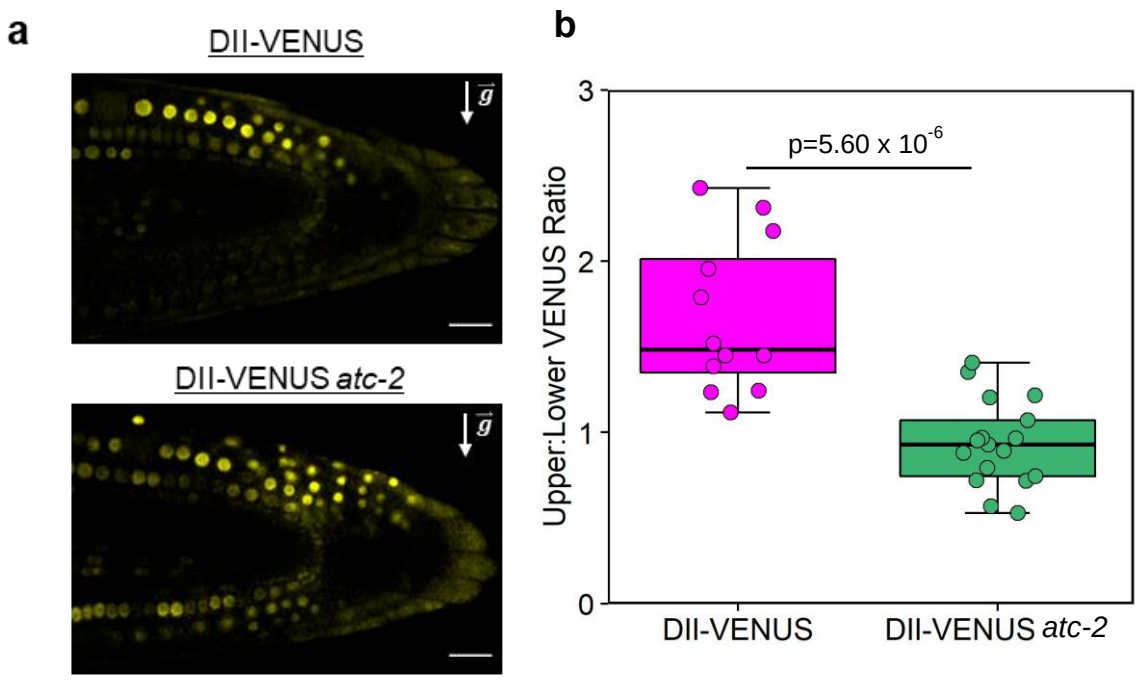

Figure 3.3. Distribution of DII-VENUS in the root tip during gravistimulation. a) DII-VENUS localization in wild-type and *atc-2* roots that have been turned at 90 degrees for one hour on 0.01 mM NO_3^-. b) Quantification of VENUS signal ratio of the upper to lower side of the primary root tip representing auxin distribution to the lower side of the root in DII-VENUS (n=12) and DII-VENUS *atc-2* (n=17). Results of a Student's *t*-test between wild-type and *atc-2* comparisons are indicated on each figure. $p<0.05$ indicates significant differences. Boxplots range from first to third quartile with median values indicated by the thick line and whiskers range from lowest to highest values. Scale bars = 20 μm. White arrows indicate direction of the gravity vector.

The expression of a second auxin-responsive reporter, DII-VENUS, was also examined in Col-0 and *atc-2* background (Figure 3.3). This reporter, which is degraded in the presence of auxin, was more responsive than *DR5::GFP* and a 60-minute turn for 90 degrees was sufficient to visualize the asymmetric shift in auxin distribution (Figure 3.3a). Analysis of VENUS signal ratio in the upper and lower halves of the root tip as a measurement of auxin distribution further confirm that there is a reduction in auxin

transport to the lower side of the root in the *atc-2* mutant line (Figure 3.3b). Thus, it was concluded that ATC leads to an inhibition of auxin transport in the root tip during gravistimulation events.

ATC regulates expression of PIN3 to maintain root gravitropism

Changes in auxin distribution in response to gravity are facilitated in part by key members of the PIN family of auxin efflux transporters[109]. Within the columella cells of the root tip, PIN3 and PIN7 function redundantly to facilitate the flow of auxin to the lower side of the root through rapid relocalization to the sides of the cells aligning with the direction of the gravity vector[110,111]. Concurrently, PIN2 expressed in root epidermal cells is degraded on the upper side of the root, which further contributes to asymmetric shootward auxin flow integral for gravitropic bending[120,121]. Therefore, the expression of PIN2, PIN3, and PIN7 fused to GFP, each driven by their native promoters, was observed in wild-type and *atc-2* background.

PIN2-GFP showed no significant difference (Appendix Figure B.1a) in accumulation and localization in *atc-2* compared to the wild-type background. In contrast, PIN3-GFP levels were significantly reduced in *atc-2* in both the vasculature and columella cells (Figure 3.4a). There also was a noticeable expansion of the domain of PIN7-GFP expression in the columella cells of *atc-2* (Appendix Figure B.1b); however, this result is likely due to a compensation for large reduction of PIN3 in the *atc-2* mutant line as previously shown with PIN7-GFP expressed in the *pin3* knockout mutant[23].

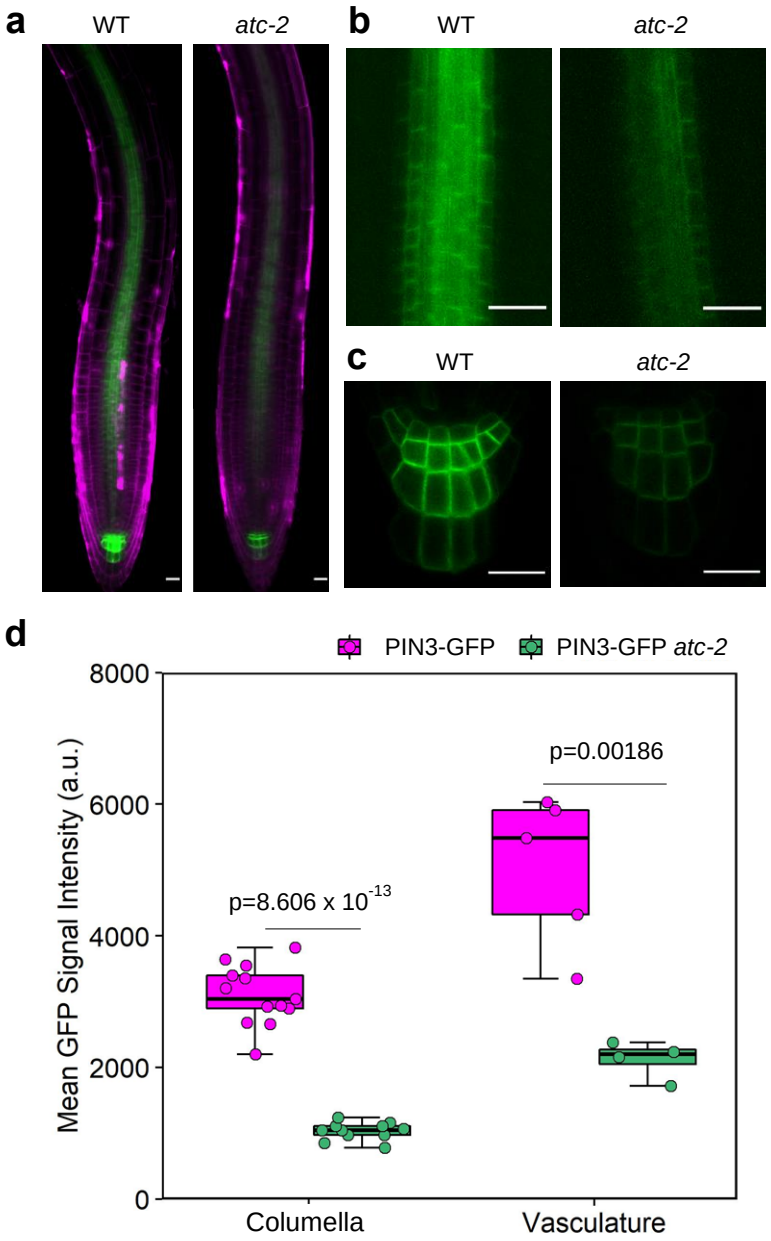

Figure 3.4. Reduction of PIN3-GFP expression in *atc-2* mutant lines. a) PIN3-GFP expression in WT and *atc-2* primary roots from the root tip to elongation zone. The PI counter staining is shown in magenta. b-c) Representative images of PIN3-GFP expression in WT and *atc-2* in the vasculature of the transition zone (b) and columella cells (c). Scale bars = 20 µm. d) Mean GFP intensity of PIN3-GFP and PIN3-GFP *atc-2* in the columella cells (n=11-13) and vasculature (n=4-5). Results of a Student's *t*-test between wild-type and *atc-2* comparisons are indicated on each figure. $p<0.05$ indicates significant differences. Boxplots range from first to third quartile with median values indicated by the thick line and whiskers range from lowest to highest values.

The expression of the PIN3 auxin efflux transporter was greatly diminished in the roots of *atc-2* compared to Col-0 (Figure 3.4). This reduction was qualitatively observed throughout the vasculature (Figure 3.4b) as well as in the columella cells (Figure 3.4c). Quantification of PIN3-GFP signal in these two regions separately confirm this significant reduction in the *atc-2* mutant line (Figure 3.4d). The reduction of PIN3 in the columella cells especially is proposed to result in the lack of auxin redistribution during gravistimulation, as PIN3 exports auxin from this region towards the lateral root cap[110].

ATC does not affect PIN3 relocalization but may stabilize expression at the columella during gravistimulation

In order to contribute to the asymmetric flow of auxin, PIN3 relocalizes to the lower side of the columella cells in response to gravistimuli[110]. The ratio of PIN3-GFP signal of the upper outer membrane of the columella cell region compared to the lower outer membrane was used as an indicator of PIN3 relocalization[119] in vertically growing seedlings and gravistimulated seedlings. A change in membrane localization of PIN3-GFP was seen in both Col-0 and *atc-2* after turning for 60 minutes (Figure 3.5). This result indicates that despite a significant reduction in the levels of PIN3 in the columella cells of the *atc-2* mutant, loss of ATC function does not affect the behavior of PIN3 transcytosis in response to gravistimulation.

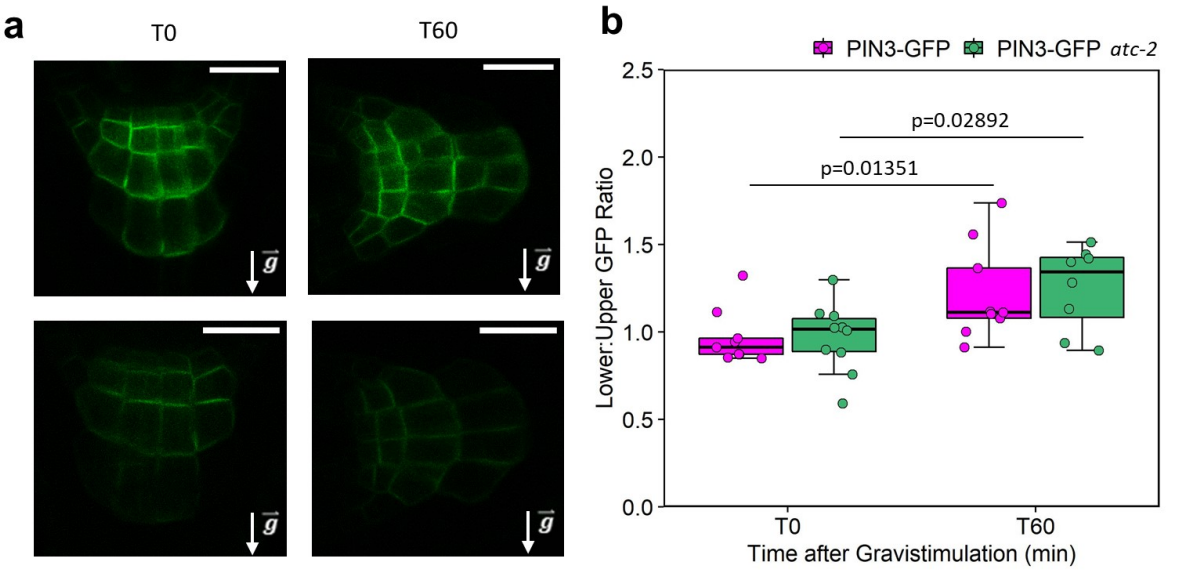

Figure 3.5. Relocalization of PIN3 in the columella is unaffected by *ATC* mutation. a) *PIN3::PIN3-GFP* expressed in wild-type (upper) and *atc-2* (lower) before and after 60 minutes of 90-degree gravistimulation on 0.01 mM NO_3^- media. Scale bars = 20 µm. White arrow indicates the direction of the gravity vector. b) Ratio of lower to upper GFP signal on the outer membranes of the columella cells (n=8-10 roots). Results of a two-tailed Student's *t*-test between the zero and 60-minute time points within each genotype are indicated on each figure (Supplementary Table S2). $p<0.05$ indicates significant differences. Boxplots range from first to third quartile with median values indicated by the thick line and whiskers range from lowest to highest values excluding outliers.

In addition to an overall reduction of PIN3-GFP signal in the *atc-2* mutant line, PIN3-GFP signal changes during gravistimulation. PIN3-GFP signals significantly decreased in the columella cells of *atc-2* after turning, but the corresponding signals were retained in Col-0 background, suggesting the ATC function is necessary to maintain the PIN3 expression levels in the root tip during the gravistimulation events (Figure 3.6). This change was only observed in the columella region of the root tip (Figure 3.6b-c) and not in the vasculature (Figure 3.6a, c), which could correlate with the accumulation of ATC in the columella cells after turning (Chapter 2, Figure 2.8).

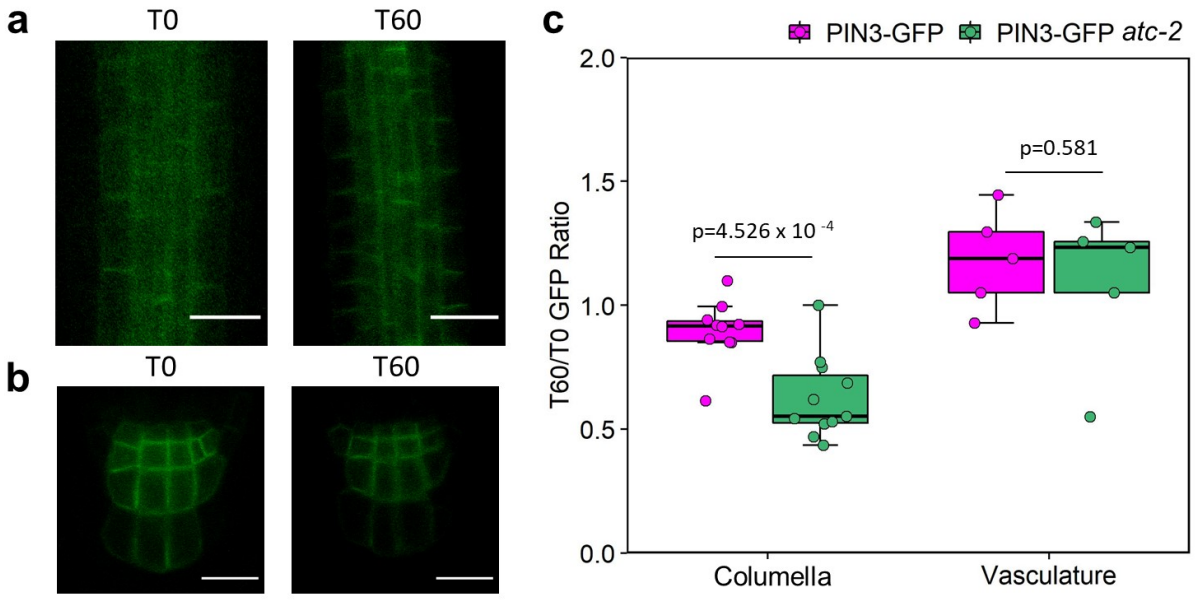

Figure 3.6. PIN3 expression is reduced in *atc-2* during gravistimulation. a-b) PIN3-GFP expression in the vasculature (a) and columella cells (b) of *atc-2* before and after 60 minutes of 90-degree gravistimulation. c) Change in PIN3-GFP signal intensity in the columella cells of the root tip (n=10) and in the vasculature (n=5) of wild-type and *atc-2* after turning. Ratios were calculated as the mean GFP signal intensity in each region after 60 minutes of 90-degree gravistimulation compared to the average GFP intensity of vertically grown seedlings. Results of a Student's *t*-test between wild-type and *atc-2* comparisons are indicated. $p<0.05$ indicates significant differences. Boxplots range from first to third quartile with median values indicated by the thick line and whiskers range from lowest to highest values excluding outliers.

N-dependent ATC signaling mediates *PIN3* expression and root gravitropism

In support of the suggested role of ATC in the maintenance of PIN3 expression, there was a decrease in *PIN3* transcript levels in whole root tissue of *atc-2* and *atc-4* relative to Col-0 at 0.01 mM NO_3^-. This reduction, however, were not detected with the higher 1.0 mM NO_3^- treatment (Figure 3.7a-b). Furthermore, a significant weakening of gravitropism in *pin3* mutants was observed at 0.01 mM NO_3^- but not with 1.0 mM NO_3^-

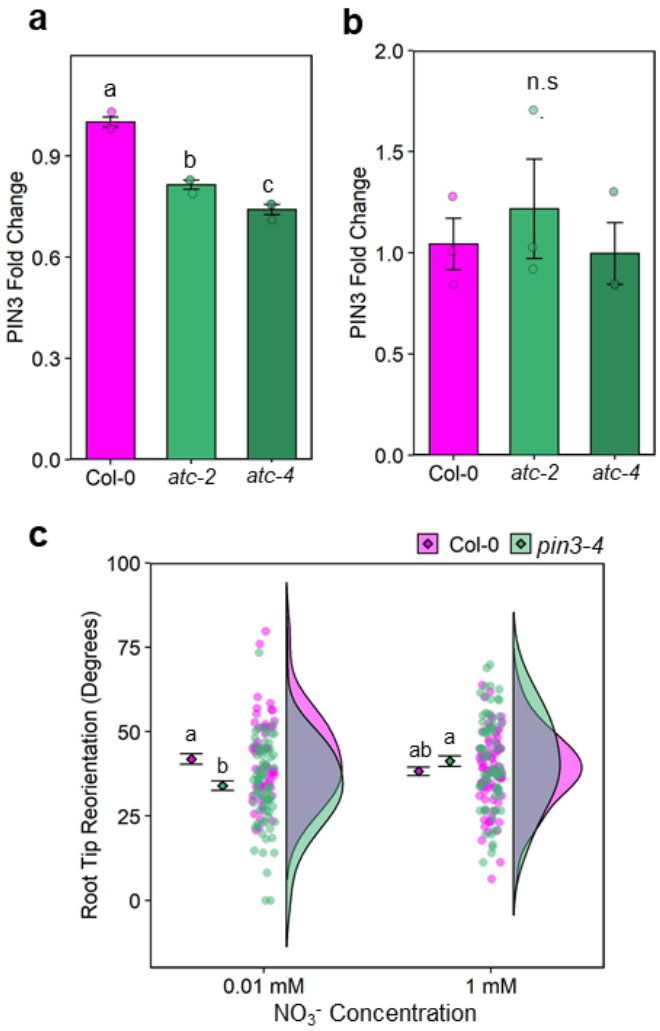

Figure 3.7. *PIN3* expression in *atc* mutant lines and its influence on root gravitropic response. a-b) *PIN3* transcript expression in Col-0 compared to *atc* mutant lines grown on 0.01 mM NO_3^- (a) and 1 mM NO_3^- (b) MGRL media. Fold change values were determined from 3 biological replicates and bars show standard error. c) Root tip reorientation of the *pin3-4* mutant compared to Col-0 on 0.01 mM NO_3^- and 1 mM NO_3^- MGRL media (n=59-78). Mean-and-error plots are shown alongside raincloud plots indicating individual data points and distributions by genotype. Letters indicate significant groupings from Tukey's test ($p<0.05$) following a significant one-way (a-b) or two-way (c) ANOVA. n.s.: not significant.

supplementation (Figure 3.6e, Appendix Figure B.2a), while there was no significant changes in the root growth rate (Appendix Figure B.2b). Thus, the observed weakening

of gravitropism in *atc-2* and *atc-4* under low NO_3^- availability was attributed to the reduction in PIN3 expression.

Discussion

The work presented here shows the involvement of the CLE-CLV1-ATC pathway in the regulation of auxin-dependent mechanisms governing root gravitropic response. Primarily, ATC functions to promote the expression of the PIN3 auxin efflux transporter in this process. I hypothesize this effect predominantly occurs under low NO_3^- availability when *ATC* expression levels are highest (Chapter 2, Figure 2.3b), which is further supported by the weakening of root gravitropic response in *pin3* knockout mutants under this condition. These results expand our understanding of how N availability regulates root gravitropic response.

As shown in Chapter 2, the CLE-CLV1-ATC pathway is also proposed to have a moderate impact on lateral root emergence under N-limited conditions. While this phenotype was not investigated specifically in relation to the regulation of PIN3 via ATC, a reduction of PIN3 levels in the vasculature of *atc* mutants as well as in the columella cells was observed (Figure 3.4). In addition to its involvement in the transport of auxin in the root cap, PIN3 expressed in the transition zone is proposed to function in auxin reflux into the vasculature from the cortex cells to maintain acropetal auxin transport[116]; however, changes to auxin transport in this region remain to be determined. PIN3 expressed distally from the root tip has also been shown to be involved in auxin transport processes necessary for early lateral root development[122]. While CLE-CLV1 signaling has been shown to inhibit the late stage progression of lateral root primordia to

emergence[14], these processes may be connected to altered auxin transport process. Further work is thus necessary to elucidate the role of CLE-CLV1-ATC signaling in PIN3-mediated lateral root development.

The nature of the regulation of PIN3 via ATC activity also remains to be considered. While mutation of *ATC* impacts transcriptional regulation of *PIN3* under low NO_3^- availability (Figure 3.7a-b), this does not rule out other potential mechanisms of control. PIN3 protein levels are known to be regulated by endocytic cycling mechanisms that are integral for the polarization of PIN3 during gravistimulation and that gravity does not enhance PIN3 degradation[111]. The trans-cytotic relocalization of PIN3 is unaffected in the *atc-2* mutant despite a strong reduction in overall signal (Figure 3.5), providing alternative evidence that ATC may be involved in the replacement of PIN3 during the turning process (Figure 3.6). One possibility is that the reduction of PIN3 expression occurs during turning when plants are experiencing N starvation; further experiments would be necessary to observe PIN3 protein dynamics under a spectrum of N conditions.

Another mechanism by which ATC could regulate *PIN3* expression at the transcriptional level could involve the known interaction between ATC and the transcription factor FLOWERING LOCUS D (FD). FD has been shown to interact with both ATC and its homolog FT in the regulation of flowering time; specifically, FD binding to ATC competitively inhibits binding with FT, which leads to suppression of flowering[77]. Furthermore, recent chromatin immunoprecipitation (ChIP)-based evidence suggests the presence of FD binding sites in the promoter region and gene body of PIN3[123,124]. The putative role of ATC-FD interaction in the regulation of the PIN3 auxin efflux transporter as well as the characterization of ATC lipid binding will be further discussed in Chapter 4.

CHAPTER 4

Characterization of the flowering repressor protein *Arabidopsis thaliana* CENTRORADIALIS as a novel regulator of root growth

Lipid binding results from this chapter have been submitted for publication as part of the following manuscript:

Lay-Pruitt, K. S., Araya, T., Abualia, R., Giehl, R. F. H., Benková, E., von Wirén, N. & Takahashi, H. Nitrogen-responsive small peptide signaling modulates root gravitropism.

Abstract

Arabidopsis thaliana CENTRORADIALIS (ATC) serves a dual function as a novel regulator of N-responsive root architectural traits and of flowering time under short-day conditions. ATC is a homolog of the major florigen in plants, FLOWERING LOCUS T (FT), and contains a putative phosphatidylethanolamine binding domain that may play a role in the activity of this protein. In its capacity as a floral repressor, ATC also interacts with the transcription factor FLOWERING LOCUS D (FD) to alter the expression of key flowering time genes. Despite the novel role of ATC in the regulation of auxin transport in response to gravistimulation, the effect of the ATC-FD interaction on the regulation of the PIN3 auxin efflux transporter has not been determined. In this chapter, integral properties of ATC are characterized in the context of root growth regulatory processes. ATC binds to phosphatidic acid and phosphatidylserine, which is contrary to the binding of phosphatidylcholine observed for FT and may indicate another facet of environmental control. FD has been shown to bind to regions of the *PIN3* promoter and gene body; however, data presented in this chapter indicates a repressive effect of FD on *PIN3* transcription despite promotion in *PIN3* expression downstream of ATC. These findings contribute to the novel characterization of flowering regulatory pathways in the maintenance of N-responsive root system architecture.

Introduction

While the work presented thus far has focused on a novel mechanism involving the regulation of key auxin transport processes via the activity of *Arabidopsis thaliana* CENTRORADIALIS, this protein has been previously studied for its role in floral

development. ATC is a small (19.8 kDa) protein that has been shown to repress flowering under short-day conditions[77]. ATC was first identified as a homolog of TERMINAL FLOWER 1 and was named as such due sharing closer sequence similarity to the *Antirrhinum* CENTRORADIALIS (CEN) protein involved in the maintenance of the inflorescence meristem in this species[125]. Like TFL1, ATC also belongs to the same family as the major florigen in plants FLOWERING LOCUS T (FT), although both proteins exhibit contrary effects on floral development compared to FT[95]. Due to the predicted lipid binding domain shared among its members, this protein family is referred to as phosphatidylethanolamine (PE) binding proteins (PEBPs)[95]. Multiple members of this family, including ATC and FT, have been shown to bind to the transcription factor FLOWERING LOCUS D (FD) to affect the expression of key floral regulatory genes, such as *APETALA1* (AP1)[77,126].

ATC::GUS activity has been shown to be localized to the phloem companion cells in the roots, hypocotyl and leaves of *A. thaliana*[77]. Due to the lack of expression detection in the apex, it was proposed that ATC is able to move to this location from the vasculature; this mobility was further supported by grafting experiments that showed that both ATC protein and mRNA are graft transmissible[77]. Results presented in Chapter 2 indicate that ATC protein is expressed in root tissue types outside of the phloem companion cells, specifically to the root tip columella cells and the pericycle and endodermal cells of the transition zone where phloem unloading predominantly occurs. Further characterization of ATC based on features of its role as a flowering time regulator may contribute to better understanding of the function of ATC in the development of root architecture in response to N.

An important characteristic of FT that has been shown to be integral for its function is its ability to bind lipids. Although the protein domain shared by PEBPs was predicted to bind to phosphatidylethanolamine (PE) as their name suggests, FT was shown to bind instead to phosphatidylcholine (PC) through lipid binding overlay experiments[127]. The species of PC that binds to FT oscillates throughout the day and is predominantly present in plants in the daytime, which is proposed to contribute to flowering promotion[127]. A recent study by Nakamura *et al*. (2019) shows that this binding does not occur as predicted in the anion-binding pocket of FT, but instead occurs between FT and the acyl chains of the PC[128]. The PC binding site in FT is present near the region of FT that is proposed to bind to DNA during the formation of the florigen activator complex between FT and FD[128]. Mutation in PC binding sites alters flowering time, suggesting this interaction is necessary for proper FT function[128]. Thus, it is of importance to determine the lipid binding capacity of ATC, which may or may not involve PC due to the divergence in FT and ATC function during flowering. This interaction also serves as an example of how environmental changes to plant lipid composition can influence when these proteins are active as certain lipid species may potentially be present in greater abundance under limited N conditions when ATC is also most highly expressed (Fig 2.3b).

As described in Chapter 3, ATC function appears to be important for the expression of the PIN3 auxin efflux transporter to maintain auxin transport processes when plants experience a gravity stimulus. This regulation is proposed to occur at the transcriptional level as *PIN3* transcript expression level was significantly reduced in *atc* mutant lines under low nitrate (NO_3^-) treatments (Figure 3.7a-b). Since ATC is involved in the transcriptional regulation of floral identity genes through its interaction with FD, this

interaction may regulate *PIN3* expression in the roots. Recently, large-scale chromatin immunoprecipitation (ChIP) experiments probing for targets of the FD transcription factor point to a potential link between FD and *PIN3*. In ChIP-seq experiments performed by Collani *et al.* (2019), FD has been shown to bind to a canonical bZIP binding motif (CACGTG) in the *PIN3* promoter region approximately 3 kB upstream of the start codon[123]. Similarly, an independent experiment performed by Zhu *et al.* (2020) has shown that FD also binds to an exon in the *PIN3* gene body; this binding does not occur in the *tfl1* mutant background, suggesting that the interaction of TFL1-FD is necessary for DNA binding in this region[124]. Despite the binding of FD in these regions, it has not yet been observed whether these interactions elicit changes in *PIN3* transcript expression or if FD is involved in the regulation of root gravitropic responses.

The work shown in this chapter expands our understanding of ATC as a regulator of auxin and root gravitropic response is through providing evidence for the distinct lipid binding capacity of ATC and the potential effect of the ATC-FD interaction on *PIN3* gene expression. The lipid binding analysis of ATC indicates that it does not bind to PC, but instead to phosphatidic acid and phosphatidylserine, two phospholipids with negatively charged head groups. With regard to the potential involvement of FD as a downstream component of the CLE-CLVi-ATC pathway, phenotypes of *fd* mutants suggest that FD is also necessary for the maintenance of root gravitropic response under low NO_3^- availability. However, the results of transactivation experiments suggest that FD can repress *PIN3* promoter-driven gene expression, indicating ATC and FD may be interacting with other regulatory components to elicit divergent effects on auxin transport mechanisms to modulate root gravitropic response.

Methods

Plant growth and culture

Plant growth conditions for *A. thaliana* are described in Chapter 2 Methods. The mutant lines used in study are *atc-2* (isolated from SALK_021699C)[34], *fd-3* (isolated from SALK_054421C) and *fd-4* (isolated from SALK_118487C). *Nicotiana benthamiana* seeds were sown on Ready Earth (Sun Gro Horticulture) soil mixture in pots and germinated in growth chambers set at 25°C with 16-hour day/ 8-hour night light cycle. Plants were grown for 6 weeks prior to agroinfiltration and watered with 1/2x Hoagland nutrient solution.

Root phenotyping

Root tip reorientation and growth rate were measured as described in Chapter 2 Methods.

Agroinfiltration of *N. benthamiana* leaves

The pEAQ-HT[129] (which contains the anti-posttranscriptional gene silencing protein p19) and pBGCN[88] binary vectors were used for generating constructs for tobacco infiltration. The coding sequences of FD and ATC were PCR amplified from cDNA using the NruI-FD-F and XhoI-FD-R primer pairs and NruI-ATC-F and XhoI-ATC-R primer pairs, respectively. These products were then introduced into NruI and XhoI digested pEAQ through InFusion cloning to generate *p35S::FD* and *p35S::ATC* overexpression constructs. A construct overexpressing *Renilla* luciferase (*RLuc*) downstream of the *p35S* promoter with an omega enhancer sequence (*p35SΩ::RLuc*) was generated by PCR amplifying this region from a *p35SΩ::RLuc* construct generated in pTH2 (Bohrer *et al.*

unpublished) using the HindIII-p35S-F and SacI-RLuc-R primers and inserting it into pBGCN that had been digested with HindIII and SacI. The pBGCN construct was also used to generate a binary vector containing the 4-kb promoter region upstream of the *PIN3* transcriptional start site driving the expression of the gene encoding firefly luciferase (*FLuc*). The *FLuc* sequence downstream of the *p35S* promoter with an omega enhancer sequence (*p35SΩ::FLuc*) was PCR amplified from a *p35SΩ::FLuc* construct generated in pTH2 (Bohrer *et al.* unpublished) using the HindIII-p35S-F and SacI-FLuc-R primers and also inserted into HindIIII and SacI digested pBGCN using InFusion cloning. This construct was then digested again with HindIII and XbaI to remove the p35S promoter and Ω sequence. The *PIN3* promoter sequence amplified from genomic DNA using HindIII-PIN3-F and XbaI-PIN3-R primers was inserted upstream of FLuc using InFusion cloning. Primer sequences are listed in Appendix Table C.1.

The *p35S::ATC*, *p35S::FD*, *p35SΩ::RLuc*, *PIN3::Fluc*, and pEAQ-HT-GFP[129] (negative control) constructs were introduced into *Agrobacterium tumefaciens* GV3101 (pMP90)[91] by freeze-thaw transformation[92]. Pairwise combinations of *p35S::ATC, p35S::FD,* and pEAQ-HT-GFP were agroinfiltrated with *p35SΩ::RLuc* and *PIN3::Fluc*, into 6-week *N. benthamiana* leaves. Equal ratios (1:1:1:1) of the *Agrobacterium* cultures diluted in a mixture of water and 200 µM acetosyringone to an OD_{600} of 1.0 were infiltrated into the abaxial side of the leaf. A 2:1:1 ratio of pEAQ-HT-GFP to *p35SΩ::RLuc* and *PIN3::Fluc* was used as a control to maintain levels of the p19 silencing protein. Three leaves per plant were infiltrated with the same construct combinations to generate experimental triplicates. Plants were returned to the growth chamber for 72 hours and leaf tissue was harvested for further analysis.

Luciferase transactivation assay

Total protein was extracted from infiltrated tobacco leaves. Leaf tissue was ground in liquid N and approximately 1 mL of powder was mixed with protein extraction buffer (50 mM Tris-HCl, pH 8; 150 nM NaCl, 10 mM NaF, 0.1 mM Na3VO4, 10% glycerol, 1% Triton X-100, 0.005X protease inhibitor cocktail p9599). The protein extract was centrifuged twice to remove solid debris and then protein concentration was determined using a Bradford assay. The protein extract was then diluted to 0.05 µg/µL. To assess the effect of each co-infiltrated effector construct on *PIN3::FLuc* activity, a Dual-Luciferase Reporter Assay (Promega) was performed according to the manufacturer's protocol and luminescence was measured using a Berthold Centro XS LB 960 luminometer. The diluted protein extracts were mixed with the firefly luciferase reagent LAR II and luminescence readings were measured to detect firefly luciferase activity. Next, Stop & Glo Reagent was added to the samples and luminescence readings were taken again to detect *Renilla* luciferase activity, which was used as an internal standard. The ratio of *Fluc* to *Rluc* was then determined for each replicate and measured in technical duplicate.

Protein expression and lipid binding assay

ATC coding sequence was PCR amplified from Arabidopsis root cDNA using NdeI-ATC-F and NdeI-ATC-R and was inserted into NdeI-digested pET15b vector through InFusion cloning to generate ATC with an N-terminal 6xHis tag (His-ATC). Primer sequences are listed in Appendix Table C1. The pET15b-ATC construct was introduced into *E. coli* C41 competent cells and protein expression was induced using IPTG. His-ATC protein was purified using a His SpinTrap Column (GE Healthcare) and desalted

using a PD MiniTrap G-25 column according to the manufacturer's protocols. The cleared lysate, flow through, wash, and elution fractions from the protein extraction procedure were analyzed through SDS-PAGE using a Mini-Protean TGX gel (4-20%) (Bio-Rad) and a Western blotting using an Anti-6xHis-HRP antibody (Rockland Antibodies).

For the lipid binding assay[130], 8 µg in 1uL of each phospholipid species was spotted onto a Protran Supported nitrocellulose membrane (Amersham). The phospholipid species used in this study are as follows: PA: 1,2-dioleoyl-sn-glycero-3-phosphate, PC: 1,2-dioleoyl-sn-glycero-3-phosphocholine, PE: 1,2-dioleoyl-sn-glycero-3-phosphoethanolamine, PS: 1,2-dioleoyl-sn-glycero-3-phospho-L-serine, PG: 1,2-dioleoyl-sn-glycero-3-phospho-(1'-rac-glycerol), and PI: 1,2-dioleoyl-sn-glycero-3-phospho-(1'-myo-inositol). The membrane was incubated in blocking buffer (3% fatty-acid free BSA in TBST: 10 mM Tris–HCl, pH 8.0, 150 mM NaCl, 0.2% Tween 20) for one hour and incubated overnight in blocking buffer with 1 ug/ml of the His-ATC protein. The membrane was then rinsed twice with TBST, incubated in a 1:5000 dilution of the Anti-6xHis-HRP antibody for one hour, and rinsed three times with TBST. Chemiluminescence was detected after incubation with ECL reagent (Amersham) and imaged using a ChemiDoc Imaging System (Bio-Rad).

Results

ATC binds to phosphatidic acid and phosphatidylserine

A construct containing the ATC protein with a 6xHis-tag on the N-terminus (Appendix Figure C.1a) was generated to express protein in the C41 *Escherichia coli* system. After protein extraction, the size of the protein and specificity of the 6XHis-HRP

antibody binding were validated via SDS-PAGE and Western blotting (Appendix Figure C.1b-c) The ATC protein was incubated with various phospholipid species to assess its lipid binding profile due to the PET binding domain contained within its protein sequence (Figure 4.1).

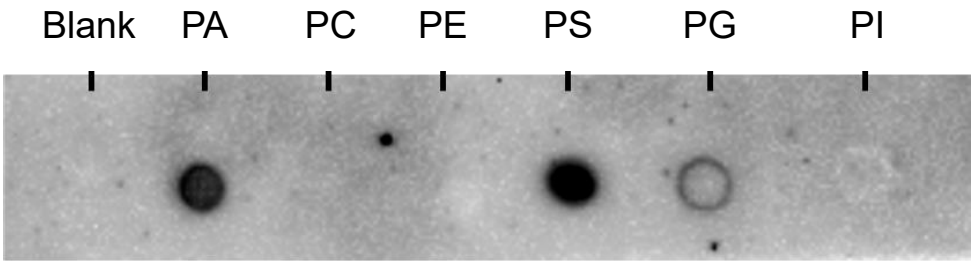

Figure 4.1 Lipid binding profiling of His-ATC. The amount of each lipid spotted to the membrane was 8 µg.

ATC was found to bind to phosphatidic acid (PA) and phosphatidylserine (PS), phospholipids that contain negatively charged polar head groups (Figure 4.1). Furthermore, ATC binds to PA preferentially over PS (Figure 4.2). ATC also shows absence of binding to PC, deviating from the binding profile of FT[127]. As the binding of PC has been shown to be integral to the activity of the FT protein and may be implicated in the ability of FT to bind to DNA during its interaction with the FD transcription factor, that the biochemical difference in lipid binding capacity of ATC may contribute to its divergence in function.

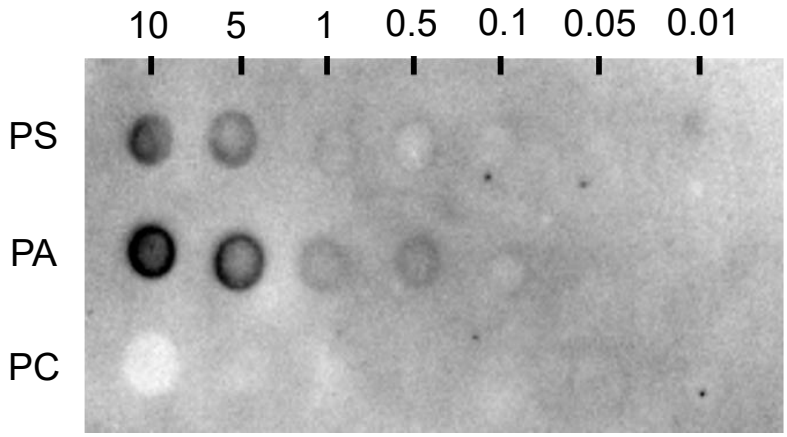

Figure 4.2 Overlay of His-ATC on a dilution series of PS, PA, and PC. Numbers indicate micrograms of lipid spotted on the nitrocellulose membrane in 1 µl volumes.

FD function influences root gravitropic response

To determine the relevance of the FD transcription factor to the root gravitropism phenotype, *fd-3* and *fd-4* mutant lines containing T-DNA insertions within the coding region of the FD gene were obtained (Figure 4.3a). Root tip reorientation assays indicate that these mutations result in significant weakening of root gravitropic response under low NO_3^- availability (Figure 4.3b). Thus, the observed phenotypes are consistent with the weakening of gravitropic response in *atc* mutant lines (Figure 2.3c, Appendix Figure A.3a-b).

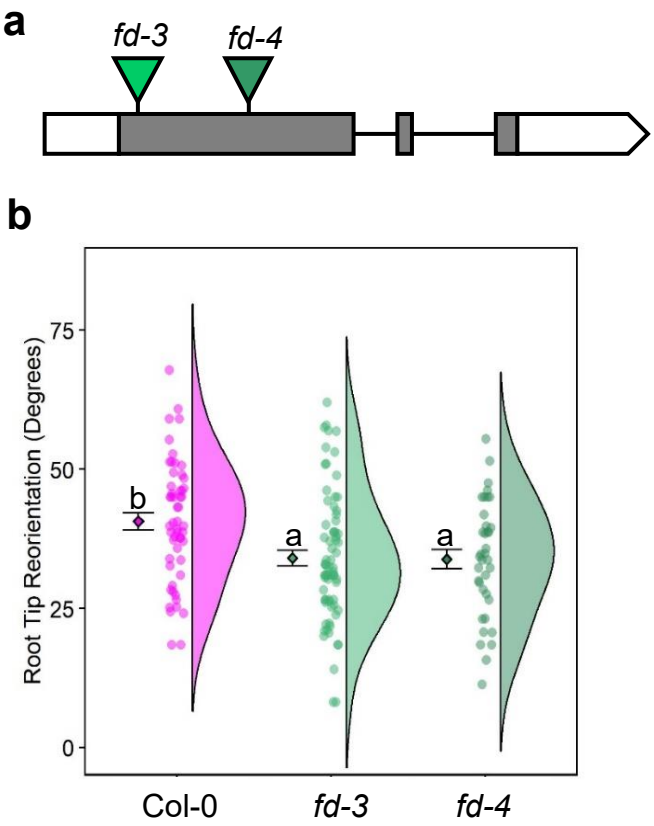

Figure 4.3. Root gravitropic response in *fd* mutants. a) Gene model of *FD* (AT4G35900) with locations of *fd-3* (SALK_054421C) and *fd-4* (SALK_118487C) mutations. Green triangles indicate T-DNA insertions. b) Root tip reorientation of 5-day-old *fd* mutants compared to Col-0 on 0.01 mM NO_3^- media. Mean-and-error plots are shown alongside raincloud plots indicating individual data points with distributions by genotype. Significant differences between genotype and condition combinations were determined using Tukey's test (p<0.05) following a one-way ANOVA and are indicated by lowercase letters.

ATC and FD independently influence *PIN3* expression

To investigate if the interaction of ATC and FD affects PIN3 expression to govern root gravitropic response, a dual-luciferase transactivation assay was performed. The 4-kB *PIN3* promoter, which contains the putative CACGTG binding site for FD and other bZIP transcription factors, was cloned upstream of the firefly luciferase gene (*FLuc*).

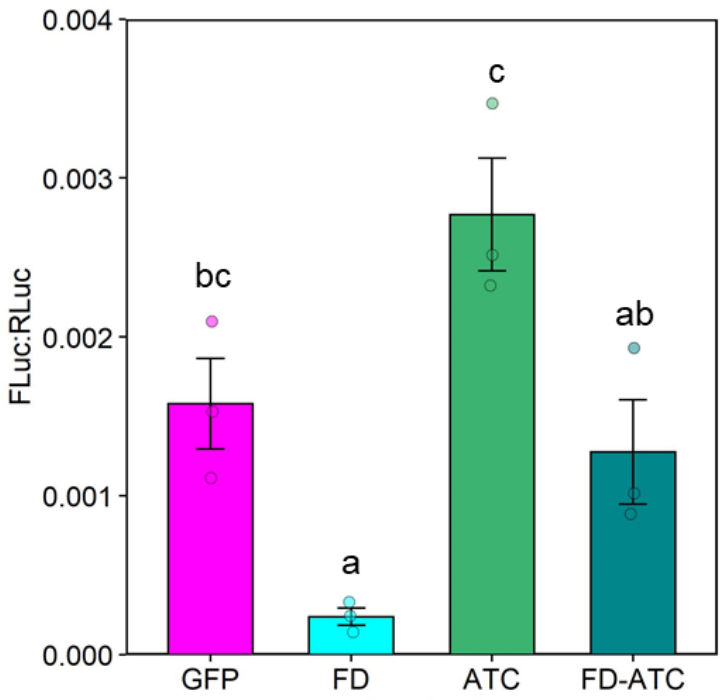

Figure 4.4. *PIN3::Fluc* transactivation assay. Ratios between *PIN3::FLuc* and *p35SΩ::RLuc* expression values following infiltration of pEAQ plasmid combinations were determined from 3 biological replicates and bars show standard error. Letters indicate significant groupings from Tukey's test (p<0.05) following a one-way ANOVA .

Along with a construct driving the constitutive expression of *Renilla* luciferase (*p35SΩ::Rluc*) to serve as an internal standard, the *PIN3::Fluc* construct was co-infiltrated in a combinatorial manner with constructs containing *p35S::FD*, *p35S::ATC*, and pEAQ-HT-GFP (to serve as a negative control). Co-infiltration of *p35S::FD* and *PIN3::FLuc* appears to repress the activity of the *PIN3* promoter as measured by the ratio of *FLuc/RLuc* (Figure 4.4). Infiltration of *p35S::ATC* with *PIN3::Fluc* increases luciferase activity but not to statistically significant levels compared to the GFP control. However, infiltration of *p35S::ATC* alone elicits a significantly higher level of *PIN3::FLuc* expression compared to co-infiltration of both *p35S::ATC* and *p35S::FD* constructs, indicating that the presence of FD reduces the positive regulatory effect of ATC. Likewise, co-infiltration

of *p35S::ATC* and *p35S::FD* restores *PIN3* expression to control levels compared to *p35S::FD* alone. These results may suggest that the interaction of ATC-FD prevents the repression of *PIN3* expression by FD and may also imply that other interacting partners of ATC and FD contribute to their respective changes to *PIN3* gene expression.

Discussion

The work presented in this chapter further characterizes the ATC flowering repressor protein as a novel regulator of plant root architecture and supports a more integrated role of this phloem-mobile signaling protein in plant development. Flowering time exhibits a U-shaped pattern in *Arabidopsis*, requiring a longer period of time to flower when N supply is severely limited or in excess[131]. ATC may therefore be involved in repression of flowering while simultaneously contributing to strengthening root gravitropism under conditions with severely limited N supply. The divergence in lipid binding profiles observed between ATC and the florigen FT (Figure 4.1) may indicate another facet of environmental control of this signaling protein. Phospholipases that generate phosphatidic acid have been shown to be involved in the regulation of root growth under N-limited conditions[132], suggesting the relevance of phospholipid species binding for the functionality of ATC, which may find parallels in phosphatidylcholine binding to FT[128].

Although the interaction of ATC and FD plays a role in the regulation of flowering time, it was not observed in this study that this interaction promotes the expression of the PIN3 auxin efflux transporter. While mutants in *FD* had weaker root gravitropic response under low NO_3^- availability (Figure 4.3b), nevertheless in transactivation assay

transfection of FD repressed the expression of *PIN3::FLuc* (Figure 4.4). These divergent effects of ATC and FD on *PIN3* expression could imply that there are alternative binding partners for either ATC or FD to regulate this response. In Arabidopsis, there are 6 members of the PEBP family, most of which are already known to interact with FD to regulate transcription[77,124,126,133]. Likewise, FD is only one of the 78 bZIP transcription factors in Arabidopsis[134]; the most closely related FD homolog, FLOWERING LOCUS D PARALOGUE (FDP) has been shown to independently influence the expression of FD targets that are not involved in flowering[135]. Members of the bZIP family also function as homo- or heterodimers[134], which could mean that both ATC and FD interact with multiple bZIPs in a regulatory complex to influence PIN3 expression. It remains to be tested whether ATC interacts with FDP or other FD homologs to coordinate the transcriptional activity of *PIN3*, but the potential integration of these floral regulatory networks in the development of root architecture has significant implications for understanding systemic signaling coordinating plant development in response to the nutrient environment.

CHAPTER 5

Conclusions and future directions

Summary

The research presented in this dissertation broadens our understanding of a small peptide signaling process governing how the plant root system responds to the availability of N. N-responsive CLE peptides interact with the CLV1 receptor kinase to induce the expression of ATC (Figure 2.2, Appendix Table A.2), a small, mobile flowering repressor protein, to regulate root phenotypes. ATC acts as a moderate repressor of lateral root development (Figure 2.4c), consistent with previous findings of the CLE-CLV1 pathway. However, ATC has a more prominent role in the regulation of root gravitropic response (Figure 2.3c, Appendix Figure A.3a-b) by promoting expression of the PIN3 auxin efflux transporter (Figure 3.4) to maintain the asymmetric flow of auxin in response to gravity stimuli (Figure 3.2, Figure 3.3). This regulation is proposed to occur via transcriptional regulation of *PIN3* by ATC (Figure 3.7a-b), but this promotion appears not simply due to the known interaction between ATC and the FD transcription factor (Figure 4.4). Instead, it may involve another binding partner, potentially from the bZIP transcription factor family functioning in a homo- or heterodimeric complex. Alteration of root system architecture through this SSP pathway may have biological significance based on the way that NO_3^- stratifies in the soil environment. Negatively charged NO_3^- is highly mobile in soil as it may move through negatively charged soil particles and is typically found at higher concentrations in deeper soils. Thus, the CLE-CLV-ATC pathway demonstrated in this study potentially prevents lateral root outgrowth in NO_3^- poor environments and directs root growth toward deeper soil layers through the promotion of root gravitropic response mechanisms downstream of ATC activity (Figure 5.1). Increased ATC expression under limited N availability may also promote gravitropic response in lateral roots to promote

steeper root growth, although the involvement of PIN3-mediated auxin transport in this process have not been characterized.

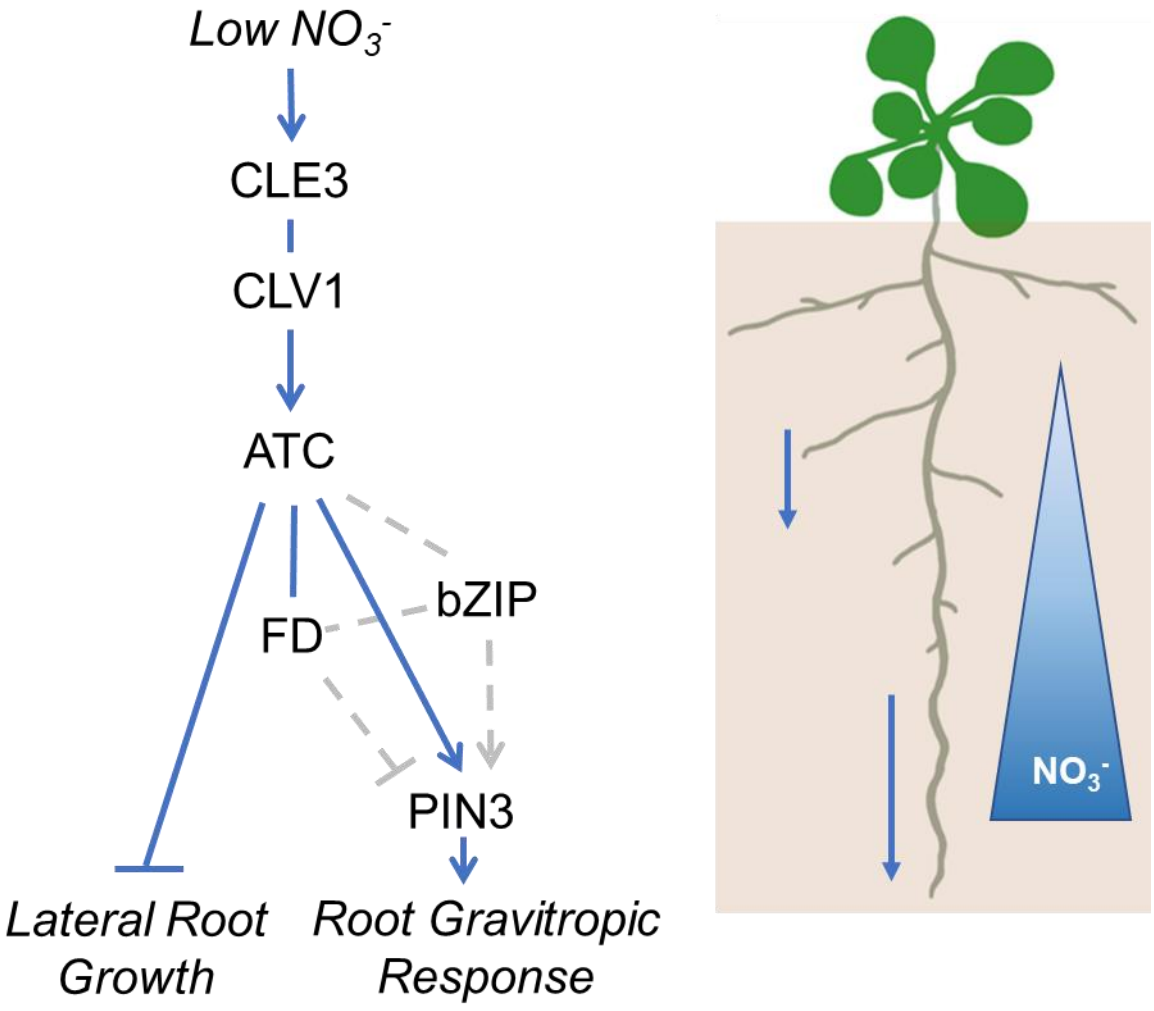

Figure 5.1. Proposed model of N-responsive CLE-CLV1-ATC signaling to regulate root architecture. Gray arrows indicate hypothetical connections.

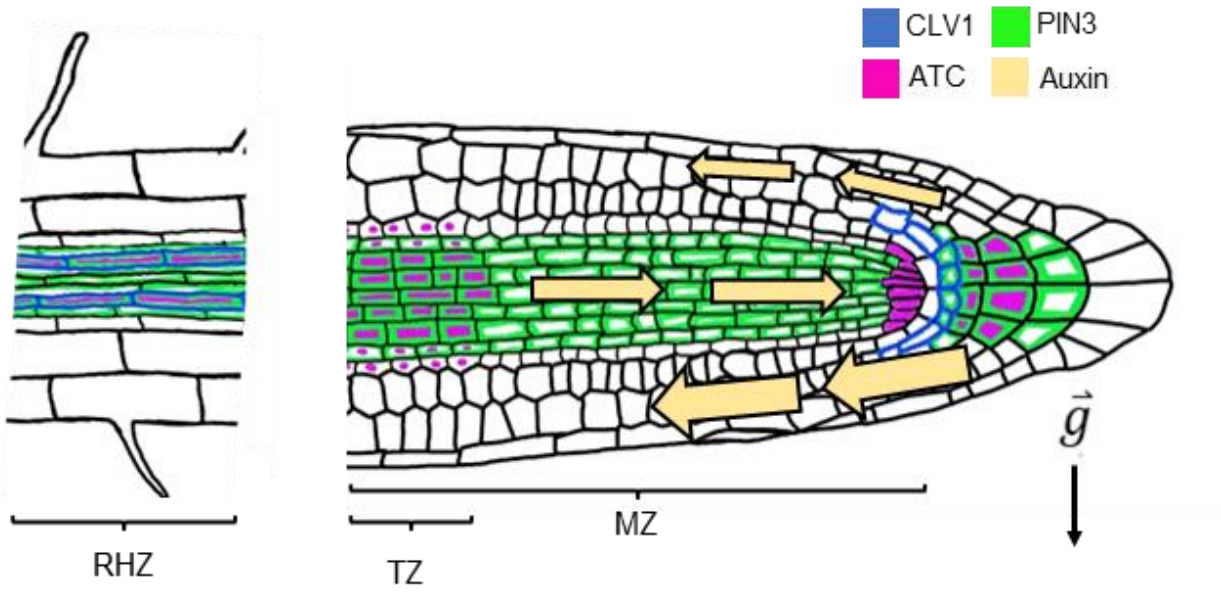

Figure 5.2. Localization of CLV1 and ATC modulating PIN3-mediated auxin transport during gravitropic response. RHZ: root hair zone, TZ: transition zone, MZ: meristematic zone. Black arrow indicates the direction of the gravity vector**.**

Additionally, the localization of CLE-CLV1-ATC pathway components within the root provides a means by which spatially distinct auxin transport pathways may be regulated by the same nutritional stimulus. For example, CLE-CLV1 interaction, while phloem localized, appears to be limited by the location of the membrane-bound receptor kinase within the phloem of the root hair zone and the first tier of the columella cells. ATC as a smaller, phloem-mobile protein may act as an additional mobile signal to regulate PIN3 expression in the columella cells and the pericycle cells of the transition and elongation zones, both locations that have been demonstrated to be regions where PIN3 is expressed[110]. Regulation of PIN3 in the columella cells alters auxin transport to the lower side of the root during root-tip bending in response to gravity[110], while in the transition zone it may impact the reflux of auxin into the vasculature and acropetal

transport towards the root tip[116], although the effect of ATC on the latter phenotype remains to be determined. Regulation of both these relative domains would allow for collective control of auxin distribution in the root tip, which may contribute to efficient and quick manipulation of root system architecture in response to N (Figure 5.2).

The original role of ATC as a flowering repressor protein also provides interesting implications for the coordination of regulatory processes throughout the plant. The novel functions of this protein described in the dissertation imply an integrated role of nutrient-dependent signaling in not only the developmental regulation of the root and shoot but also connecting vegetative and reproductive growth processes. The function of these mobile proteins and small peptides would allow for efficient systemic signaling when plants undergo significant environmental stressors, such as severe N deprivation.

Future work

Lateral root development

Although a link between the regulation of PIN3 via ATC signaling in both the root tip and vasculature has been presented, this research does not encompass the effect of ATC on PIN3-mediated lateral root development. Examination of PIN3 dynamics in older seedlings under different NO_3^- supply to determine if altered levels of PIN3 in the vasculature of *atc* mutants affect this phenotype would be necessary. It would also be interesting to examine crosses of *clv1* mutants and *CLE3* overexpressing lines (*CLE3ox*) with *PIN3::PIN3-GFP* lines to observe changes in PIN3 levels in both the root tip and vasculature, especially since these components have more substantial impact on lateral root development.

Additionally, due to the moderate effect of ATC on lateral root development (Figure 2.4c), potentially other signaling components downstream of the CLE-CLV1 interaction may have a more substantial or additive effect on this phenotype. Microarray analysis of *CLE3ox* lines and the *clv1-15* mutant identified 20 potential downstream candidates including ATC (Figure 2.2a, Appendix Table A.2). Candidates that were not chosen for further analysis in this study did include genes with known effect on auxin-mediated root architectural changes. Multiple NF-YA transcription factors were differentially expressed in the *CLE3*ox and *clv1-15* dataset. Members of the NF-YA family have been shown to be induced by N starvation[136] and have been involved in the regulation of lateral root development[137]; additionally, select members of this family regulate auxin transport mechanisms to promote leaf development[138]. Potential targets of CLE-CLV1 are also involved in other phytohormone or abiotic stress response pathways. For example, CYP78A5, which is repressed by CLE-CLV1, has been shown to activate cytokinin signaling and N assimilation[139]. Multiple heat shock proteins (HSPs) were identified in this dataset as well and can be involved in various nutrient-responsive signaling processes downstream of CLE-CLV1 interaction. These results may indicate more complex signaling integration of the CLE-CLV1 pathway in the regulation of these phenotypes, which could allow for fine-tuning in response to N availability.

ATC-mediated regulation of PIN3

Although ATC is known to bind to FD to regulate genes involved in floral development, the interaction of ATC and FD was not shown in this study to promote the activity of the *PIN3* promoter in dual-luciferase transactivation assays. Instead, the

expression of FD significantly repressed *PIN3* expression (Figure 4.4). These results could indicate that ATC and FD are potentially binding to other partners to regulate the expression of PIN3 in an opposing manner. Nevertheless, *fd* mutants showed weak gravitropic response on low-N medium (Figure 4.3b), similar to *atc* (Figure 2.3c, Appendix Figure A.3a-b) and *pin3* mutants (Figure 3.7c, Appendix Figure B2.a). Future work characterizing the binding partners of these two proteins through targeted protein-protein interaction experiments such as yeast-two hybrid assays may elucidate other components downstream of the CLE-CLV1-ATC signaling pathway. Further confirmation on the effect of these interactions on PIN3 expression may be tested using the validated dual-luciferase transactivation system described in Chapter 4 with or without site directed mutagenesis of the putative bZIP binding sites within the *PIN3* genomic region.

The lipid binding capacity of ATC (Figure 4.1, Figure 4.2) also presents an interesting facet for future study. Under N limited conditions, phosphatidic acid (PA) levels and the expression of key enzymes involved in the production of PA are altered[132,140], which could influence these phenotypes if PA is necessary for ATC function. This presents a further mechanism of environmental control of ATC that is independent of upstream CLE-CLV1 signaling mechanisms promoting its transcription. Analyzing root gravitropism in plant systems in which the levels of these phospholipids can be artificially adjusted, such as in mutants or overexpressing lines of PLDε phospholipases to generate PA from PC[132], could help determine if this lipid binding specificity serves a developmental function.

Expanding the CLE-CLV1-ATC signaling model

The results presented in this dissertation focus on the NO_3^- availability since this is the preferred source of N for *A. thaliana*. Other forms of inorganic N, such as NH_4^+, have also been shown to influence lateral root development[20,79] and root gravitropic response[141,142]. There exists a potential role of NH_4^+ derived signals acting on this pathway through the expression of CLE3. CLE3 has been shown to be induced by N starvation and is even further induced by NH_4^+ re-supplementation[28]. This could be a means to respond to NH_4^+ availability in higher soil layers that would drive the repression of lateral root growth and redirection of root growth to deeper soils to acquire preferential NO_3^- resources. Different CLEs interacting through CLV1 could also be a means of other nutritional cues to act through this pathway to regulate RSA. For example, CLE2 interacts with CLV1 and is responsive to S availability[143]. Further work examining different CLE peptide overexpressing lines or the effects of different combinatorial nutritional conditions on ATC-mediated root gravitropism could aid in elucidating these effects.

The findings presented in this dissertation may also be studied in crop systems or in soil environments in more applied approaches. Gravitropic response is emerging as an important root growth trait to consider for crop systems in N-limited soils. The root system of maize has also been shown to have steeper root angles in low N soils[113]. Likewise, alleles that confer stronger root gravitropism have been connected to increased N uptake in rice[144]. Numerous orthologs of the CLE peptide family[145], CLV1 receptor kinase[146,147], and PEPB families[148–150] are present in many plant species and can be utilized as candidates for further characterization of these N-dependent changes in RSA.

Conclusion

Taken together, the results presented in this dissertation have demonstrated the importance of the N-responsive CLE-CLV1-ATC pathway in the regulation of root system architecture. This signaling module acts as a novel integrator of nutrient signaling and plant hormone transport processes to control root growth. The key component of this module, ATC, suggests the presence of coordinated systemic signaling pathways governing plant development in response to the nutrient environment due to its dual role as a regulator of root growth and flowering. This study provides new insights into nutrient-responsive SSP pathways and their integration with hormone transport and signaling processes central to root development.

APPENDICES

APPENDIX A

Supplemental Data for Chapter 2

Appendix Table A.1. List of primers used in Chapter 2

Primer Name	Sequence
NheI-ATC-F-2047-2	GCTAGCGTGTCACAGATTGTTGTGGGAGCATATGCTAAAG
NcoI-ATC-R-2	CCATGGCTCGATTGCTTGGTTAAGAATTTAGACGAAGAAATGAAGAATAAGTGAAAG
NcoI-GFP-F-3	CCATGGTGAGCAAGGGCGAGGAGCTGTTCACCGGGGTG
SacI-GFP-R-3	GAGCTCTTACTTGTACAGCTCGTCCATGCCGTGAGTGATCCCGG
SacI-NLS-F	GACGAGCTGTACAAGTCCGGACTCAGATCTCGAGC
SacI-NLS-R	GATCGGGGAAATTCGAGCTCTTATCTAGATCCGGTGAATC
SacI-ATC-F	GACGAGCTGTACAAGATGGCCAGGATTTCCTCAGA
SacI-ATC-R	GATCGGGGAAATTCGAGCTCTCAACGGCGTCTAGCGGCGG
ACT2-F	CTTGCACCAAGCAGCATGAA
ACT2-R	CCGATCCAGACACTGTACTTCCTT
EF1a-F	TGAGCACGCTCTTCTTGCTTTCA
EF1a-R	GGTGGTGGCATCCATTTCGTTACA
ATC-qF	CGCGGCTGTTTTCTTCAACT
ATC-qR	GAAAGTCATTCAACGGCGTCTA

Appendix Table A.2. Differentially expressed genes in *CLE3* overexpressing lines and *clv1-15*. Log_2 fold changes (FC) in transcript abundance and adjusted *p*-values are shown for each gene.

AGI Code	Gene ID	*clv1-15* log_2 FC	Adj. *p*-value	*CLE3ox- 17* log_2 FC	Adj. *p*-value	*CLE3ox-12* log_2 FC	Adj. *p*-value
AT1G33340	PICALM8	-1.786	2.19E-04	1.078	1.22E-02	0.959	7.72E-02
AT1G59730	TH7	-2.184	1.10E-04	1.158	1.28E-02	0.933	1.19E-01
AT2G27550	ATC	-1.941	7.51E-04	2.198	2.14E-03	1.585	3.20E-02
AT5G35480	unknown protein	-5.947	5.55E-04	5.021	6.63E-03	3.297	1.34E-01
AT5G48485	DIR1	-1.782	4.09E-03	1.540	3.28E-02	0.934	4.28E-01
AT3G15650	unknown protein	-1.924	2.25E-04	1.944	1.32E-03	1.190	4.93E-02
AT5G12020	HSP17.6II	-1.025	3.55E-02	1.778	1.88E-02	1.017	3.49E-01
AT1G69880	TH8	-2.619	4.48E-04	2.700	2.14E-03	1.092	2.80E-01
AT5G12030	HSP17.6A	-2.098	1.17E-03	2.575	2.14E-03	1.053	2.71E-01
AT1G53540	HSP17.6C	-1.995	1.66E-02	3.311	8.28E-03	1.582	3.60E-01
AT3G46230	HSP17.4	-1.334	4.37E-03	3.421	1.66E-04	1.675	2.33E-02
AT4G25200	HSP23.6-MITO	-1.140	4.21E-02	3.424	1.92E-03	1.553	1.94E-01
AT1G52700	unknown protein	-1.489	1.21E-02	2.379	7.11E-03	0.779	5.87E-01
AT1G13710	CYP78A5	1.595	6.32E-03	-1.826	1.61E-02	-2.152	2.33E-02
AT3G60270	unknown protein	1.398	5.42E-03	-1.929	5.63E-03	-1.904	2.04E-02
AT3G61400	unknown protein	2.455	2.25E-04	-1.315	2.59E-02	-0.974	2.49E-01
AT3G05690	NF-YA2	2.483	9.23E-06	-1.798	3.01E-04	-1.345	6.08E-03
AT1G72830	NF-YA3	1.250	5.02E-04	-1.845	3.16E-04	-1.304	8.21E-03
AT1G01380	ETC1	1.066	1.89E-02	-1.332	3.30E-02	-0.752	4.79E-01
AT5G24860	FPF1	1.444	7.51E-05	-1.944	8.82E-05	-0.607	8.40E-02

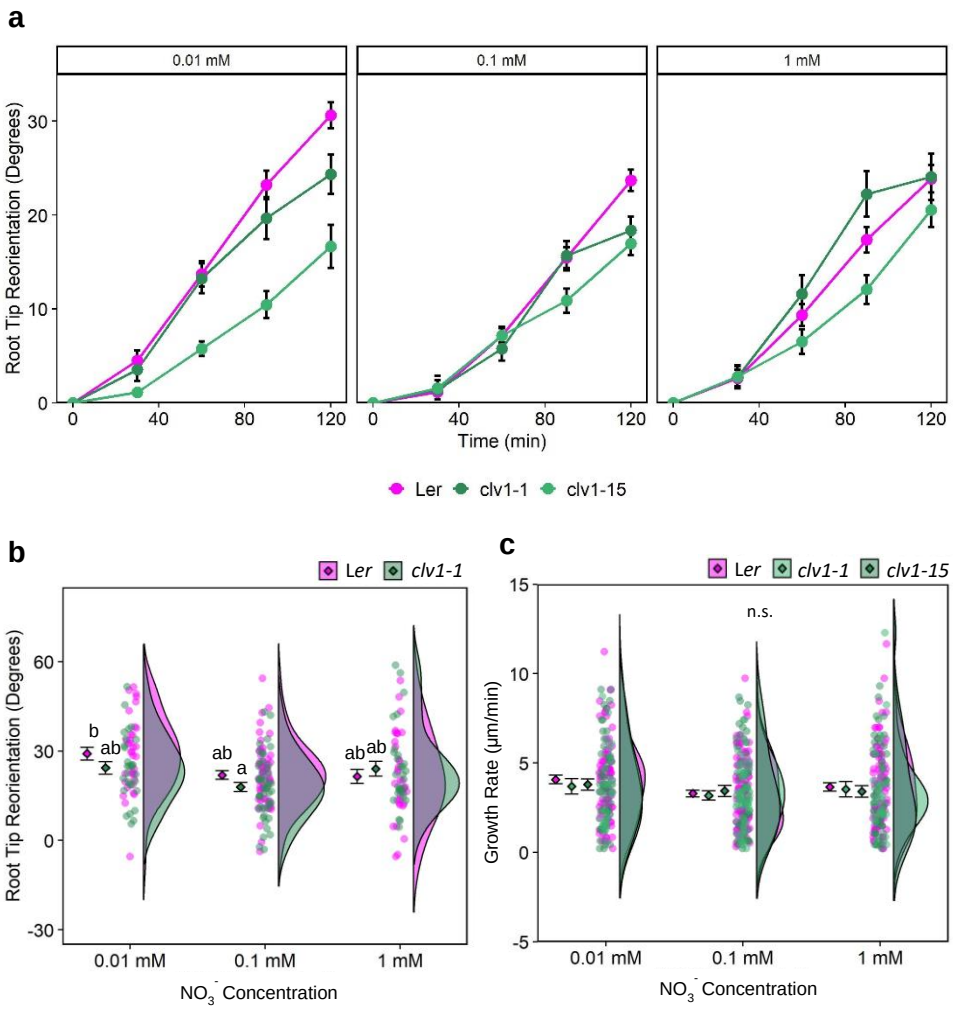

Appendix Figure A.1. Root phenotyping of *clv1* mutants. a). Root tip reorientation of *clv1* mutants compared to L*er* over a two-hour 90-degree gravistimulation time course. b). Root gravitropism of *clv1-1* mutant compared to L*er* after two hours of gravistimulation. c) Root growth rates of *clv1* mutants during the two-hour time course. Mean-and-error plots are shown alongside raincloud plots indicating individual data points and distributions by genotype. Significant differences between genotype and condition combinations were determined using Tukey's test (p<0.05) following a two-way ANOVA and are indicated by lowercase letters n.s.: not significant.

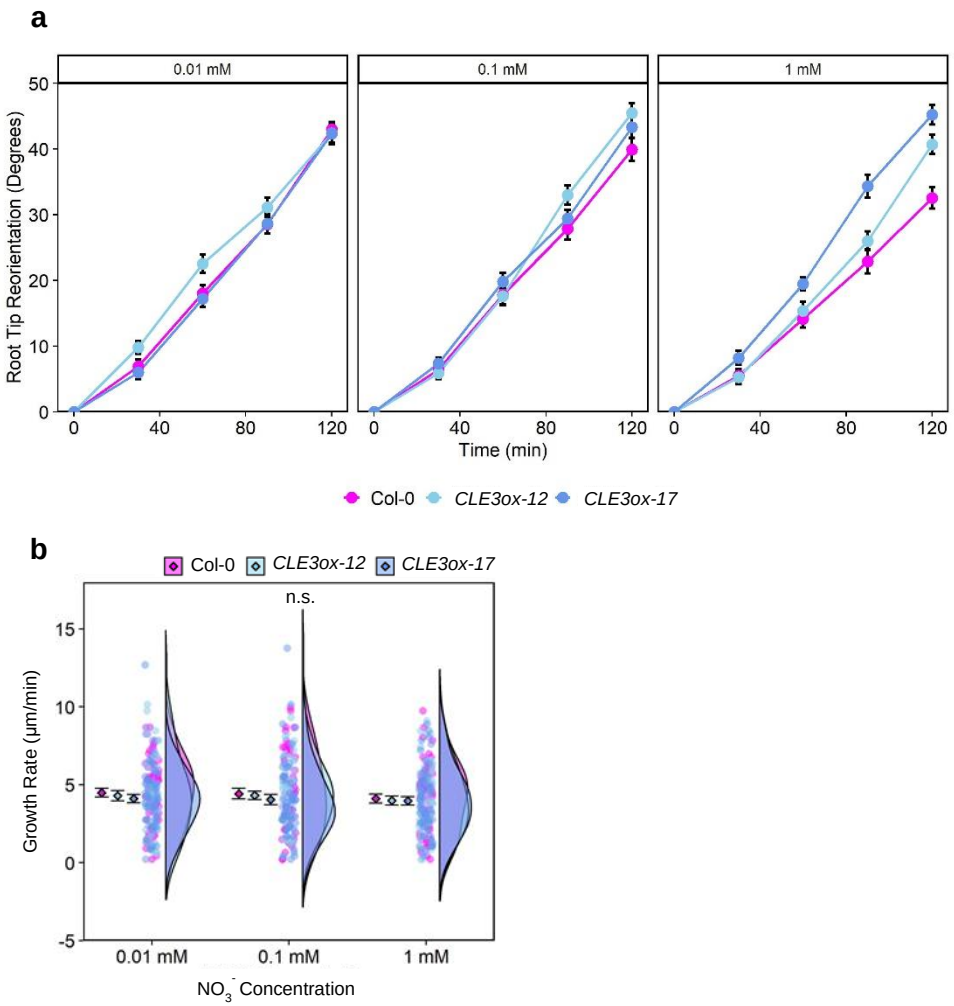

Appendix Figure A.2. Root phenotyping of *CLE3* overexpressing lines. a). Root tip reorientation of *CLE3ox* lines compared to Col-0 over a two-hour 90-degree gravistimulation time course. b) Root growth rates of *CLE3ox* lines during the two-hour time course. Mean-and-error plots are shown alongside raincloud plots indicating individual data points and distributions by genotype. Mean-and-error plots are shown alongside raincloud plots indicating individual data points and distributions by genotype. Significant differences between genotype and condition combinations were determined using Tukey's test (p<0.05) following a two-way ANOVA and are indicated by lowercase letters n.s.: not significant.

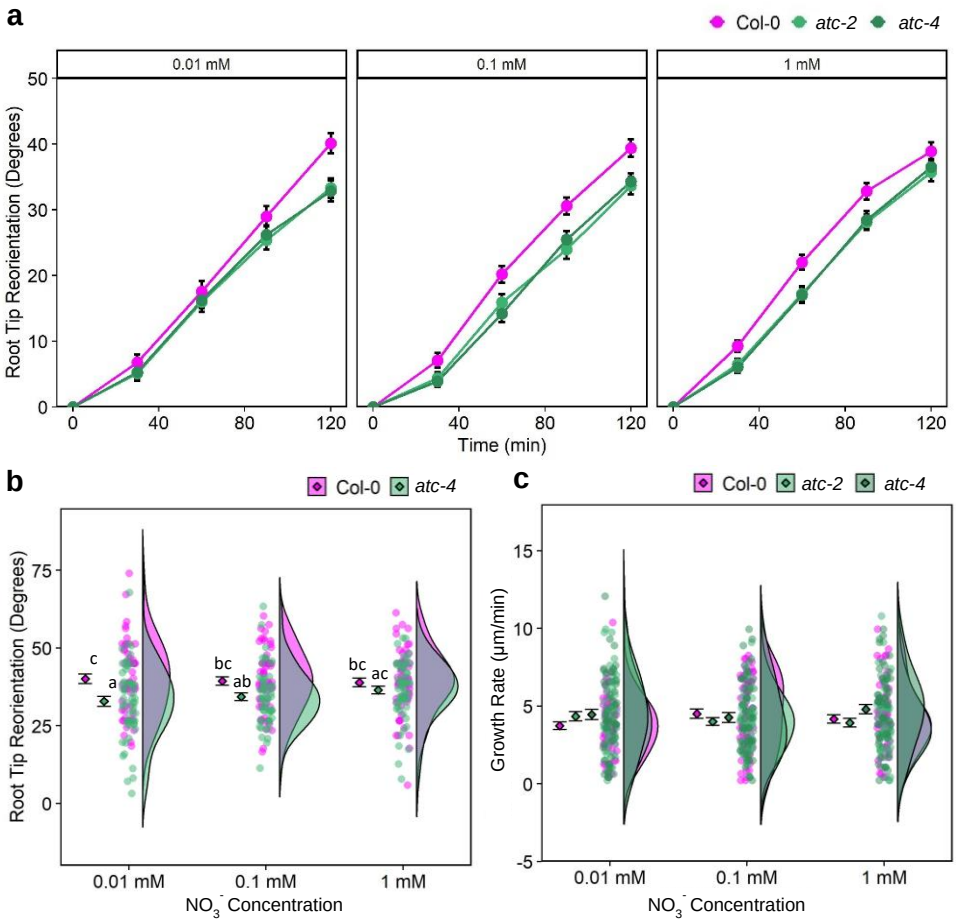

Appendix Figure A.3. Root phenotyping of *atc* mutants. a). Root tip reorientation of *atc* mutants compared to Col-0 over a two-hour 90-degree gravistimulation time course. b). Root tip reorientation of *atc-4* overexpressing lines compared to Col-0 at the two-hour time point of the gravistimulation time course under a spectrum of NO_3^- concentration. c) Root growth rates of *atc* mutants during the two-hour time course. Mean-and-error plots are shown alongside raincloud plots indicating individual data points and distributions by genotype. Significant differences between genotype and condition combinations were determined using Tukey's test ($p<0.05$) following a two-way ANOVA and are indicated by lowercase letters n.s.: not significant.

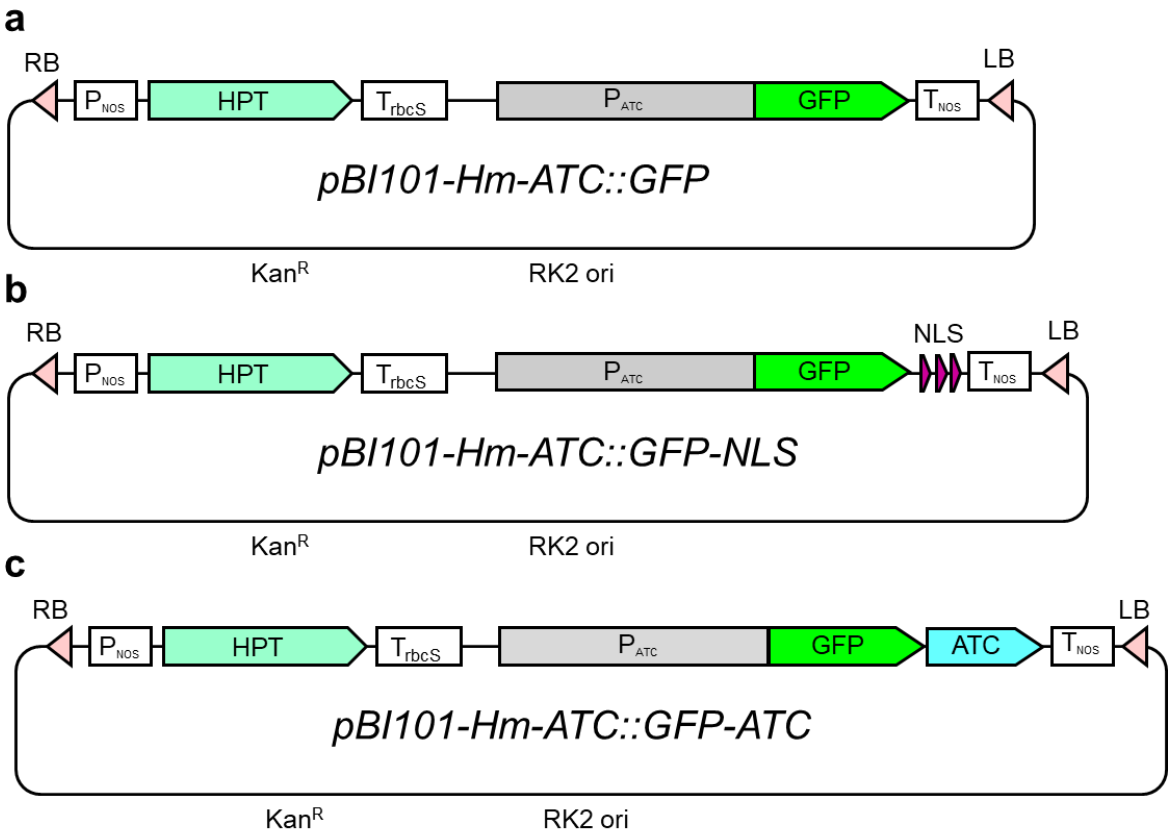

Appendix Figure A.4. Plasmid maps of ATC reporter constructs. a) pBI101-Hm-ATC::GFP, b) pBI101-Hm-ATC::GFP-NLS, c) pBI101-Hm-ATC::GFP-ATC. P_{NOS} : NOS promoter, T_{rbcS}: rbcS terminator, P_{ATC}: *ATC* promoter, T_{NOS}: NOS terminator, NLS: nuclear localization signal.

APPENDIX B

Supplemental Data for Chapter 3

Appendix Table B.1. List of primers used in Chapter 3

Primer Name	Sequence
ACT2-F	CTTGCACCAAGCAGCATGAA
ACT2-R	CCGATCCAGACACTGTACTTCCTT
EF1a-F	TGAGCACGCTCTTCTTGCTTTCA
EF1a-R	GGTGGTGGCATCCATTTCGTTACA
PIN3-F	GAGGGAGAAGGAAGAAAGGGAAAC
PIN3-R	CTTGGCTTGTAATGTTGGCATCAG

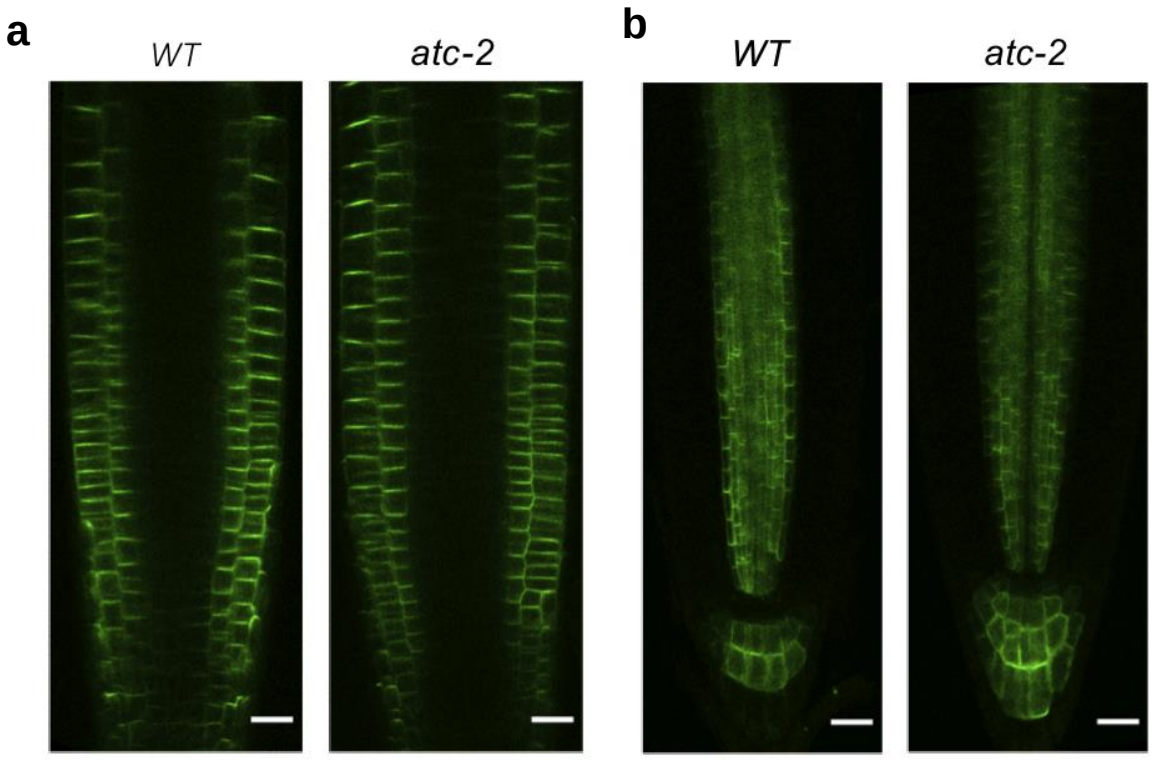

Appendix Figure B.1. Effect of *ATC* mutation on PIN2 and PIN7 expression. a) *PIN2::PIN2-GFP* expression in wild-type and *atc-2* background. b) *PIN7::PIN7-GFP* expression in wild-type and *atc-2* background. Root tip images are of 5-day-old seedlings grown on 0.01 mM NO_3^- media. Scale bars: 20 μm.

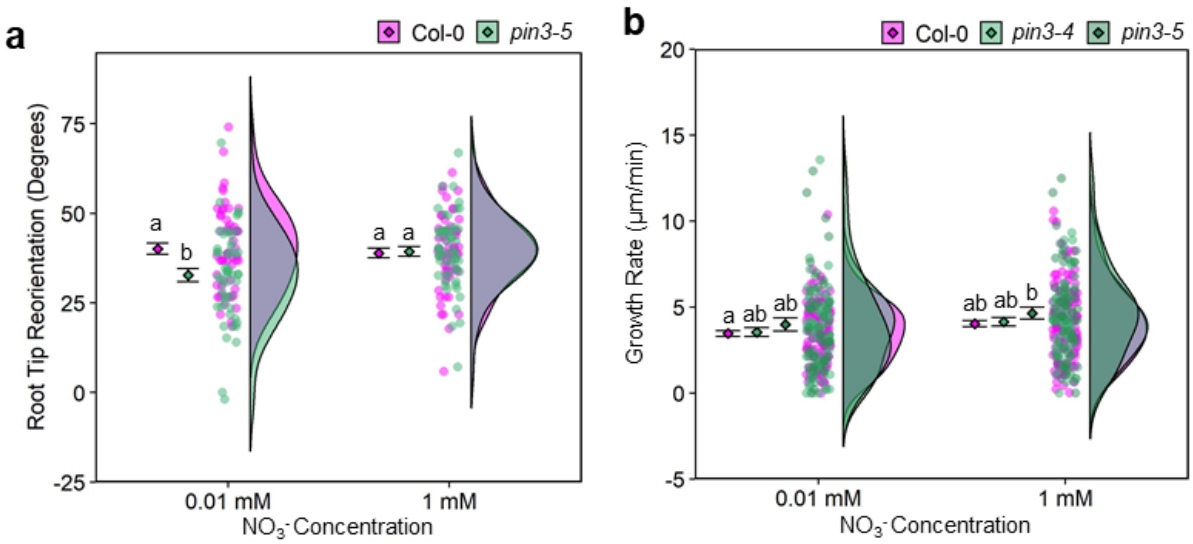

Appendix Figure B.2. Root phenotyping of *pin3* mutant lines. a) Root tip reorientation of *pin3-5* compared to Col-0 after two hours of 90-degree gravistimulation on 0.01 mM and 1 mM NO_3^- media (n=51-59). b) Root growth rates of *pin3* mutants compared to Col-0 (n=51-139). Mean-and-error plots are shown alongside raincloud plots indicating individual data points and distributions by genotype. Significant differences between genotype and condition combinations were determined using Tukey's test (p<0.05) following a two-way ANOVA and are indicated by lowercase letters (Supplementary Table S2).

APPENDIX C

Supplemental Data for Chapter 4

Appendix Table C.1. List of primers used in Chapter 4

Primer Name	Sequence
NruI-FD-F	TTCTGCCCAAATTCGCGAATGTTGTCATCAGCTAAGCATCAGAGA
XhoI-FD-R	AGTTAAAGGCCTCGAGTCAAAATGGAGCTGTGGAAGACCG
NruI-ATC-F	TTCTGCCCAAATTCGCGAATGGCCAGGATTTCCTCAGAC
XhoI-ATC-R	AGTTAAAGGCCTCGAGTCAACGGCGTCTAGCGGC
HindIII-p35S-F	TATATGTTTGAAGCTTTGAGACTTTTCAACAAAGGGTAATATCGG
SacI-Rluc-R	GATCGGGGAAATTCGAGCTCTTATTGTTCATTTTTGAGAACTCGCTCAAC
SacI-Fluc-R	GATCGGGGAAATTCGAGCTCTTACACGGCGATCTTTCCGC
HindIII-PIN3-F	TATATGTTTGAACTTCGCGATGTTAATATGTGAATAGCTTATAGCAT
XbaI-PIN3-R	CCATGGATCCTCTAGACTTGAAGGGACAAAAATGGAAAACC
NdeI-ATC-F	GGATCCTCGAGCATATGTCAACGGCGTCTAGCGGC
NdeI-ATC-R	CGCGCGGCAGCCATATGGCCAGGATTTCCTCAGAC

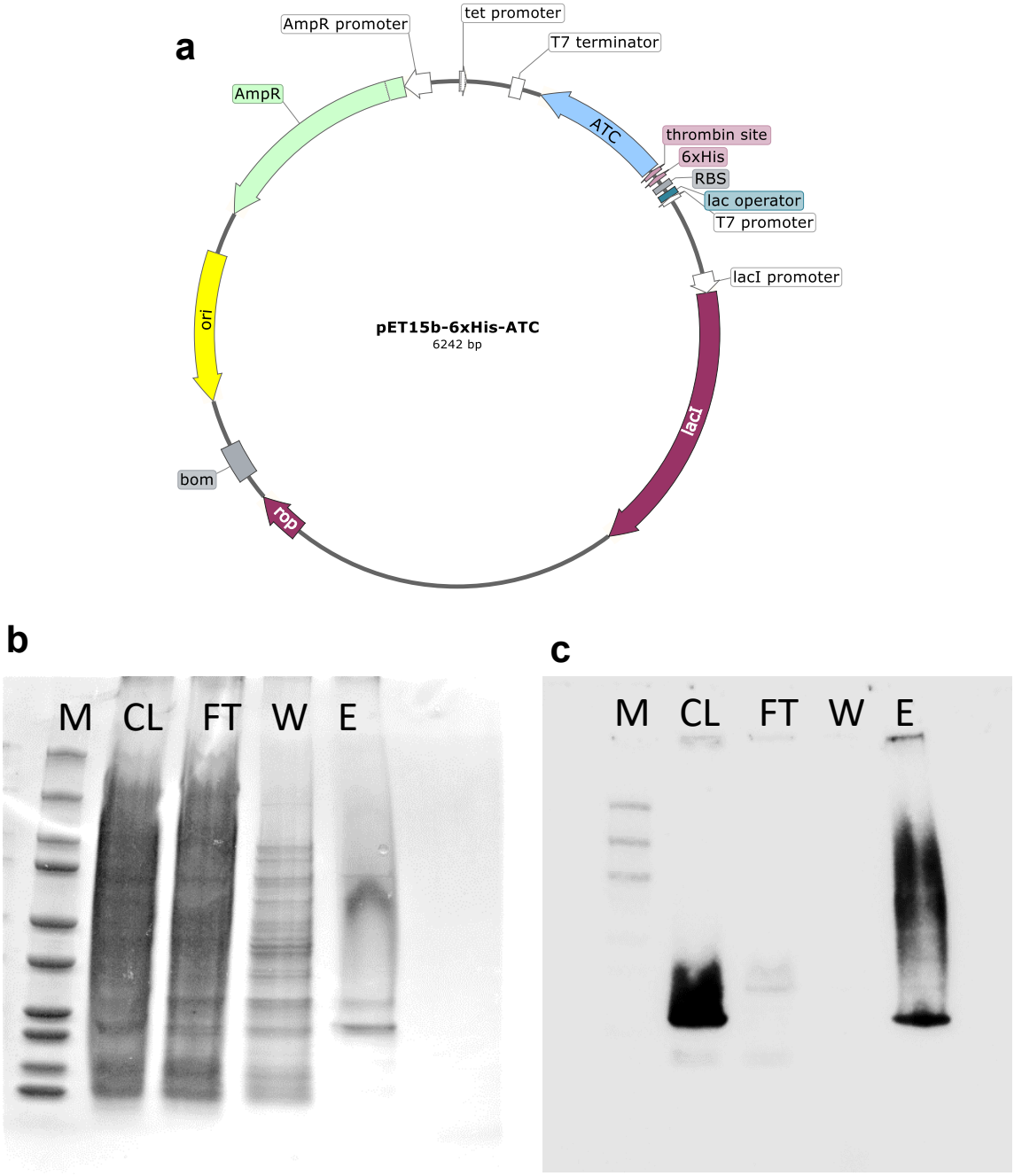

Appendix Figure C.1. Validation of His-ATC through SDS-PAGE and Western Blot. a) Plasmid map of *pET15b-6xHis-ATC* construct. b) SDS-PAGE gel of protein extraction fractions. c) Western blot of protein extraction fractions probed with the 6xHis-HRP antibody. M: marker, CL: cleared lysate, FT: flow-through, W: wash, E: elution.

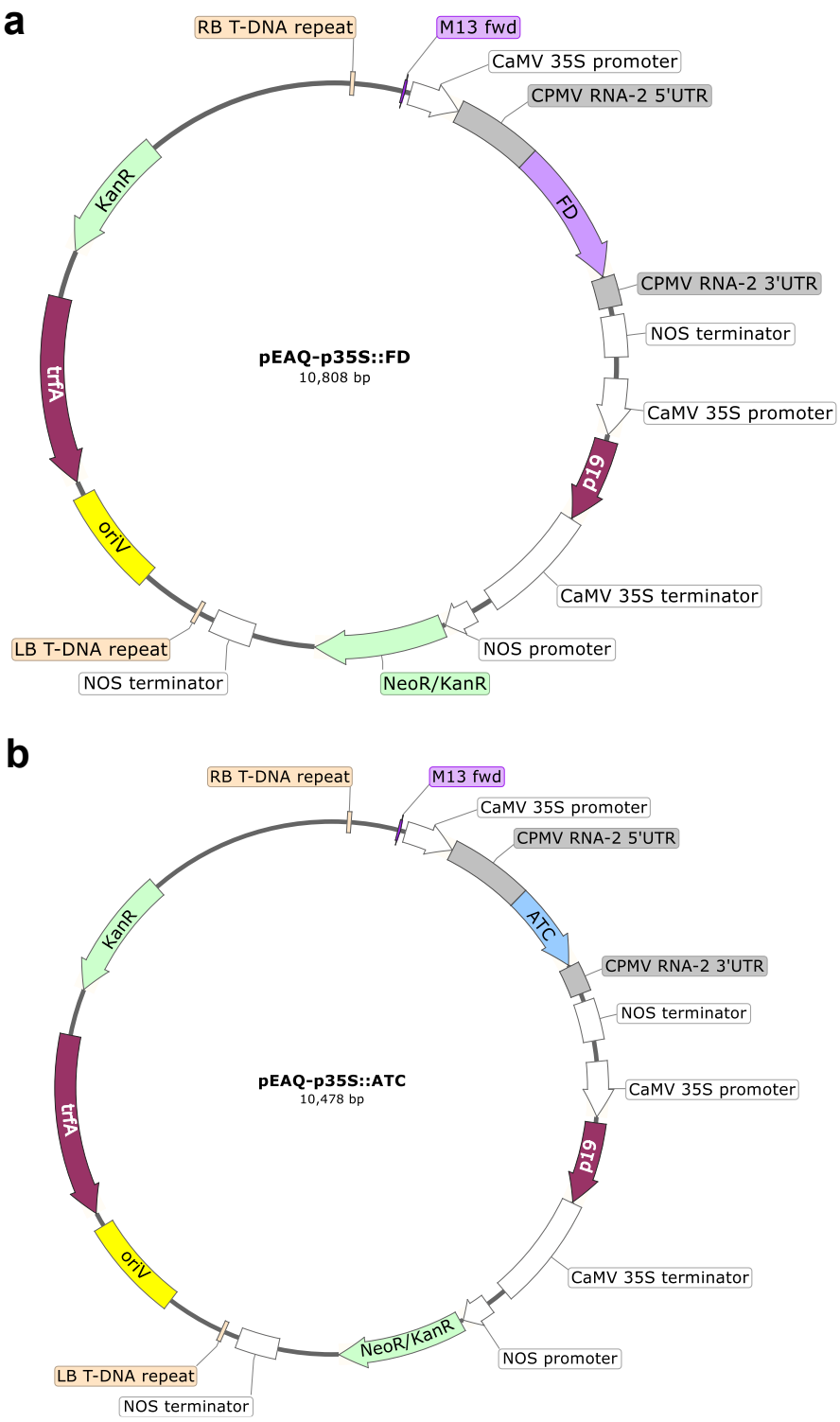

Appendix Figure C.2. Plasmid maps of pEAQ vectors. a) *pEAQ-p35S::FD*. b) *pEAQ-p35S::ATC*

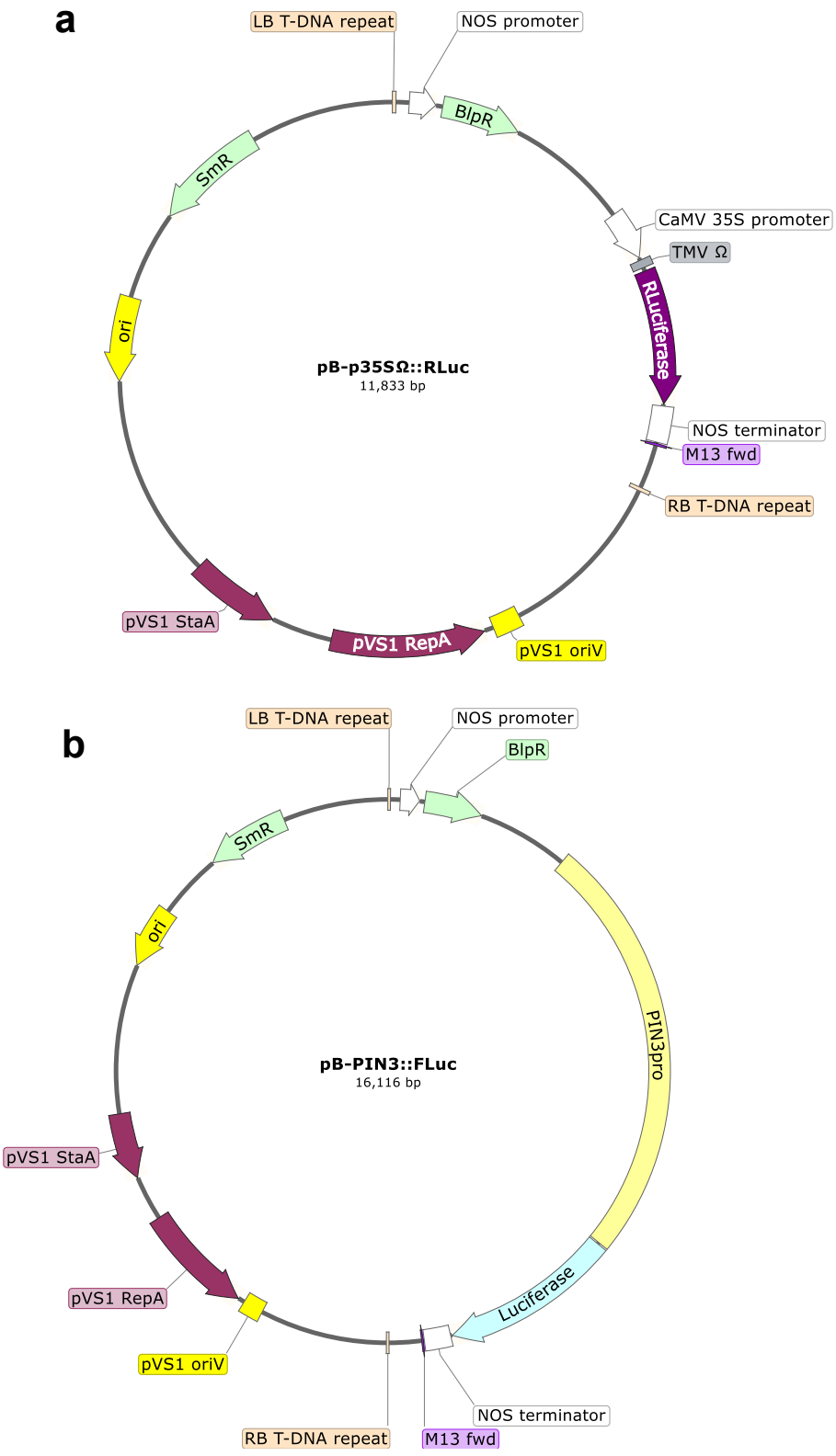

Appendix Figure C.3. Plasmid maps of dual luciferase vectors. A) *pB-p35SΩ::RLuc*. B) *pB-PIN3::FLuc.*

REFERENCES

REFERENCES

1. Giehl, R. F. H. & von Wiren, N. Root Nutrient Foraging. *PLANT Physiol.* **166,** 509–517 (2014).

2. Osmont, K. S., Sibout, R. & Hardtke, C. S. Hidden Branches: Developments in Root System Architecture. *Annu. Rev. Plant Biol.* **58,** 93–113 (2007).

3. Gruber, B. D., Giehl, R. F. H., Friedel, S. & von Wirén, N. Plasticity of the Arabidopsis Root System under Nutrient Deficiencies. *Plant Physiol.* **163,** 161–179 (2013).

4. Shahzad, Z. & Amtmann, A. Food for thought: how nutrients regulate root system architecture. *Curr. Opin. Plant Biol.* **39,** 80–87 (2017).

5. Tavormina, P., Coninck, B. D., Nikonorova, N., Smet, I. D. & Cammue, B. P. A. The Plant Peptidome: An Expanding Repertoire of Structural Features and Biological Functions. *Plant Cell* **27,** 2095–2118 (2015).

6. Czyzewicz, N. & De Smet, I. The *Arabidopsis thaliana* CLAVATA3/EMBRYO-SURROUNDING REGION 26 (CLE26) peptide is able to alter root architecture of *Solanum lycopersicum* and *Brassica napus*. *Plant Signal. Behav.* **11,** e1118598 (2016).

7. Velde, W. V. de, Zehirov, G., Szatmari, A., Debreczeny, M., Ishihara, H., Kevei, Z., Farkas, A., Mikulass, K., Nagy, A., Tiricz, H., Satiat-Jeunemaître, B., Alunni, B., Bourge, M., Kucho, K., Abe, M., Kereszt, A., Maroti, G., Uchiumi, T., Kondorosi, E. & Mergaert, P. Plant Peptides Govern Terminal Differentiation of Bacteria in Symbiosis. *Science* **327,** 1122–1126 (2010).

8. Shiu, S.-H. & Bleecker, A. B. Receptor-like kinases from Arabidopsis form a monophyletic gene family related to animal receptor kinases. *Proc. Natl. Acad. Sci.* **98,** 10763–10768 (2001).

9. Matsubayashi, Y. Post-translational modifications in secreted peptide hormones in plants. *Plant Cell Physiol.* **52,** 5–13 (2011).

10. Hobe, M., Müller, R., Grünewald, M., Brand, U. & Simon, R. Loss of CLE40, a protein functionally equivalent to the stem cell restricting signal CLV3, enhances root waving in Arabidopsis. *Dev. Genes Evol.* **213,** 371–381 (2003).

11. Suzaki, T., Yoshida, A. & Hirano, H.-Y. Functional Diversification of CLAVATA3-Related CLE Proteins in Meristem Maintenance in Rice. *Plant Cell* **20,** 2049–2058 (2008).

12. Ikeuchi, M., Yamaguchi, T., Kazama, T., Ito, T., Horiguchi, G. & Tsukaya, H. ROTUNDIFOLIA4 regulates cell proliferation along the body axis in Arabidopsis shoot. *Plant Cell Physiol.* **52,** 59–69 (2011).

13. Yang, S.-L., Xie, L.-F., Mao, H.-Z., Puah, C. S., Yang, W.-C., Jiang, L., Sundaresan, V. & Ye, D. TAPETUM DETERMINANT1 Is Required for Cell Specialization in the Arabidopsis Anther. *Plant Cell* **15,** 2792–2804 (2003).

14. Araya, T., Miyamoto, M., Wibowo, J., Suzuki, A., Kojima, S., Tsuchiya, Y. N., Sawa, S., Fukuda, H., Wirén, N. von & Takahashi, H. CLE-CLAVATA1 peptide-receptor signaling module regulates the expansion of plant root systems in a nitrogen-dependent manner. *Proc. Natl. Acad. Sci.* **111,** 2029–2034 (2014).

15. Kumpf, R. P., Shi, C.-L., Larrieu, A., Stø, I. M., Butenko, M. A., Péret, B., Riiser, E. S., Bennett, M. J. & Aalen, R. B. Floral organ abscission peptide IDA and its HAE/HSL2 receptors control cell separation during lateral root emergence. *Proc. Natl. Acad. Sci.* **110,** 5235–5240 (2013).

16. Mortier, V., Den Herder, G., Whitford, R., Van de Velde, W., Rombauts, S., D'haeseleer, K., Holsters, M. & Goormachtig, S. CLE Peptides Control *Medicago truncatula* Nodulation Locally and Systemically. *Plant Physiol.* **153,** 222–237 (2010).

17. Fernandez, A., Drozdzecki, A., Hoogewijs, K., Nguyen, A., Beeckman, T., Madder, A. & Hilson, P. Transcriptional and Functional Classification of the GOLVEN/ROOT GROWTH FACTOR/CLE-Like Signaling Peptides Reveals Their Role in Lateral Root and Hair Formation. *Plant Physiol.* **161,** 954–970 (2013).

18. Lynch, J. P. Steep, cheap and deep: an ideotype to optimize water and N acquisition by maize root systems. *Ann. Bot.* **112,** 347–357 (2013).

19. Remans, T., Nacry, P., Pervent, M., Filleur, S., Diatloff, E., Mounier, E., Tillard, P., Forde, B. G. & Gojon, A. The Arabidopsis NRT1.1 transporter participates in the signaling pathway triggering root colonization of nitrate-rich patches. *Proc. Natl. Acad. Sci.* **103,** 19206–19211 (2006).

20. Lima, J. E., Kojima, S., Takahashi, H. & Wirén, N. von. Ammonium Triggers Lateral Root Branching in Arabidopsis in an AMMONIUM TRANSPORTER1;3-Dependent Manner. *Plant Cell* **22,** 3621–3633 (2010).

21. Canales, J., Contreras-López, O., Álvarez, J. M. & Gutiérrez, R. A. Nitrate induction of root hair density is mediated by TGA1/TGA4 and CPC transcription factors in Arabidopsis thaliana. *Plant J. Cell Mol. Biol.* **92,** 305–316 (2017).

22. Krouk, G., Lacombe, B., Bielach, A., Perrine-Walker, F., Malinska, K., Mounier, E., Hoyerova, K., Tillard, P., Leon, S., Ljung, K., Zazimalova, E., Benkova, E., Nacry, P. & Gojon, A. Nitrate-Regulated Auxin Transport by NRT1.1 Defines a Mechanism for Nutrient Sensing in Plants. *Dev. Cell* **18,** 927–937 (2010).

23. Maghiaoui, A., Bouguyon, E., Cuesta, C., Perrine-Walker, F., Alcon, C., Krouk, G., Benková, E., Nacry, P., Gojon, A. & Bach, L. The Arabidopsis NRT1.1 transceptor coordinately controls auxin biosynthesis and transport to regulate root branching in response to nitrate. *J. Exp. Bot.* **71,** 4480–4494 (2020).

24. Cock, J. M. & McCormick, S. A Large Family of Genes That Share Homology withCLAVATA3. *Plant Physiol.* **126,** 939–942 (2001).

25. Okamoto, S., Shinohara, H., Mori, T., Matsubayashi, Y. & Kawaguchi, M. Root-derived CLE glycopeptides control nodulation by direct binding to HAR1 receptor kinase. *Nat. Commun.* **4,** 2191 (2013).

26. Brand, U., Fletcher, J. C., Hobe, M., Meyerowitz, E. M. & Simon, R. Dependence of stem cell fate in Arabidopsis on a feedback loop regulated by CLV3 activity. *Science* **289,** 617–619 (2000).

27. Stahl, Y., Wink, R. H., Ingram, G. C. & Simon, R. A signaling module controlling the stem cell niche in Arabidopsis root meristems. *Curr. Biol. CB* **19,** 909–914 (2009).

28. Patterson, K., Cakmak, T., Cooper, A., Lager, I., Rasmusson, A. G. & Escobar, M. A. Distinct Signaling Pathways and Transcriptome Response Signatures Differentiate Ammonium- and Nitrate-supplied Plants. *Plant Cell Environ.* **33,** 1486–1501 (2010).

29. Ohyama, K., Ogawa, M. & Matsubayashi, Y. Identification of a biologically active, small, secreted peptide in Arabidopsis by in silico gene screening, followed by LC-MS-based structure analysis. *Plant J. Cell Mol. Biol.* **55,** 152–160 (2008).

30. Delay, C., Imin, N. & Djordjevic, M. A. CEP genes regulate root and shoot development in response to environmental cues and are specific to seed plants. *J. Exp. Bot.* **64,** 5383–5394 (2013).

31. Ohkubo, Y., Tanaka, M., Tabata, R., Ogawa-Ohnishi, M. & Matsubayashi, Y. Shoot-to-root mobile polypeptides involved in systemic regulation of nitrogen acquisition. *Nat. Plants* **3,** 1–6 (2017).

32. Tabata, R., Sumida, K., Yoshii, T., Ohyama, K., Shinohara, H. & Matsubayashi, Y. Perception of root-derived peptides by shoot LRR-RKs mediates systemic N-demand signaling. *Science* **346,** 343–346 (2014).

33. Roberts, I., Smith, S., Stes, E., De Rybel, B., Staes, A., van de Cotte, B., Njo, M. F., Dedeyne, L., Demol, H., Lavenus, J., Audenaert, D., Gevaert, K., Beeckman, T. & De Smet, I. CEP5 and XIP1/CEPR1 regulate lateral root initiation in Arabidopsis. *J. Exp. Bot.* **67,** 4889–4899 (2016).

34. Imin, N., Mohd-Radzman, N. A., Ogilvie, H. A. & Djordjevic, M. A. The peptide-encoding CEP1 gene modulates lateral root and nodule numbers in Medicago truncatula. *J. Exp. Bot.* **64,** 5395–5409 (2013).

35. Mohd-Radzman, N. A., Laffont, C., Ivanovici, A., Patel, N., Reid, D., Stougaard, J., Frugier, F., Imin, N. & Djordjevic, M. A. Different Pathways Act Downstream of the CEP Peptide Receptor CRA2 to Regulate Lateral Root and Nodule Development. *Plant Physiol.* **171,** 2536–2548 (2016).

36. Djordjevic, M. A., Mohd-Radzman, N. A. & Imin, N. Small-peptide signals that control root nodule number, development, and symbiosis. *J. Exp. Bot.* **66,** 5171–5181 (2015).

37. Lynch, J. P. & Brown, K. M. Topsoil foraging - an architectural adaptation of plants to low phosphorus availability. *Plant Soil* **237,** 225–237 (2001).

38. Linkohr, B. I., Williamson, L. C., Fitter, A. H. & Leyser, H. M. O. Nitrate and phosphate availability and distribution have different effects on root system architecture of Arabidopsis. *Plant J. Cell Mol. Biol.* **29,** 751–760 (2002).

39. Ticconi, C. A., Lucero, R. D., Sakhonwasee, S., Adamson, A. W., Creff, A., Nussaume, L., Desnos, T. & Abel, S. ER-resident proteins PDR2 and LPR1 mediate the developmental response of root meristems to phosphate availability. *Proc. Natl. Acad. Sci.* **106,** 14174–14179 (2009).

40. Deb, S., Sankaranarayanan, S., Wewala, G., Widdup, E. & Samuel, M. A. The S-Domain Receptor Kinase Arabidopsis Receptor Kinase2 and the U Box/Armadillo Repeat-Containing E3 Ubiquitin Ligase9 Module Mediates Lateral Root Development under Phosphate Starvation in Arabidopsis. *Plant Physiol.* **165,** 1647–1656 (2014).

41. Song, L., Yu, H., Dong, J., Che, X., Jiao, Y. & Liu, D. The Molecular Mechanism of Ethylene-Mediated Root Hair Development Induced by Phosphate Starvation. *PLoS Genet.* **12,** e1006194 (2016).

42. Cederholm, H. M. & Benfey, P. N. Distinct sensitivities to phosphate deprivation suggest that RGF peptides play disparate roles in Arabidopsis thaliana root development. *New Phytol.* **207,** 683–691 (2015).

43. Matsuzaki, Y., Ogawa-Ohnishi, M., Mori, A. & Matsubayashi, Y. Secreted Peptide Signals Required for Maintenance of Root Stem Cell Niche in Arabidopsis. *Science* **329,** 1065–1067 (2010).

44. Shinohara, H., Mori, A., Yasue, N., Sumida, K. & Matsubayashi, Y. Identification of three LRR-RKs involved in perception of root meristem growth factor in Arabidopsis. *Proc. Natl. Acad. Sci.* **113,** 3897–3902 (2016).

45. de Bang, T. C., Lundquist, P. K., Dai, X., Boschiero, C., Zhuang, Z., Pant, P., Torres-Jerez, I., Roy, S., Nogales, J., Veerappan, V., Dickstein, R., Udvardi, M. K., Zhao, P. X. & Scheible, W.-R. Genome-Wide Identification of Medicago Peptides Involved in Macronutrient Responses and Nodulation. *Plant Phys.* **175,** 1669-1689 (2017).

46. Doblas, V. G., Smakowska-Luzan, E., Fujita, S., Alassimone, J., Barberon, M., Madalinski, M., Belkhadir, Y. & Geldner, N. Root diffusion barrier control by a vasculature-derived peptide binding to the SGN3 receptor. *Science* **355,** 280-284 (2017).

47. Nakayama, T., Shinohara, H., Tanaka, M., Baba, K., Ogawa-Ohnishi, M. & Matsubayashi, Y. A peptide hormone required for Casparian strip diffusion barrier formation in Arabidopsis roots. *Science* **355,** 284-286 (2017).

48. Robbins, N. E., Trontin, C., Duan, L. & Dinneny, J. R. Beyond the Barrier: Communication in the Root through the Endodermis. *Plant Phys.* **166,** 551-559 (2014).

49. Haruta, M., Sabat, G., Stecker, K., Minkoff, B. B. & Sussman, M. R. A peptide hormone and its receptor protein kinase regulate plant cell expansion. *Science* **343,** 408–411 (2014).

50. Wu, J., Kurten, E. L., Monshausen, G., Hummel, G. M., Gilroy, S. & Baldwin, I. T. NaRALF, a peptide signal essential for the regulation of root hair tip apoplastic pH in Nicotiana attenuata, is required for root hair development and plant growth in native soils. *Plant J. Cell Mol. Biol.* **52,** 877–890 (2007).

51. Matsubayashi, Y., Ogawa, M., Kihara, H., Niwa, M. & Sakagami, Y. Disruption and Overexpression of Arabidopsis Phytosulfokine Receptor Gene Affects Cellular Longevity and Potential for Growth. *Plant Physiol.* **142,** 45–53 (2006).

52. de Bang, T., Lay, K., Scheible, W. & Takahashi, H. Small peptide signaling pathways modulating macronutrient utilization in plants. *Curr. Opin. Plant Biol.* **39,** 31–39 (2017).

53. Ruffel, S., Krouk, G., Ristova, D., Shasha, D., Birnbaum, K. D. & Coruzzi, G. M. Nitrogen economics of root foraging: Transitive closure of the nitrate–cytokinin relay and distinct systemic signaling for N supply vs. demand. *Proc. Natl. Acad. Sci.* **108,** 18524-18529 (2011).

54. Chen, Y.-L., Lee, C.-Y., Cheng, K.-T., Chang, W.-H., Huang, R.-N., Nam, H. G. & Chen, Y-R. Quantitative Peptidomics Study Reveals That a Wound-Induced Peptide from PR-1 Regulates Immune Signaling in Tomato. *Plant Cell.* **26,** 4135-4148 (2014).55. Chien, P.-S., Nam, H. G. & Chen, Y.-R. A salt-regulated peptide derived from the CAP superfamily protein negatively regulates salt-stress tolerance in Arabidopsis. *J. Exp. Bot.* **66,** 5301–5313 (2015).

55. Chien, P.-S., Nam, H. G. & Chen, Y.-R. A salt-regulated peptide derived from the CAP superfamily protein negatively regulates salt-stress tolerance in Arabidopsis. *J. Exp. Bot.* **66,** 5301–5313 (2015).

56. Kellermeier, F., Armengaud, P., Seditas, T. J., Danku, J., Salt, D. E. & Amtmann, A. Analysis of the Root System Architecture of Arabidopsis Provides a Quantitative Readout of Crosstalk between Nutritional Signals. *Plant Cell.* **26,** 1480-1496 (2014).

57. Scheible, W.-R., Morcuende, R., Czechowski, T., Fritz, C., Osuna, D., Palacios-Rojas, N., Schindelasch, D., Thimm, O., Udvardi, M. K. & Stitt, M. Genome-Wide Reprogramming of Primary and Secondary Metabolism, Protein Synthesis, Cellular Growth Processes, and the Regulatory Infrastructure of Arabidopsis in Response to Nitrogen. *Plant Physiol.* **136,** 2483–2499 (2004).

58. Czyzewicz N., Shi, C.-L., Vu, L. D., Van De Cotte, B., Hodgman, C., Butenko, M. A. & De Smet, I. Modulation of Arabidopsis and monocot root architecture by CLAVATA3/EMBRYO SURROUNDING REGION 26 peptide. *J. Exp. Bot.* **66,** 5229-5243 (2015).

59. Lease, K. A. & Walker, J. C. The Arabidopsis unannotated secreted peptide database, a resource for plant peptidomics. *Plant Physiol.* **142,** 831–838 (2006).

60. Ghorbani, S., Lin, Y.-C., Parizot, B., Fernandez, A., Njo, M. F., Van de Peer, Y., Beeckman, T. & Hilson, P. Expanding the repertoire of secretory peptides controlling root development with comparative genome analysis and functional assays. *J. Exp. Bot.* **66,** 5257–5269 (2015).

61. Czyzewicz, N., Wildhagen, M., Cattaneo, P., Stahl, Y., Pinto, K. G., Aalen, R. B., Butenko, M. A., Simon, R., Hardtke, C. S. & De Smet, I. Antagonistic peptide technology for functional dissection of CLE peptides revisited. *J. Exp. Bot.* **66,** 5367–5374 (2015).

62. Strabala, T. J., O'Donnel, P. J., Smit, A.-M., Ampomah-Dwamena, C., Martin, E. J., Netzler, N., Nieuwenhuizen, N. J., Quinn, B. D., Foote, H. C. C. & Hudson, K. R. Gain-of-Function Phenotypes of Many CLAVATA3/ESR Genes, Including Four New Family Members, Correlate with Tandem Variations in the Conserved CLAVATA3/ESR Domain. *Plant Phys.* **140,** 1331-1344 (2006).

63. Yamaguchi, Y. L., Ishida, T., Yoshimura, M., Imamura, Y., Shimaoka, C. & Sawa, S. A Collection of Mutants for CLE-Peptide-Encoding Genes in Arabidopsis Generated by CRISPR/Cas9-Mediated Gene Targeting. *Plant Cell Physiol.* **58,** 1848–1856 (2017).

64. Peterson, B. A., Haak, D. C., Nishimura, M. T., Teixeira, P. J. P. L., James, S. R., Dangl, J. L. & Nimchuk, Z. L. Genome-Wide Assessment of Efficiency and Specificity in CRISPR/Cas9 Mediated Multiple Site Targeting in Arabidopsis. *PLOS ONE* **11,** e0162169 (2016).

65. Bollig, K., Lamshöft, M., Schweimer, K., Marner, F.-J., Budzikiewicz, H. & Waffenschmidt, S. Structural analysis of linear hydroxyproline-bound O-glycans of Chlamydomonas reinhardtii—conservation of the inner core in Chlamydomonas and land plants. *Carbohydr. Res.* **342,** 2557–2566 (2007).

66. Ohyama, K., Shinohara, H., Ogawa-Ohnishi, M. & Matsubayashi, Y. A glycopeptide regulating stem cell fate in Arabidopsis thaliana. *Nat. Chem. Biol.* **5,** 578–580 (2009).

67. DeYoung, B. J. & Clark, S. E. BAM Receptors Regulate Stem Cell Specification and Organ Development Through Complex Interactions With CLAVATA Signaling. *Genetics* **180,** 895–904 (2008).

68. Bleckmann, A., Weidtkamp-Peters, S., Seidel, C. A. M. & Simon, R. Stem cell signaling in Arabidopsis requires CRN to localize CLV2 to the plasma membrane. *Plant Physiol.* **152,** 166–176 (2010).

69. Zhu, Y., Wang, Y., Li, R., Song, X., Wang, Q., Huang, S., Jin, J. B., Liu, C.-M. & Lin, J. Analysis of interactions among the CLAVATA3 receptors reveals a direct interaction between CLAVATA2 and CORYNE in Arabidopsis. *Plant J. Cell Mol. Biol.* **61,** 223–233 (2010).

70. Kinoshita, A., Betsuyaku, S., Osakabe, Y., Mizuno, S., Nagawa, S., Stahl, Y., Simon, R., Yamaguchi-Shinozaki, K., Fukuda, H. & Sawa, S. RPK2 is an essential receptor-like kinase that transmits the CLV3 signal in Arabidopsis. *Development.* **137,** 3911-3920 (2010).

71. Guo, Y., Han, L., Hymes, M., Denver, R. & Clark, S. E. CLAVATA2 forms a distinct CLE-binding receptor complex regulating Arabidopsis stem cell specification. *Plant J. Cell Mol. Biol.* **63,** 889–900 (2010).

72. Stahl, Y., Grabowski, S., Bleckmann, A., Kühnemuth, R., Weidtkamp-Peters, S., Pinto, K. G., Kirschner, G. K., Schmid, J. B., Wink, R. H., Hülsewede, A., Felekyan, S., Seidel, C. A. M. & Simon, R. Moderation of Arabidopsis Root Stemness by CLAVATA1 and ARABIDOPSIS CRINKLY4 Receptor Kinase Complexes. *Curr. Biol.* **23,** 362–371 (2013).

73. Hazak, O. & Hardtke, C. S. CLAVATA 1-type receptors in plant development. *J. Exp. Bot.* **67,** 4827–4833 (2016).

74. Brandt, B. & Hothorn, M. SERK co-receptor kinases. *Curr. Biol.* **26,** R225–R226 (2016).

75. Santiago, J., Henzler, C. & Hothorn, M. Molecular Mechanism for Plant Steroid Receptor Activation by Somatic Embryogenesis Co-Receptor Kinases. *Science* **341,** 889–892 (2013).

76. Araya, T., von Wirén, N. & Takahashi, H. CLE peptide signaling and nitrogen interactions in plant root development. *Plant Mol. Biol.* **91,** 607–615 (2016).

77. Huang, N.-C., Jane, W.-N., Chen, J. & Yu, T.-S. Arabidopsis thaliana CENTRORADIALIS homologue (ATC) acts systemically to inhibit floral initiation in Arabidopsis. *Plant J.* **72,** 175–184 (2012).

78. Krapp, A. Plant nitrogen assimilation and its regulation: a complex puzzle with missing pieces. *Curr. Opin. Plant Biol.* **25,** 115–122 (2015).

79. Meier, M., Liu, Y., Lay-Pruitt, K. S., Takahashi, H. & von Wirén, N. Auxin-mediated root branching is determined by the form of available nitrogen. *Nat. Plants* **6,** 1136–1145 (2020).

80. Araya, T., Wirén, N. von & Takahashi, H. CLE peptides regulate lateral root development in response to nitrogen nutritional status of plants. *Plant Signal. Behav.* **9,** e29302 (2014).

81. Schoof, H., Lenhard, M., Haecker, A., Mayer, K. F. X., Jürgens, G. & Laux, T. The Stem Cell Population of Arabidopsis Shoot Meristems Is Maintained by a Regulatory Loop between the CLAVATA and WUSCHEL Genes. *Cell* **100,** 635–644 (2000).

82. Fujiwara, T., Hirai, M. Y., Chino, M., Komeda, Y. & Naito, S. Effects of Sulfur Nutrition on Expression of the Soybean Seed Storage Protein Genes in Transgenic Petunia. *Plant Physiol.* **99,** 263–268 (1992).

83. Koornneef, M., van Eden, J., Hanhart, C. J., Stam, P., Braaksma, F. J. & Feenstra, W. J. Linkage map of Arabidopsis thaliana. *J. Hered.* **74,** 265–272 (1983).

84. Sundaresan, V., Springer, P., Volpe, T., Haward, S., Jones, J. D., Dean, C., Ma, H. & Martienssen, R. Patterns of gene action in plant development revealed by enhancer trap and gene trap transposable elements. *Genes Dev.* **9,** 1797–1810 (1995).

85. Alonso, J. M., Stepanova, A. N., Leisse, T. J., Kim, C. J., Chen, H., Shinn, P., Stevenson, D. K., Zimmerman, J., Barajas, P., Cheuk, R., Gadrinab, C., Heller, C., Jeske, A., Koesema, E., Meyers, C. C., Parker, H., Prednis, L., Ansari, Y., Choy, N., Deen, H., Geralt, M., Hazari, N., Hom, E., Karnes, M., Mulholland, C., Ndubaku, R., Schmidt, I., Guzman, P., Aguilar-Henonin, L., Schmid, M., Weigel, D., Carter, D. E., Marchand, T., Risseeuw, E., Brogden, D., Zeko, A., Crosby, W. L., Berry, C. C. & Ecker, J. R. Genome-Wide Insertional Mutagenesis of Arabidopsis thaliana. *Science* **301,** 653–657 (2003).

86. Schindelin, J., Arganda-Carreras, I., Frise, E., Kaynig, V., Longair, M., Pietzsch, T., Preibisch, S., Rueden, C., Saalfeld, S., Schmid, B., Tinevez, J.-Y., White, D. J., Hartenstein, V., Eliceiri, K., Tomancak, P. & Cardona, A. Fiji: an open-source platform for biological-image analysis. *Nat. Methods* **9,** 676–682 (2012).

87. Allen, M., Poggiali, D., Whitaker, K., Marshall, T. R. & Kievit, R. A. Raincloud plots: a multi-platform tool for robust data visualization. *Wellcome Open Res.* **4,** (2019).

88. Kubo, M., Udagawa, M., Nishikubo, N., Horiguchi, G., Yamaguchi, M., Ito, J., Mimura, T., Fukuda, H. & Demura, T. Transcription switches for protoxylem and metaxylem vessel formation. *Genes Dev.* **19,** 1855–1860 (2005).

89. Yoshimoto, N., Inoue, E., Watanabe-Takahashi, A., Saito, K. & Takahashi, H. Posttranscriptional Regulation of High-Affinity Sulfate Transporters in Arabidopsis by Sulfur Nutrition. *Plant Physiol.* **145,** 378–388 (2007).

90. Chiu, W., Niwa, Y., Zeng, W., Hirano, T., Kobayashi, H. & Sheen, J. Engineered GFP as a vital reporter in plants. *Curr. Biol. CB* **6,** 325–330 (1996).

91. Koncz, C. & Schell, J. The promoter of TL-DNA gene 5 controls the tissue-specific expression of chimaeric genes carried by a novel type of Agrobacterium binary vector. *Mol. Gen. Genet. MGG* **204,** 383–396 (1986).

92. Höfgen, R. & Willmitzer, L. Storage of competent cells for Agrobacterium transformation. *Nucleic Acids Res.* **16,** 9877 (1988).

93. Davis, A. M., Hall, A., Millar, A. J., Darrah, C. & Davis, S. J. Protocol: Streamlined sub-protocols for floral-dip transformation and selection of transformants in Arabidopsis thaliana. *Plant Methods* **5,** 3 (2009).

94. Blancaflor, E. B., Fasano, J. M. & Gilroy, S. Mapping the Functional Roles of Cap Cells in the Response of Arabidopsis Primary Roots to Gravity. *Plant Physiol.* **116,** 213–222 (1998).

95. Kobayashi, Y. A Pair of Related Genes with Antagonistic Roles in Mediating Flowering Signals. *Science* **286,** 1960–1962 (1999).

96. Chapman, K., Ivanovici, A., Taleski, M., Sturrock, C. J., Ng, J. L. P., Mohd-Radzman, N. A., Frugier, F., Bennett, M. J., Mathesius, U. & Djordjevic, M. A. CEP receptor signalling controls root system architecture in Arabidopsis and Medicago. *New Phytol.* **226,** 1809–1821 (2020).

97. Winter, D., Vinegar, B., Nahal, H., Ammar, R., Wilson, G. V. & Provart, N. J. An “Electronic Fluorescent Pictograph” Browser for Exploring and Analyzing Large-Scale Biological Data Sets. *PLOS ONE* **2,** e718 (2007).

98. Brady, S. M., Orlando, D. A., Lee, J.-Y., Wang, J. Y., Koch, J., Dinneny, J. R., Mace, D., Ohler, U. & Benfey, P. N. A High-Resolution Root Spatiotemporal Map Reveals Dominant Expression Patterns. *Science* **318,** 801–806 (2007).

99. Li, B., Li, G., Kronzucker, H. J., Baluška, F. & Shi, W. Ammonium stress in Arabidopsis: signaling, genetic loci, and physiological targets. *Trends Plant Sci.* **19,** 107–114 (2014).

100. Ogura, T., Goeschl, C., Filiault, D., Mirea, M., Slovak, R., Wolhrab, B., Satbhai, S. B. & Busch, W. Root System Depth in Arabidopsis Is Shaped by EXOCYST70A3 via the Dynamic Modulation of Auxin Transport. *Cell* **178,** 400-412.e16 (2019).

101. Péret, B., De Rybel, B., Casimiro, I., Benková, E., Swarup, R., Laplaze, L., Beeckman, T. & Bennett, M. J. Arabidopsis lateral root development: an emerging story. *Trends Plant Sci.* **14,** 399–408 (2009).

102. Ötvös, K., Marconi, M., Vega, A., O'Brien, J., Johnson, A., Abualia, R., Antonielli, L., Montesinos, J. C., Zhang, Y., Tan, S., Cuesta, C., Artner, C., Bouguyon, E., Gojon, A., Friml, J., Gutiérrez, R. A., Wabnik, K. & Benková, E. Modulation of plant root growth by nitrogen source-defined regulation of polar auxin transport. *EMBO J.* **n/a,** e106862 (2021).

103. Zhang, Y., Xiao, G., Wang, X., Zhang, X. & Friml, J. Evolution of fast root gravitropism in seed plants. *Nat. Commun.* **10,** 3480 (2019).

104. Su, S.-H., Gibbs, N. M., Jancewicz, A. L. & Masson, P. H. Molecular Mechanisms of Root Gravitropism. *Curr. Biol.* **27,** R964–R972 (2017).

105. Baldwin, K. L., Strohm, A. K. & Masson, P. H. Gravity Sensing and Signal Transduction in Vascular Plant Primary Roots. *Am. J. Bot.* **100,** 126–142 (2013).

106. Leitz, G., Kang, B.-H., Schoenwaelder, M. E. A. & Staehelin, L. A. Statolith Sedimentation Kinetics and Force Transduction to the Cortical Endoplasmic Reticulum in Gravity-Sensing *Arabidopsis* Columella Cells. *Plant Cell* **21,** 843–860 (2009).

107. Overvoorde, P., Fukaki, H. & Beeckman, T. Auxin Control of Root Development. *Cold Spring Harb. Perspect. Biol.* **2,** a001537 (2010).

108. Bennett, M. J., Marchant, A., Green, H. G., May, S. T., Ward, S. P., Millner, P. A., Walker, A. R., Schulz, B. & Feldmann, K. A. Arabidopsis AUX1 Gene: A Permease-Like Regulator of Root Gravitropism. *Science* **273,** 948–950 (1996).

109. Adamowski, M. & Friml, J. PIN-Dependent Auxin Transport: Action, Regulation, and Evolution. *Plant Cell* **27,** 20–32 (2015).

110. Friml, J., Wiśniewska, J., Benková, E., Mendgen, K. & Palme, K. Lateral relocation of auxin efflux regulator PIN3 mediates tropism in Arabidopsis. *Nature* **415,** 806–809 (2002).

111. Kleine-Vehn, J., Ding, Z., Jones, A. R., Tasaka, M., Morita, M. T. & Friml, J. Gravity-induced PIN transcytosis for polarization of auxin fluxes in gravity-sensing root cells. *Proc. Natl. Acad. Sci.* **107,** 22344–22349 (2010).

112. Philosoph-Hadas, S., Friedman, H. & Meir, S. in *Vitam. Horm.* (ed. Litwack, G.) **72,** 31–78 (Academic Press, 2005).

113. Trachsel, S., Kaeppler, S. M., Brown, K. M. & Lynch, J. P. Maize root growth angles become steeper under low N conditions. *Field Crops Res.* **140,** 18–31 (2013).

114. Friml, J., Vieten, A., Sauer, M., Weijers, D., Schwarz, H., Hamann, T., Offringa, R. & Jürgens, G. Efflux-dependent auxin gradients establish the apical–basal axis of Arabidopsis. *Nature* **426,** 147–153 (2003).

115. Xu, J. & Scheres, B. Dissection of Arabidopsis ADP-RIBOSYLATION FACTOR 1 Function in Epidermal Cell Polarity. *Plant Cell* **17,** 525–536 (2005).

116. Blilou, I., Xu, J., Wildwater, M., Willemsen, V., Paponov, I., Friml, J., Heidstra, R., Aida, M., Palme, K. & Scheres, B. The PIN auxin efflux facilitator network controls growth and patterning in Arabidopsis roots. *Nature* **433,** 39–44 (2005).

117. Zádníková, P., Petrásek, J., Marhavy, P., Raz, V., Vandenbussche, F., Ding, Z., Schwarzerová, K., Morita, M. T., Tasaka, M., Hejátko, J., Van Der Straeten, D., Friml, J. & Benková, E. Role of PIN-mediated auxin efflux in apical hook development of Arabidopsis thaliana. *Dev. Camb. Engl.* **137,** 607–617 (2010).

118. Brunoud, G., Wells, D. M., Oliva, M., Larrieu, A., Mirabet, V., Burrow, A. H., Beeckman, T., Kepinski, S., Traas, J., Bennett, M. J. & Vernoux, T. A novel sensor to map auxin response and distribution at high spatio-temporal resolution. *Nature* **482,** 103–106 (2012).

119. Grones, P., Abas, M., Hajný, J., Jones, A., Waidmann, S., Kleine-Vehn, J. & Friml, J. PID/WAG-mediated phosphorylation of the Arabidopsis PIN3 auxin transporter mediates polarity switches during gravitropism. *Sci. Rep.* **8,** 10279 (2018).

120. Wiśniewska, J., Xu, J., Seifertová, D., Brewer, P. B., Růžička, K., Blilou, I., Rouquié, D., Benková, E., Scheres, B. & Friml, J. Polar PIN Localization Directs Auxin Flow in Plants. *Science* **312,** 883–883 (2006).

121. Abas, L., Benjamins, R., Malenica, N., Paciorek, T., Wišniewska, J., Moulinier–Anzola, J. C., Sieberer, T., Friml, J. & Luschnig, C. Intracellular trafficking and proteolysis of the Arabidopsis auxin-efflux facilitator PIN2 are involved in root gravitropism. *Nat. Cell Biol.* **8,** 249–256 (2006).

122. Marhavý, P., Vanstraelen, M., De Rybel, B., Zhaojun, D., Bennett, M. J., Beeckman, T. & Benková, E. Auxin reflux between the endodermis and pericycle promotes lateral root initiation. *EMBO J.* **32,** 149–158 (2013).

123. Collani, S., Neumann, M., Yant, L. & Schmid, M. *Effects of FLOWERING LOCUS T on FD during the transition to flowering at the shoot apical meristem of* Arabidopsis thaliana. (Plant Biology, 2018). doi:10.1101/483925

124. Zhu, Y., Klasfeld, S., Jeong, C. W., Jin, R., Goto, K., Yamaguchi, N. & Wagner, D. TERMINAL FLOWER 1-FD complex target genes and competition with FLOWERING LOCUS T. *Nat. Commun.* **11,** 5118 (2020).

125. Mimida, N., Goto, K., Kobayashi, Y., Araki, T., Ahn, J. H., Weigel, D., Murata, M., Motoyoshi, F. & Sakamoto, W. Functional divergence of the TFL1-like gene family in Arabidopsis revealed by characterization of a novel homologue. *Genes Cells* **6,** 327–336 (2001).

126. Abe, M., Kobayashi, Y., Yamamoto, S., Daimon, Y., Yamaguchi, A., Ikeda, Y., Ichinoki, H., Notaguchi, M., Goto, K. & Araki, T. FD, a bZIP Protein Mediating Signals from the Floral Pathway Integrator FT at the Shoot Apex. *Science* **309,** 1052–1056 (2005).

127. Nakamura, Y., Andrés, F., Kanehara, K., Liu, Y., Dörmann, P. & Coupland, G. Arabidopsis florigen FT binds to diurnally oscillating phospholipids that accelerate flowering. *Nat. Commun.* **5,** 3553 (2014).

128. Nakamura, Y., Lin, Y.-C., Watanabe, S., Liu, Y., Katsuyama, K., Kanehara, K. & Inaba, K. High-Resolution Crystal Structure of Arabidopsis FLOWERING LOCUS T Illuminates Its Phospholipid-Binding Site in Flowering. *iScience* **21,** 577–586 (2019).

129. Sainsbury, F., Thuenemann, E. C. & Lomonossoff, G. P. pEAQ: versatile expression vectors for easy and quick transient expression of heterologous proteins in plants. *Plant Biotechnol. J.* **7,** 682–693 (2009).

130. Benning, U. F., Tamot, B., Guelette, B. S. & Hoffmann-Benning, S. New Aspects of Phloem-Mediated Long-Distance Lipid Signaling in Plants. *Front. Plant Sci.* **3,** (2012).

131. Lin, Y.-L. & Tsay, Y.-F. Influence of differing nitrate and nitrogen availability on flowering control in Arabidopsis. *J. Exp. Bot.* **68,** 2603–2609 (2017).

132. Hong, Y., Devaiah, S. P., Bahn, S. C., Thamasandra, B. N., Li, M., Welti, R. & Wang, X. Phospholipase Dε and phosphatidic acid enhance Arabidopsis nitrogen signaling and growth. *Plant J.* **58,** 376–387 (2009).

133. Ryu, J. Y., Lee, H.-J., Seo, P. J., Jung, J.-H., Ahn, J. H. & Park, C.-M. The Arabidopsis floral repressor BFT delays flowering by competing with FT for FD binding under high salinity. *Mol. Plant* **7,** 377–387 (2014).

134. Dröge-Laser, W., Snoek, B. L., Snel, B. & Weiste, C. The Arabidopsis bZIP transcription factor family—an update. *Curr. Opin. Plant Biol.* **45,** 36–49 (2018).

135. Romera-Branchat, M., Severing, E., Pocard, C., Ohr, H., Vincent, C., Née, G., Martinez-Gallegos, R., Jang, S., Andrés, F., Madrigal, P. & Coupland, G. Functional Divergence of the Arabidopsis Florigen-Interacting bZIP Transcription Factors FD and FDP. *Cell Rep.* **31,** 107717 (2020).

136. Krapp, A., Berthomé, R., Orsel, M., Mercey-Boutet, S., Yu, A., Castaings, L., Elftieh, S., Major, H., Renou, J.-P. & Daniel-Vedele, F. Arabidopsis Roots and Shoots

Show Distinct Temporal Adaptation Patterns toward Nitrogen Starvation1[W]. *Plant Physiol.* **157,** 1255–1282 (2011).

137. Sorin, C., Declerck, M., Christ, A., Blein, T., Ma, L., Lelandais-Brière, C., Njo, M. F., Beeckman, T., Crespi, M. & Hartmann, C. A miR169 isoform regulates specific NF-YA targets and root architecture in Arabidopsis. *New Phytol.* **202,** 1197–1211 (2014).

138. Zhang, M., Hu, X., Zhu, M., Xu, M. & Wang, L. Transcription factors NF-YA2 and NF-YA10 regulate leaf growth via auxin signaling in Arabidopsis. *Sci. Rep.* **7,** 1395 (2017).

139. Jiang, L., Yoshida, T., Stiegert, S., Jing, Y., Alseekh, S., Lenhard, M., Pérez-Alfocea, F. & Fernie, A. R. Multi-omics approach reveals the contribution of KLU to leaf longevity and drought tolerance. *Plant Physiol.* **185,** 352–368 (2021).

140. Angkawijaya, A. E., Nguyen, V. C. & Nakamura, Y. LYSOPHOSPHATIDIC ACID ACYLTRANSFERASES 4 and 5 are involved in glycerolipid metabolism and nitrogen starvation response in Arabidopsis. *New Phytol.* **224,** 336–351 (2019).

141. Zou, N., Li, B., Dong, G., Kronzucker, H. J. & Shi, W. Ammonium-induced loss of root gravitropism is related to auxin distribution and TRH1 function, and is uncoupled from the inhibition of root elongation in Arabidopsis. *J. Exp. Bot.* **63,** 3777–3788 (2012).

142. Zou, N., Li, B., Chen, H., Su, Y., Kronzucker, H. J., Xiong, L., Baluška, F. & Shi, W. GSA-1/ARG1 protects root gravitropism in Arabidopsis under ammonium stress. *New Phytol.* **200,** 97–111 (2013).

143. Dong, W., Wang, Y. & Takahashi, H. CLE-CLAVATA1 Signaling Pathway Modulates Lateral Root Development under Sulfur Deficiency. *Plants* **8,** 103 (2019).

144. Arai-Sanoh, Y., Takai, T., Yoshinaga, S., Nakano, H., Kojima, M., Sakakibara, H., Kondo, M. & Uga, Y. Deep rooting conferred by DEEPER ROOTING 1 enhances rice yield in paddy fields. *Sci. Rep.* **4,** 5563 (2014).

145. Yamaguchi, Y. L., Ishida, T. & Sawa, S. CLE peptides and their signaling pathways in plant development. *J. Exp. Bot.* **67,** 4813–4826 (2016).

146. Schnabel, E., Journet, E.-P., de Carvalho-Niebel, F., Duc, G. & Frugoli, J. The Medicago truncatula SUNN Gene Encodes a CLV1-like Leucine-rich Repeat Receptor Kinase that Regulates Nodule Number and Root Length. *Plant Mol. Biol.* **58,** 809–822 (2005).

147. Yamamoto, E., Karakaya, H. C. & Knap, H. T. Molecular characterization of two soybean homologs of Arabidopsis thaliana CLAVATA1 from the wild type and fasciation mutant11The sequence data reported in this paper have been submitted to the GenBank data libraries under the accession numbers AF197946 for GmCLV1A

and AF197947 for GmCLV1B. *Biochim. Biophys. Acta BBA - Gene Struct. Expr.* **1491,** 333–340 (2000).

148. Kikuchi, R., Kawahigashi, H., Ando, T., Tonooka, T. & Handa, H. Molecular and Functional Characterization of PEBP Genes in Barley Reveal the Diversification of Their Roles in Flowering. *Plant Physiol.* **149,** 1341–1353 (2009).

149. Harig, L., Beinecke, F. A., Oltmanns, J., Muth, J., Müller, O., Rüping, B., Twyman, R. M., Fischer, R., Prüfer, D. & Noll, G. A. Proteins from the FLOWERING LOCUS T-like subclade of the PEBP family act antagonistically to regulate floral initiation in tobacco. *Plant J.* **72,** 908–921 (2012).

150. Karlgren, A., Gyllenstrand, N., Källman, T., Sundström, J. F., Moore, D., Lascoux, M. & Lagercrantz, U. Evolution of the PEBP Gene Family in Plants: Functional Diversification in Seed Plant Evolution. *Plant Physiol.* **156,** 1967–1977 (2011).